OPTIMISATION OF THE PRESERVATION OF MICROBIAL CELL BANKS FOR ENHANCED FERMENTATION PROCESS PERFORMANCE.

by

NICHOLA HELEN HANCOCKS

A thesis submitted to The University of Birmingham
For the degree of
DOCTOR OF PHILOSOPHY

Department of Chemical Engineering
College of Engineering and Physical Sciences
University of Birmingham
September 2009

Abstract

This work discusses optimisation of the cryopreservation of *Bacillus licheniformis* cell banks, used as inoculum for α-amylase producing 5 L batch fermentations. The effect of the presence of various cryopreservants including glycerol, Tween 80 and dimethyl sulphoxide on final fermentation performance measured by biomass and α-amylase concentration was investigated using optical density, dry cell weight, colony forming units, and multi-parameter flow cytometry. The application of multi-parameter flow cytometry using the fluorophores $DiBac_4(3)$ and PI allowed real time viability measurements of individual microbial cells to be monitored before and after cryopreservation and during the fermentation process; viability here being defined as a cell having an intact and fully polarised cytoplasmic membrane. It was found that the concentration and type of cryopreservant used had a significant effect on microbial cell physiology and population heterogeneity during resuscitation recovery immediately after thawing. Cell banks prepared with Tween 80 were fastest to recover after freezing in comparison to cell banks prepared with dimethyl sulphoxide which showed the slowest growth rates. Interestingly cells preserved in glycerol recovered at a similar rate to cells frozen without cryopreservant. Despite different responses to the freezing process when each cell bank was used as inoculum for 5 L batch fermentations very little difference was noticed in overall process performance with respect to α-amylase production, growth rate and final biomass concentration.

Acknowledgements

I would like to thank the following people who have made it possible for me to complete this research project:

My academic supervisors, Professor Christopher Hewitt and Professor Colin Thomas and my industrial supervisor Dr. Stuart Stocks for their help, encouragement and guidance throughout this project.

Novozymes A/S (Bagsværd, Denmark) for sponsoring my PhD project and for their hospitality and informative tour of the facility during my stay in Denmark.

Dr. Gerhard Nebe-von-Caron for his expertise with the flow cytometry.

Fellow colleagues for their help and practical assistance.

My husband, Mr Robin Hancocks for his help and encouragement.

My father, Professor Gordon Foxall, and my mother, Mrs Jean Foxall, for their love and support.

Abbreviations and Nomenclature

ADP	Adenosine diphosphate
ATP	Adenosine triphosphate
BSA	Bovine serum albumen
CcpA	Catabolite control protein
CCR	Carbon catabolite repression
CFU	Colony forming unit ($CFUmL^{-1}$)
CV	Coefficient of variance (%)
DCW	Dry cell weight (gL^{-1})
DE	Dextrose equivalent
$DiBac_4(3)$	Bis-(1, 3-dibutylbarbituric acid) trimethine oxonol
$DiOC_6(3)$	3, 3'-dihexyloxacarbocyanine iodide
DKK	Danish Krone
DMSO	Dimethyl sulphoxide
DOT	Dissolved oxygen tension (%)
DP	Degree of polymerisation
EDTA	Ethylene diamine tetra acetic acid
EGTA	Ethylene glycol tetra acetic acid
F	Feed rate (Lh^{-1})
FACS	Fluorescence activated cell sorting
FADH	Flavin adenine dinucleotide

FALS	Forward angle light scatter (°)
FDA	U.S. Food and Drug Administration
GlpK	Phosphorylating glycerol kinase
GRAS	Generally regarded as safe
GDP	Guanosine diphosphate
GTP	Guanosine triphosphate
HPLC	High pressure liquid chromatography
HPr	Histidine protein
HPrK	Histidine protein kinase
IFCC	International Federation of Clinical Chemistry and Laboratory Medicine
kDa	kiloDalton
LPS	Lipopolysaccharide
M	Maintenance coefficient ($gg^{-1}h^{-1}$)
mV	milliVolt
NADH	Nicotinamide adenine dinucleotide
nm	nanometer
PBS	Phosphate buffered saline
P_i	Inorganic phosphate
PI	Phenanthridium, 3,8-diamino-5-[3-(diethylmethylammonio) propyl]-6-phenyl-, di-iodide
PMT	Photomultiplier tube

PPG	Polypropylene glycol
PRD	phosphoenolpyruvate-carbohydrate phosphotransferase system regulatory domain
RALS	Right angle light scatter (°)
RI	Refractive index
S	Substrate concentration (gL^{-1})
SSF	Solid state fermentation
STR	Stirred tank reactor
UV	Ultraviolet
v/v	by volume
X_0	Total amount of cells (g)
Y_{xs}	Yield coefficient (gg^{-1})
μ	Specific growth rate (h^{-1})
ΔΨ	Membrane potential (mV)

To Robin, Gordon and Jean

for their love and support

Contents

Chapter 3 Materials and Methods

Chapter 4 Results and Discussion – Shake Flask Fermentation

List of Tables

List of Figures

Chapter 1

Introduction

An enzyme (from the Greek ‘to leaven’) is defined as a naturally occurring or synthetic macromolecular substance composed wholly or largely of protein, that catalyses more or less specifically one or more (bio) chemical reactions. Throughout history man has made use of these natural biological catalysts sometimes unknowingly to produce products which enhanced daily life. Wine, beer, bread and cheese have all been produced for many centuries and rely on natural enzymes. It was in the 19th century that Louis Pasteur was studying the process of fermentation of sugar into ethanol by yeast that he realised the process was catalysed by something associated with the yeast cells which he called ‘ferments’. Wilhelm Kuhne in 1878 first used the term enzyme. In 1897 Eduard Buchner showed that it was extracts of yeast cells, and not whole yeast cells that caused the fermentation and he named the enzyme zymase, and, in 1907 he received a Nobel Prize in chemistry for his discovery of cell free fermentation. The science known as zymotechnology was born, and became the start of the modern science of biotechnology. It was an exciting time, when recent advances in the field of agriculture, coupled with vast amounts of financial investment resulted in the creation of institutes dedicated to brewing such as Birmingham University’s British School of Malting and Brewing and

Copenhagen's Carlsberg Institute. The use of enzymes replaced traditional chemical processes which were not highly favoured at the time as summed up by Wilhelm Koenig:

Synthetic the coffee, Synthetic the wine
Synthetic the Milk and the butter gloss shine
on top of it all, even beer is not pure
Natural nutrition, you won't find to be sure.
They do let the devil take it for free
That wretched synthetic-made chemistry.
(Quoted by Bud, 1994)

In 1896 Emil Christian Hansen published a book entitled *Practical Studies in Fermentation* in which the concluding statement sums up the enthusiasm for the new science of zymotechnology:

"Nowadays it must be clear to every zymotechnologist who has made himself familiar with the results of recent investigation, that wherever fermentation organisms are made use of, the aim must be the same, namely to give up the old traditional method which depended on mere chance. In this entire field a new era has now commenced" (Quoted by Bud, 1994).

Enzymes have many advantages over chemical synthesis. They often provide a more specific reaction route, using a lower energy of activation. The products are of a higher purity and more easily extracted from the reaction mixture. Chemical reactions can produce unwanted side products which contaminate the end result.

Enzymes are produced naturally only in relatively low quantities, and only in response to specific conditions and although they are produced in most organisms bacteria are one of the most economically viable producers of enzymes. This is because there are many different types of bacteria which leads to a vast array of potential commercial products; they can be grown in large quantities which generates a large amount of product, and they can be manipulated at a genetic level or strain selected to enhance productivity. Today the enzyme industry is a huge growth industry and in 2008 Novozymes A/S who are the leading global enzyme manufacturer reported its overall sales to be DKK 8,146 million (http://www.novozymes.com).

One example of a commercially viable enzyme is α-amylase which is able to break down large starch molecules into small low molecular weight sugars and has a highly thermostable nature. This makes α-amylase important in a number of different industries such as the food and drink industry for the manufacture of high quality sugar syrups for fizzy drinks and in baking bread. In the textile and paper industry enzymes are used to produce size for protecting threads and paper from harsh mechanical processes and in the detergent industry they are

used to remove starch based stains from clothes and crockery. Most recently they are being used in the production of biofuels. The increased demand for α-amylase has led to ways to improve the quantity and quality of the enzyme for industrial production, and this has led to numerous studies aimed at a better understanding of enzyme production (Section 2.4).

The substrate for α-amylase is starch which is produced by plants in the process of photosynthesis. Starch is synthesised in leaf plastids for use as a storage compound for respiration during dark periods and it is also synthesised in amyloplasts of tubers, seeds and roots as an energy store where it accumulates as water soluble granules. Starch is a polymer of glucose; each glucose is linked by a glycosidic bond. The glycosidic bonds are stable at high pH but hydrolyse at low pH. At the end of the glucose polymer is an aldehyde group known as the reducing end. Figure 1.1 shows the two types of glucose polymers that exist in starch (i) amylose and (ii) and amylopectin (Martin *et al*., 1995).

(i) Amylose is a linear polymer of α-1,4 linked glucose units; there can be up to 6000 glucose units in an amylose polymer (Figure 1.1). The precise number of glucose units is termed the degree of polymerisation (DP) and varies with the origin of the starch. The average amylose content of a starch varies from 0 to 75% but is usually between 20-25% (Van der Maarel *et al*., 2002).

(ii) Amylopectin is a branched chain polymer composed of short linear sections of between 10 and 60 α-1,4 linked glucose units and branched side chains of between 15 and 45 α-1,6 linked glucose units (Figure 1.1). The

complete amylopectin molecule can contain as many as 2,000,000 glucose units making it one of the largest naturally occurring molecules (Van der Maarel *et al*., 2002). Starch converting enzymes have been grouped into four categories: (i) endoamylases, (ii) exoamylases, (iii) debranching enzymes and (iv) transferase enzymes.

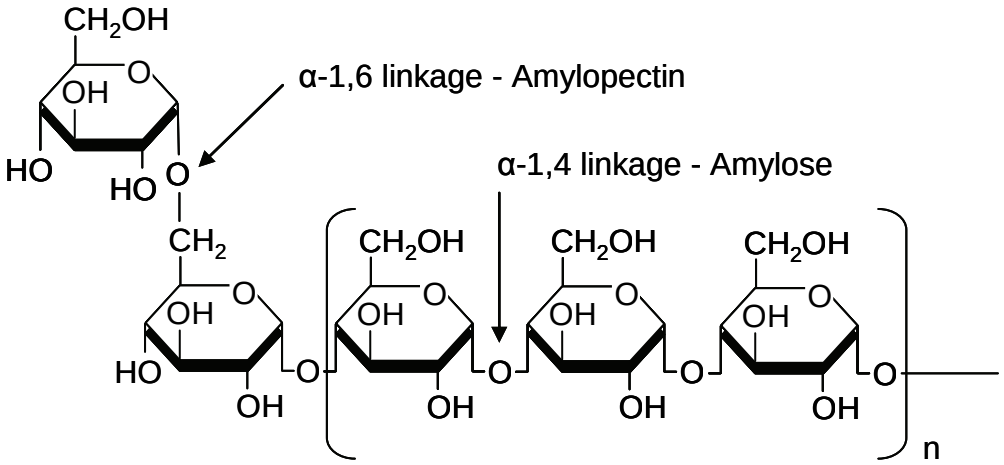

Figure 1.1 A representation of a starch molecule. It contains two polymers of glucose amylose and amylopectin (adapted from Martin *et al*., 1995).

Endoamylases which include α-amylase (EC 3.2.1.1) or 1,4-α-D-glucanglucanohydrolase cleaves the α-1,4 glycosidic bonds in the internal region of amylose and amylopectin polymers in a random fashion to produce shorter oligosaccharides such as maltose, maltotriose, glucose and limit dextrins from amylopectin (Van der Maarel *et al*., 2002).

The α-amylases are used in a wide range of roles and represent one of the most commercially successful industrial enzymes. In each process they are rarely

used alone, but in combination with other enzymes. Most processes make use of the unique specificity of a variety of different enzymes to complete each stage of a process and some examples include.

(i) Starch liquefaction and saccharification

In 1811 the German scientist Kirchhoff discovered that sweet syrup was obtained when a starch water slurry was treated with diluted acid. The sweetness of starch syrup was dependent on the degree of hydrolysis, with complete hydrolysis producing only glucose or dextrose (Van der Maarel *et al*., 2002). In 1930 Ohlsson concluded that amylase enzymes hydrolyse starch into smaller sugar molecules (Gupta *et al*., 2003). Acid hydrolysis has been replaced by enzymatic treatment which involves a number of different enzymes and different processing conditions. Figure 1.2 shows the stages involved and the conditions required for each process.

Amylopectin is completely soluble in water, but amylose and the starch granule itself are not soluble in cold water. Starch processing into syrups involves three main steps: (i) gelatinisation, (ii) liquefaction and (iii) saccharification. (i) Gelatinisation is the process of heating a water starch slurry, a process which causes the starch granules to swell irreversibly. The process causes the amylose to leach out of the granules resulting in a viscous slurry. Prolonged heating increases the viscosity of the slurry, and yields a viscous colloidal suspension, which once cooled, forms an elastic gel (Van der Maarel *et al*., 2002).

(ii) Starch liquefaction involves the partial hydrolysis of starch and a loss of viscosity. The amount of glucose contained in the slurry is dependent on the amount of enzyme added and the length of incubation (Van der Maarel *et al*., 2002).

(iii) Starch saccharification during which the starch-hydrolysate syrup is converted into a highly concentrated glucose syrup.

The percentage hydrolysis of the glycosidic bonds is given by the dextrose equivalent (DE) value. Termamyl 120 L and Termamyl 2X are α–amylases produced by Novozymes A/S from *B. licheniformis*.

They are marketed as producing high yields of dextrose with limited by-products, they reduce viscosity efficiently, they do not adversely colour the product thereby reducing refinery costs and do not require additional calcium which saves on production costs. Termamyl SC is also from *B. licheniformis* and can operate at reduced pH and calcium levels compared to other α–amylases (www.novozymes.com). The high quality sugar syrups generated from the saccharification process are used for the manufacture of carbonated beverages and biofuels as well as many other products.

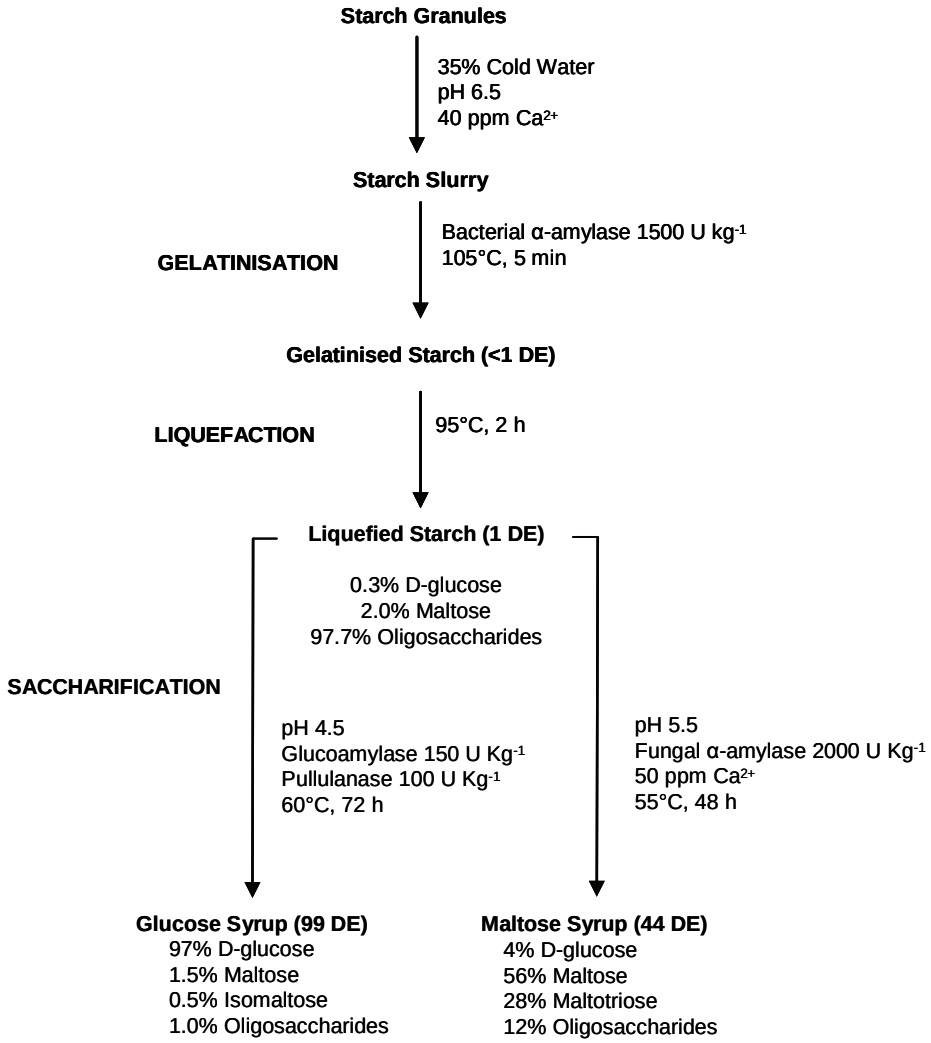

Figure 1.2 Starch saccharification and liquefaction. Typical reaction conditions are shown (http://www.lsbu.ac.uk/biology/enztech/starch.html).

(ii) The baking industry

α-amylase is used to hydrolyse starch in the preparation of the dough. This process makes the sugars more accessible to the yeast, and improves the texture and volume of a loaf of bread. Once the bread is baked, staling is a major

factor in the shelf life of bread and this is due to the process of retrogradation of the starch. Starch which has been gelatinised begins to retrograde upon cooling and affects the crispness of the crust and the flavour of the bread. The use of maltogenic amylases which hydrolyse starch into maltose and maltotriose increase the shelf life of bread by 2 days (Gil *et al*., 1999).

(iii) Detergents

α-amylases are employed for the removal of starch-based stains during laundry washing or dishwashing. The use of α-amylase in dishwashing has allowed a reduction in washing temperatures, and removed the need for harmful chemicals which can damage health and the environment and are unsuitable for delicate glass and china. The washing environment can be a harsh environment for enzymes to be active including a high pH, oxidising conditions and the presence of metal ions, surfactants and proteases. Novozymes A/S enzyme preparations Termamyl Ultra and Termamyl Ultra 300 L are capable of stable performance for long periods of time in liquid detergents and can effectively remove starch based stains and whiten laundry (www.novozymes.com).

(iv) Textile manufacture

Modern textile manufacturing processes exert large stresses on the warp threads during weaving. To avoid the breakage of the threads a removable protective coating, size, is applied to the threads. Starch is favoured for this because it is low cost widely available and easy to remove. The enzyme α-amylase is employed to produce the starch solutions applied to the textiles and

also to remove them afterwards without damaging the cloth. It does this by breaking down the starch into water soluble dextrins that are removed during washing (Gupta *et al*., 2003).

(v) Paper manufacture

During the manufacture of paper α-amylase is used to produce a low viscosity, high molecular weight starch for coating paper. The sizing of paper with starch is to protect the paper from mechanical damage during processing and improves the quality of the finished paper. The starch size improves the stiffness and strength in paper (Gupta *et al*., 2003).

Several different organisms are used commercially in the production of α-amylase with the most popular being *B.* species including *B*. *licheniformis*, *B*. *amyloliquefaciens* and *B*. *subtilis*, and the fungi *Aspergillus niger* and *Aspergillus oryzae*. The organism *B. licheniformis* used in this study is a saprophytic, Gram positive rod, spore forming, facultative anaerobe that resides in soil (Sneath *et al*., 1986) and on bird feathers (Williams *et al*., 1990). It is widely used by the biotechnology industry for the production of many commercially important enzymes and biochemicals including; alkaline proteases (Gupta *et al*., 2002), α-amylases (Gupta *et al*., 2003), penicillinase (Wittman *et al*., 1993), pentosannase, cycloglucosyltransferase, β-mannase and also some pectinolytic enzymes (Rey *et al*., 2004); several antibiotics; bacitracin (Schallmey *et al*., 2004) and proticin (Vértesy, 1972); biochemicals such as citric acid, inosine, inosinic acid and poly-γ-glutamic acid (Rey *et al*., 2004). It is closely related to the well

studied model organism *B. subtilis* and is a popular industrial micro-organism for the following reasons: (i) it is generally regarded as safe (GRAS) by the food and drug administration; (ii) it grows rapidly leading to short fermentation cycles, the high levels of extracellular enzymes it produces are secreted directly into the medium reducing the need for complex downstream processing; (iii) the α-amylase produced by *B. licheniformis* is highly thermostable and has a wide range of pH tolerance, so it is therefore of use for many applications (Schallmey *et al*., 2004); (iv) it has been widely studied and is well understood; recently the genome was sequenced and characterised (Rey *et al*., 2004). *B. licheniformis* is favoured for its high rate of growth, its overproduction of α-amylase, and because it has a "generally regarded as safe" GRAS status from the Food and Drug Administration. *B. licheniformis* SJ4628 used in this study is an industrial production strain used by Novozymes A/S, and has been the subject of a number of detailed studies (Section 2.3). However, problems have previously been encountered in the batch to batch reproducibility of some fermentations.

Product quality is dependent on reproducibility of a process making this an important area of study (Section 2.1). One possible cause of poor batch to batch reproducibility lies in the cell banks used to create the inoculum for the fermentation: studies have shown that a small variation in the quality of the inoculum leads to large variations in product yield and hence a loss of batch to batch reproducibility (Gnoth *et al*., 2007 and Webb *et al*., 1993). Both the amount of biomass and the physiology of the biomass are crucial in determining the

success of a fermentation making inoculum quality crucial to fermentation process performance. The favoured method for preparing cell banks is to freeze a sample of cells in 20% v/v glycerol and freeze at -20°C. Since its discovery in 1949 by Polge, Smith and Parkes, glycerol has become one of the most widely used cryoprotective chemicals for a number of different reasons. It is relatively non-toxic to cells; it is cheap and readily available; is well studied; and has a high rate of success not only for micro-organisms but also for mammalian cells. Novozymes A/S currently use glycerol to prepare cell banks of their α-amylase production strains of *B. licheniformis* but there are many other different cryoprotective compounds which have shown success at preserving micro-organisms including dimethyl sulphoxide (DMSO) and polyethylene glycol sorbitan monooleate (Tween 80) (Hubálek, 2003). The results of the effects of different cryopreservants on fermentation process performance are investigated in this work.

Chapter 2

Literature Review

2.1 Microbial fermentation reproducibility

Excellent product quality coupled with a high yield is the ultimate goal for any research and development programme leading to the large-scale production of microbial based products at the commercial scale. Consequently batch to batch reproducibility is of paramount importance. This has been recognised by the Food and Drug administration and has led to the development of the process analytical technology (PAT) initiative. PAT aims to design develop and operate processes consistently to ensure predefined quality at the end of the manufacturing process (http://www.fda.gov/cder/OPS/PAT.htm). This aims to reduce the substantial losses that happen in the fermentation industry each year due to variability in yields and productivity (Webb *et al*., 1993). One variable known to affect batch to batch reproducibility is the quality of the inoculum both with respect to number of cells and cellular physiology (Lee, 2006 and Webb *et al*., 1993).

The effect of inoculum cell density on final biomass formation during fed batch fermentation has been demonstrated clearly by Gnoth *et al*. (2007) and Webb *et al*. (1993) who show that small variations in initial biomass concentration lead to large variations in final biomass at the end of the fermentation. From an

industrial perspective where large scale bioprocesses are employed lack of reproducibility in inoculum preparation has a big impact on reproducibility of the overall process. Errors associated with inoculum preparation increase with the number of propagation steps especially as industrial processes tend to be as automated as possible. Work by Hornbæk *et al*. (2004) using the same organism that was used for this project *B. licheniformis* SJ4628 demonstrated the relationship between cellular physiology in the inoculum and cellular growth. They discovered that differences in cellular heterogeneity did not affect maximum growth rates of the cells or reproducibility of the process. It did result in differences in the lengths of the lag phase, and cell populations displaying greater heterogeneity had longer lag phases than more homogenous populations.

One of the driving forces for this project was the lack of reproducibility of α-amylase producing *B. licheniformis* fermentations experienced by Novozymes A/S. The probable cause for this was believed to reside in the cell banks used to create the inoculum for the process.

2.2 Cell banks and microbial preservation

The inoculum is ultimately prepared from a cell bank, and the type of preservation technique employed could have major implications on the quality of the inoculum.

Several factors must be considered when choosing a method for preserving microbes. The viability of the organism should be maintained

throughout processing and storage. Population stratification should be minimised as high levels of cell death occurring during the preservation process may lead to selection of a resistant but low producing population. A good preservation technique will avoid the possibility of genetic change arising either from strain drift through mutation or loss of plasmid. The purity of the sample should be maintained and any chance of contamination avoided (Kirsop *et al*., 1984). No single preservation technique fulfils all of these criteria and a suitable preservation method is a matter of compromise. Micro-organisms all differ in their tolerance to different preservation methods and it is unlikely that a single preservation method will be optimal for all micro-organisms in a culture collection. Preservation methods include: serial sub-culturing, drying, freeze drying and cryopreservation (Kirsop *et al*., 1984).

Cryopreservation is one of the most popular forms of microbial cell preservation used today particularly for storage of large cell banks such as those found in industry. It allows a large cell bank to be compiled from a single batch of culture with minimal expense in a short period of time. Novozymes A/S use cryopreservation for most of their cell banks. Freezing (cryopreservation) at low temperatures means that cells can be stored in a suspended state as biological processes slow to an almost un-detectable level and stop altogether at temperatures below -100 °C (Fuller, 2004). During freezing water is removed from cells and the dehydrated cells are stored at low temperatures. Damage to cells can occur during the cooling phase and in the subsequent thawing process

(Fuller, 2004). When cells are cooled slowly water in the suspending medium is converted to ice and salts become concentrated. This creates an osmotic imbalance across the cytoplasmic membrane and the cell shrinks. At cooling rates that are too fast to allow the cell to adjust by shrinkage, intracellular freezing occurs, a process which leads to the formation of damaging ice crystals inside the cell. Between the extremes of slow and fast cooling there presumably lies an optimum cooling rate for a particular cell type. The thawing process for cells which have been cryopreserved can also cause cellular damage and in practice if rapid cooling was used rapid thawing should also be used to avoid ice formation during warming. Any small ice crystals formed during rapid cooling will grow into larger crystals if slow thawing is used.

Cryoprotective chemicals are added to a sample of cells to prevent the damaging effects of ice formation. They act by hydrogen bonding to water and increasing its viscosity. The action of cryoprotective compounds is colligative however; a balance must be maintained as high concentrations may be toxic to cells (Fuller, 2004). Cryoprotective compounds are classified as penetrating and non-penetrating depending on their ability to traverse the cytoplasmic membrane. Penetrating cryoprotective compounds have low molecular weights (below 400) allowing them to enter the cytoplasmic membrane, and include glycerol and dimethyl sulphoxide. Non-penetrating cryoprotective compounds have large molecular weights and cannot enter the cytoplasmic membrane, and include polyvinylpyrrolidone and hydroxyethyl starch. The effectiveness of a

cryoprotective compound depends upon the surface area to volume ratio of a cell, the permeability of the cytoplasmic membrane, temperature, and the physiochemical properties of the cryoprotective compound (Hubálek, 2003).

Glycerol $C_3H_5(OH)_3$ has a molecular mass of 92.09 $gmol^{-1}$. It is a small polyhydroxylated molecule which is highly soluble in water, and has a low toxicity during short term exposure to cells. Glycerol can hydrogen bond with water and can penetrate the cytoplasmic membrane of a cell although the disadvantage of it is that it does this at different rates or not at all in some cells (Pagliaro *et al*., 2008). Glycerol was one of the first successful cryoprotective compounds to be used and its cryoprotective effects were first discovered by Polge *et al*. (1949). Later Smith (1950) successfully cryopreserved red blood cells with glycerol. From this point glycerol became one of the most widely used cryopreservants as it remains even today.

Dimethyl sulphoxide (DMSO) C_2H_6OS has a molecular mass of 78.13 $gmol^{-1}$. It is a small amphipathic molecule with a hydrophilic sulphoxide group and two hydrophobic methyl groups. DMSO is able to rapidly penetrate cytoplasmic membranes of cells, and it is more toxic to cells than glycerol (Gurtovenko *et al*., 2007). Like glycerol DMSO was discovered to be an effective cryopreservant early on in the history of the science of cryopreservation by Lovelock and Bishop who used it in the cryopreservation of red blood cells (Lovelock *et al*., 1959).

Polyethylene glycol sorbitan monooleate (Tween 80) $C_{64}H_{124}O_{26}$ has a molecular mass of 1310 $gmol^{-1}$, and is a non-ionic surfactant used for food

emulsification and also for cryopreservation and has the benefit of being non-toxic to cells (Chattopadhyay, 2006). It differs from both glycerol and DMSO in that it is a much larger molecule and cannot directly penetrate the lipid bilayer of the cell. Beal *et al*. (2001) postulated that the ability of a cell to resist the process of being frozen is directly related to the fatty acid composition of the cytoplasmic membrane. They showed that when the organism *Streptococcus thermophilus* was treated with oleic acid (part of the Tween 80 molecule) and cryopreserved that the oleic acid increased the ratio of unsaturated to saturated fatty acids and increased the organism's resistance to the freezing process. Work carried out by Smittle *et al*. (1974) showed that the presence of sodium oleate in the culture broth of *LactoB. bulgaricus* stimulated the production of tetradecanoic acid, hexadecanoic acid, octadecanoic acid and C19 cyclopropane fatty acid and resulted in decreased production of saturated fatty acids. Cyclopropane fatty acids are thought to prevent close packing of the fatty acids in the cytoplasmic membrane causing an increase in cytoplasmic membrane fluidity.

Despite the beneficial effects of cryopreservants caution must be observed as high concentrations of these chemicals can have toxic effects. There is no single rule for knowing which concentration is safe for a given organism, and this has to be determined empirically (Simione , 1998).

The cytoplasmic membrane of the microbial cell is directly related to the viability of the bacterium, and its ability to adapt to environmental stimuli is key to the survival of the organism. As soil dwelling organisms Bacilli have to be able to

adapt to fluctuating temperatures and they do this by the mechanism of homoviscous adaptation. When external temperatures fall changes in the fatty acid profile of the bacterial cytoplasmic membrane occur to maintain optimal fluidity. Saturated fatty acids are converted into unsaturated fatty acids by desaturase enzymes, and there is preferential synthesis of short chain fatty acids, branched chain fatty acids and anteiso-fatty acids. An increase in the number of *cis* compared to *trans* fatty acids also increases cytoplasmic membrane fluidity (Chattopadhyay, 2006).

Cryoprotective compounds such as glycerol and DMSO, which can enter the cytoplasmic membrane of the micro-organism, may mediate their effects by also helping to increase the amount of unsaturated fatty acids in the lipid bilayer. However, they can also cause toxic effects to the cell in a number of different ways. They can partition themselves within the lipid bilayer creating a concentration gradient that could disrupt the polarity of the bilayer and may cause damage to the cytoplasmic membrane in the areas of accumulation (Sikkema *et al*., 1995). The areas where the chemicals accumulate may cause localised expansion of the cytoplasmic membrane, and possibly cause pores to appear with a loss in cytoplasmic membrane integrity as seen by work on cytoplasmic membranes treated with DMSO (Gurtovenko *et al*., 2007). The changes in the integrity of the cytoplasmic membrane will also have effects on the function of the cytoplasmic membrane to carry out its role in energy transduction by dissipating the proton motive force and the sodium motive force (Sikkema *et al*., 1995). The

regulation of cellular pH may be affected and cytoplasmic membrane embedded and surface bound enzymes could be damaged (Sikkema *et al*., 1995). The possible expansion of the cytoplasmic membrane caused by high concentrations of cryopreservants would most likely disrupt these enzymes. Another detremental effect is hydration of the cytoplasmic membrane head groups of the lipid bilayer caused by apolar compounds such as DMSO because of their preferential binding to the hydrophilic head groups of the bilayer (Gurtovenko *et al*., 2007). Cytoplasmic membrane fluidity is important to the normal function of a lipid bilayer and a possible cause of toxicity would be if the fluidity was changed dramatically by changes in the fatty acid composition of the lipid bilayer. The higher the ratio of unsaturated fatty acids the more fluid the cytoplasmic membrane but, if it becomes too fluid structural integrity may become irreversibly altered (Sikkema *et al*., 1995).

The cytoplasmic membrane contains lipid soluble compounds such as cholesterol, hopanoids, and carotenoids which act to modify the fluidity and integrity of the cytoplasmic membrane. They could influence the partitioning effect of a chemical across the cytoplasmic membrane. The phospholipid composition of the cytoplasmic membrane also has a large effect on partitioning. A greater ratio of unsaturated to saturated fatty acids in the cytoplasmic membrane can increase the resistance of a cell to the toxic effects of a chemical (Sikkema *et al*., 1995). Strains of *Escherichia coli* which resisted the toxic effects of ethanol were found to have increased levels of anionic phospholipids such as

phosphatidylglycerol and cardiolipin with respect to phosphatidylethanolamine (Sikkema *et al*., 1995). Polar solvents such as acetone, DMSO and ethanol are also known to increase the unsaturated fatty acid content of the cytoplasmic membrane, although with ethanol, this is probably because it inhibits the enzyme required for biosynthesis of saturated fatty acids (Sikkema *et al*., 1995). Toxicity could be effected by a *cis* to *trans* isomerisation of fatty acids in the cytoplasmic membrane. A change from *cis* to *trans* increases the ordering of the cytoplasmic membrane and decreases fluidity (Sikkema *et al*., 1995).

This project aimed to test the effects of different cryopreservants on the organism *B. licheniformis* SJ4628 used by Novozymes A/S to produce α- amylase.

2.3 *B. licheniformis* SJ4628

Several species of *Bacillus* are used for industrial scale enzyme manufacture as they have advantageous characteristics (Chapter 1). *B. licheniformis* SJ4628 is an industrial production strain and only a few studies have been published about it. It is an asporulating mutant (Hornbæk *et al*., 2004) with a tolerance for alkaline conditions (Hornbæk *et al*., 2002). Work completed by Kocharunchitt (2007) showed *B. licheniformis* SJ4628 to be a very robust organism, and changes in micro-environment with respect to glucose and dissolved oxygen concentration had little or no effect on the final biomass or α-amylase concentration during fed batch fermentations designed to simulate large

scale fermentations with areas of poor mixing. In studies designed to simulate high glucose, low dissolved oxygen and high pH, final biomass remained unchanged when compared with cells grown in standard conditions but the yield of α-amylase was reduced by 10%. Glucose was found to be the preferred carbon source for *B. licheniformis* SJ4628 when compared to sucrose. Studies by Hornbæk *et al*. (2004) on the effect of propagation conditions on fermentation performance for *B. licheniformis* SJ4628 revealed that shorter lag phases were observed for fermentations using inoculum composed of early stationary phase cells (12 h propagation) cultured in liquid medium compared to late stationary phase cells (24 h propagation) cultured on solid media. Cells grown on solid medium showed greater heterogeneity when compared to cells grown in liquid medium. Hornbæk *et al*. (2002) also demonstrated that microbial cell viability had a significant effect on the length of the lag phase, but little effect on overall biomass production or specific growth rate for *B. licheniformis* SJ4628. Studies by Hornbæk *et al*. (2004) also revealed the effects of pH on growth of *B. licheniformis* SJ4628 and revealed interesting insights into mechanisms used by this organism to adapt to changing pH. The study found that *B. licheniformis* SJ4628 responded to changes in pH from pH 5.3 to pH 8.0 by changing the composition of the cytoplasmic membrane and increasing production of metabolites which neutralize pH. A pH of 7.0 was found to stimulate optimal growth conditions including the shortest lag phase and was associated with induction of genes involved in sucrose uptake

(*sacA* and *sacP*) and optimum growth. The lowest specific growth rates were found at pH 5.3. At pH 8.0 cells demonstrated phosphate starvation and responded with up-regulation of genes responsible for production of teichuronic acid (*tuaA*, *tuaB*, *tuaC*, *tuaD* and *yrvJ*) and synthesis of phosphate containing teichoic acid was down-regulated (*tagB*). Phosphate transporters encoded by the *pst* operon were up-regulated in increasing amounts from pH 7.0 to pH 8.0. The *phoA* gene encoding an alkaline phospatase was also up-regulated at pH 8.0. At pH 8.0 genes that were also up-regulated include those involved with fatty acid synthesis (*des*, *plsX* and *fabHA*), oxidative phosphorylation and cytoplasmic membrane bioenergetics (*ndhF*). Genes involved in acetoin biosynthesis (*alsD* and *alsS*) were down-regulated at pH 6.0, 7.0 and 8.0 and up-regulated at pH 5.3 probably to prevent the accumulation of pyruvate in the growth medium and prevent the formation of acetate (Hornbæk *et al*., 2004).

Interestingly *B. licheniformis* SJ4628 adapts to low external pH (pH 5.3) by changing the composition of the fatty acids in the cytoplasmic membrane to increase the quantity of unsaturated fatty acids and make the cytoplasmic membrane more fluid. This controls the flow of protons across the cytoplasmic membrane and is a similar response to that used to alter cytoplasmic membrane fluidity during cold shock (Section 2.2).

B. licheniformis SJ4628 is used at Novozymes A/S to produce Termamyl an amylase used to remove starch based stains and starch film. It is a robust standard amylase which whitens laundry and is suitable for dishwashing.

Termamyl has a tolerance for high temperatures and alkaline conditions (www.novozymes.com).

2.4 α-amylase

α-amylase is an extracellular enzyme with great commercial significance (Chapter 1). It is secreted into the medium surrounding the micro-organism, it does not occur in the cytoplasm, but has been found contained within vesicles bound to the extracellular side of the cytoplasmic membrane (Priest, 1977). Arnesen *et al*. (1998) discovered that the addition of Tween 80 to a shake flask culture of *Thermomyces lanuginosus* grown in low molecular weight dextran as a carbon source increased the production of α-amylase 27 fold. This may be because the detergent helped to remove the cytoplasmic membrane bound α-amylase. Coleman (1970) studied the distribution of α-amylase synthesis between cytoplasmic membrane bound and soluble fractions of ribosomes from *B. amyloliquefaciens* and showed that α-amylase concentration was five fold greater in the cytoplasmic membrane bound fraction. Both the extracellular and cytoplasmic membrane bound forms of α-amylase are encoded by the *amyE* gene and mutations of this gene prevent synthesis of α-amylase (Priest, 1977). α-amylase is described as a scavenger enzyme as it has no cellular substrate, its sole function appears to be to degrade polymers of glucose including starch, into smaller sugars to provide nutrients for the cell (Priest, 1977). α-amylase synthesis occurs before sporulation in the early or late stationary phase of growth and is

associated with depletion of carbon source and a change in culture conditions which remove the effect of carbon catabolite repression (Priest, 1977). α-amylase synthesis is induced by complex starch based molecules, Maltotetraose is an efficient inducer of α-amylase synthesis, maltotriose and higher malto-oligosaccharides (G5, G6 and G7) are good, but less efficient than maltotetraose. High yields of α-amylase can be obtained using complex starch based medium as they fail to exert carbon catabolite repression (Priest, 1977). Preferred nitrogen sources for α-amylase production include yeast extract and ammonium salts, including ammonium sulphate and ammonium nitrate (Gupta *et al*., 2003). Phosphate is important as a regulator of metabolite synthesis in micro-organisms, and if not enough phosphate is present cell growth and α-amylase production is poor. However, phosphate in too high a concentration may also be an inhibitor of α-amylase synthesis (Gupta *et al*., 2003). Metal ions particularly Mg^{2+} and Ca^{2+} are also important for α-amylase production as α-amylase is a metalloenzyme. Environmental conditions are also important and a pH of between 6.0 and 7.0 is usually maintained for *B.* species (Hornbæk *et al*., 2004). Temperature can vary depending on the organism and 37 °C is generally used for *B. licheniformis* (Gupta *et al*., 2003). Adequate aeration during the fermentation of *B. licheniformis* is essential for good yields of α-amylase because *B. licheniformis* is a facultative anaerobe (Gupta *et al*., 2003). Fed batch systems for large scale commercial production of α-amylase are favoured over batch processes as higher cell densities can be achieved and glucose can be delivered to the cells in a

controlled manner. In batch cultures the high initial concentration of glucose leads to lower cell densities and lower yield of product due to carbon catabolite repression (Priest, 1977).

2.5 Glucose metabolism

The main products of microbial glucose metabolism are shown in Figure 2.1. The production of these compounds is dependent on the concentration of glucose and oxygen in the medium during microbial growth. In order to maximize the growth and reproduction of biomass during the fermentation process glucose and oxygen concentrations must be tightly controlled for optimal process performance. At low glucose concentrations anabolism is tightly coupled to catabolism and microbial cells use the energy provided to grow and produce biomass. During glucose excess anabolism becomes uncoupled from catabolism and ATP is diverted away from growth and biomass formation into: overflow metabolism, energy spilling reactions, futile energy cycles and cellular maintenance (Sonenshein, 2007). In the presence of excess glucose *B. subtilis* metabolises glucose only as far as pyruvate and acetyl CoA. Carbon overflow pathways then convert them to the metabolic intermediates lactate, acetate and acetoin (Sonenshein, 2007). *B. licheniformis* is able to use the acetoin and 2,3-butandiol it produces as carbon sources (Veith *et al*., 2004). As a facultative anaerobe *B. licheniformis* can grow aerobically using oxygen as an electron acceptor. It can also grow anaerobically either using nitrite as an

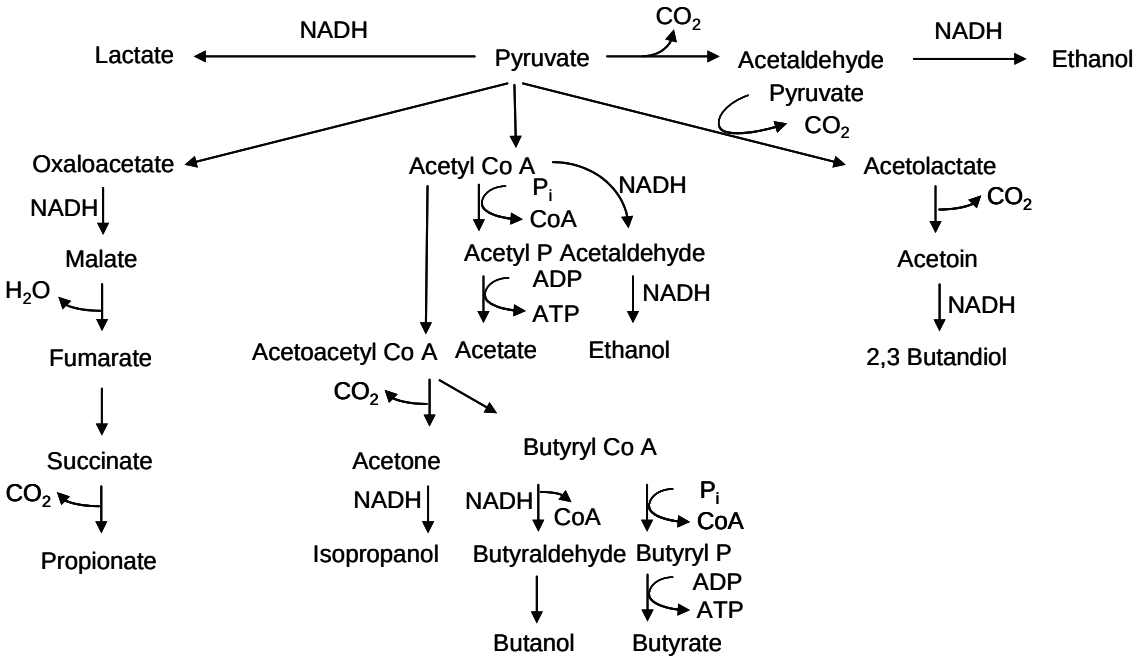

Figure 2.1 Anaerobic metabolites produced by micro-organisms. Pathways which produce NADH such as conversion of pyruvate to lactate are shown. Pathways linked to ATP production such as succinyl Co A to succinate, butyryl Co A to butyrate and acetyl Co A to acetate are also included (Ratledge *et al*., 2001).

electron acceptor or by fermentation using organic electron acceptors (Nakano *et al*., 1997). Amanullah *et al*. (2001b) showed that under fully aerobic conditions *B. subtilis* strain AJ 1992 converts glucose into pyruvate and then CO_2 and water via the citric acid cycle. They also demonstrated that for *B. subtilis* AJ 1992 in an oxygen limited environment, above 150 parts per billion (ppb) acetoin is produced. At oxygen levels below 80 ppb 2,3-butandiol is produced. Lactate is also produced at low levels of oxygenation. Acetate is also a major product for

B. subtilis grown in an aerobic batch culture with a glucose carbon source (Fuhrer *et al*., 2005). Anaerobic growth of *B. licheniformis* NCIB 6346 in the presence of glucose as a carbon source was found to produce acetate, 2,3- butandiol, ethanol, formate, lactate, succinate and pyruvate (Shariati *et al*., 1995). The dominant metabolic product was acetate which increased in concentration when nitrate was present in the growth medium (Shariati *et al*., 1995). Acetate is prevented from causing overacidification of the medium during exponential growth of *B. subtilis* by converting pyruvate into acetoin under aerobic conditions and 2,3-butandiol under anaerobic conditions both of which can be excreted into the medium (Presecan-Siedel *et al*., 1999). No formate was produced by *B. licheniformis* NCIB 6346 when nitrate and glucose were present in the medium (Shariati *et al*., 1995).

2.6 Microbial viability

An accurate measurement of microbial cell viability is of paramount importance for many applications including bioprocess engineering. During a fermentation knowledge about the number of cells and their physiological condition is crucial for optimum performance and hence product yield. Microbial viability is defined as the presence of structure, changeable genetic information, metabolic or functional ability and the capacity for reproductive growth. Table 2.1 highlights the major criteria for viability and the techniques for measuring them (Nebe-von-Caron *et al*., 2000).

Functional Cell Status	Intact Cells			Permeabilised (Dead Cells)
	Metabolically Active Cells			
	Reproductive Growing Cells			
Test Criteria	Cell Division	Metabolic Activity	Membrane Integrity	Membrane Permeability
Detection Method	**Cell Counting** • Fixed Volume Count • Time Integration • Ratiometric Counting **Cell Tracking** • Covalent Labelling (Intracellular Or Membrane)	**Energy Dependent** **Biosynthesis** • DNA/Protein Synthesis, Cell Elongation Under Antibiotic Pressure **Pump Activity** • pH Control, Dye Efflux **Membrane Potential** • Accumulation Of Cationic Dyes, Dissipation Of Anionic Dyes **Energy Independent** **Enzyme Activity** • Substrate Conversion By Esterase/ Dehydrogenase	**Selective Membrane Permeability** • Exclusion of membrane impermeable DNA stains	**Membrane Permeability** • Indiscriminate uptake of cytoplasmic stains
		Cells With Nucleic Acid Damage		

Table 2.1 Cellular viability determinants and how to measure them (Nebe-von-Caron *et al*., 2000).

Reproductive viability uses evidence of the reproductive growth of micro-organisms as evidence for microbial viability, and plate count methods have become the benchmark measure of viability by microbiologists. Plate count techniques suffer from a number of problems and often under estimate the number of viable cells, for several reasons. Plate counts are limited by the ability of the micro-organism to grow in an artificial environment, and do not take into account cells which are dead, sub-lethally damaged, viable but non culturable, dormant or inactive. The process is also time consuming and results of these tests provide information about a process in terms of days long after anything can be done to make alterations (Nebe-von-Caron *et al*., 2000).

The cytoplasmic membrane of a microbial cell is essential to the viability of a micro-organism as it performs several vital functions. Cytoplasmic membrane integrity is crucial for microbial viability as it provides a barrier between the external environment and the cellular cytoplasm. The cytoplasmic membrane is a phospholipid bilayer with proteins embedded in it. There is considerable diversity of phospholipids in prokaryotic cytoplasmic membranes, but most of the phospholipids are glycolipids with two fatty acid chains (Zhang *et al*., 2008). The phospholipid acyl chains are crucial for determining the viscosity of the cytoplasmic membrane, which has important implications for passive permeability to hydrophobic molecules, active solute transport and protein-protein interactions.

The ability of prokaryotes to change the fatty acid composition of their cytoplasmic membranes to maintain the biophysical properties of their

cytoplasmic membranes is called homoviscous adaptation (Zhang *et al*., 2008). Homoviscous adaptation may result from changes in temperature, pH, osmolarity or contact with toxic chemicals. Longer chain fully saturated fatty acids decrease the fluidity of the cytoplasmic membrane compared with unsaturated shorter fatty acids (Zhang *et al*., 2008).

The cytoplasmic membrane generates a cytoplasmic membrane potential ($\Delta\Psi$) by controlling the concentration gradients of ions including Na^+, K^+, H^+ and Cl^- across the cytoplasmic membrane; a process which is maintained by ion channels and electrogenic pumps (Shapiro, 2000). A cell with an intact cytoplasmic membrane has a net positive charge outside the cell and a net negative charge inside the cell and is polarised with a $\Delta\Psi$ of about 100 mV. The $\Delta\Psi$ may alter during normal cellular functions such as surface receptor mediated processes but, if the cytoplasmic membrane becomes damaged and loses integrity the $\Delta\Psi$ becomes 0 mV (Shapiro, 2000). Once the cytoplasmic membrane has lost integrity and can no longer generate a membrane potential a cell is dead.

Viability is also dependent on the metabolic status of a cell and its ability to produce energy during respiration using the electron transport chain which relies on enzyme activity (Nebe-von-Caron *et al*., 2000). The cytoplasmic membrane is the site for energy transduction. The electron transport chain is located in the cytoplasmic membrane of prokaryotes.

2.7 Microbial population heterogeneity

Microbial cultures are heterogeneous cell populations. Their inherent genotypic and phenotypic flexibility is crucial for their existence allowing them to adapt to adverse conditions.

Microbial population heterogeneity is caused by three main sources: (i) genotypically, as the result of mutation, (ii) phenotypically, as cells are distributed throughout the cell cycle and (iii) the physiological state of the cells relating to their environmental conditions (Davey *et al*., 1996). Even a well mixed laboratory scale bioreactor will exhibit short intervals of pH or nutrient spikes at the point of addition and larger scale systems are well characterised as having zones of poor mixing (Amanullah *et al*., 2001b).

Many techniques for measuring microbial cultures fail to take this heterogeneity into account. Techniques such as dry cell weight and spectrophotometry measure the total amount of cell biomass and fail to take into account the viability of individual cells. Because of this they may be described as “bulk analysis” techniques (Nebe-von-Caron *et al*., 2000). Spectrophotometry has the advantage of being quick and simple to perform. A sample of cells appears turbid because each cell can scatter light, and the more cells that are present the more turbid a sample appears. The spectrophotometer measures turbidity by absorbance of light of a specific wavelength and the number of photons scattered is proportional to the mass of the cells in a sample. In very concentrated samples cells can bounce the light back and forth and give inaccurate readings therefore some samples require dilution.

In order to obtain the net cell mass from a culture, cells can be centrifuged and the pellet weighed to give the wet mass. The same cells can then be dried in an oven and the dry weight determined by weighing. This is an accurate technique for measuring total cellular biomass and unlike spectrophotometry can be done on a relatively large scale. However, like spectrophotometry it does not give any information about cellular viability and it does take significant time (usually 24 h) to process samples so the results are not immediately available.

Colony forming units per mL ($CFUmL^{-1}$), microscopic cell counts, traditional staining techniques and flow cytometry are examples of single cell analysis techniques. $CFUmL^{-1}$ is a measure of the number of reproductively viable cells in a culture and is currently the benchmark for measuring microbial viability. However, it often underestimates the number of viable cells in a sample because it is limited by the ability of the micro-organism to grow in an artificial environment and does not take into account cells which are dead, sub-lethally damaged, viable but non culturable, dormant or inactive. The technique provides information 1 or 2 days after the experiment is completed which is too late to make any changes.

Microscopic cell counts are tedious to perform and are prone to human error. Traditional staining techniques for measuring microbial viability using methylene blue, methylene violet and *p*-iodonitrotetrazolium violet suffer from the same problems as manual cell counts. In addition, it is the user who determines the physiological state of the cells depending on how they perceive the uptake of the dye (Hewitt *et al*., 2004). Flow cytometry is a very powerful technique which

can measure the real time physiological state of an individual cell and can sort cells of interest for further analysis.

2.8 Multi-parameter flow cytometry

Multi-parameter flow cytometry is a powerful technique for measuring many different aspects of single cells in real time, and allows individual cells to be sorted out of a culture and analysed separately (Shapiro, 2003). A flow cytometer such as the one used for this project consists of four main systems: a fluidic system which delivers the sample into the flow cytometer, an optical system which measures properties of the sample, an electronic system which detects signals generated for a sample, processes data and allows for automation of sample measurement and a computer interface which allows the user to control the flow cytometer and to store and analyse data (Shapiro, 2003). Figure 2.2 shows a generalised picture of the major components of a flow cytometer.

The fluidic system consists of the sample of cells suspended in a flow of sheath fluid. The rate of sheath flow ensures cells are hydrodynamically focused into single file as they pass through the flow cell and then on, to be sorted or to the waste system. The optical system consists of the flow cell which is illuminated by a focused light source such as an argon (488 nm) or helium neon laser (544

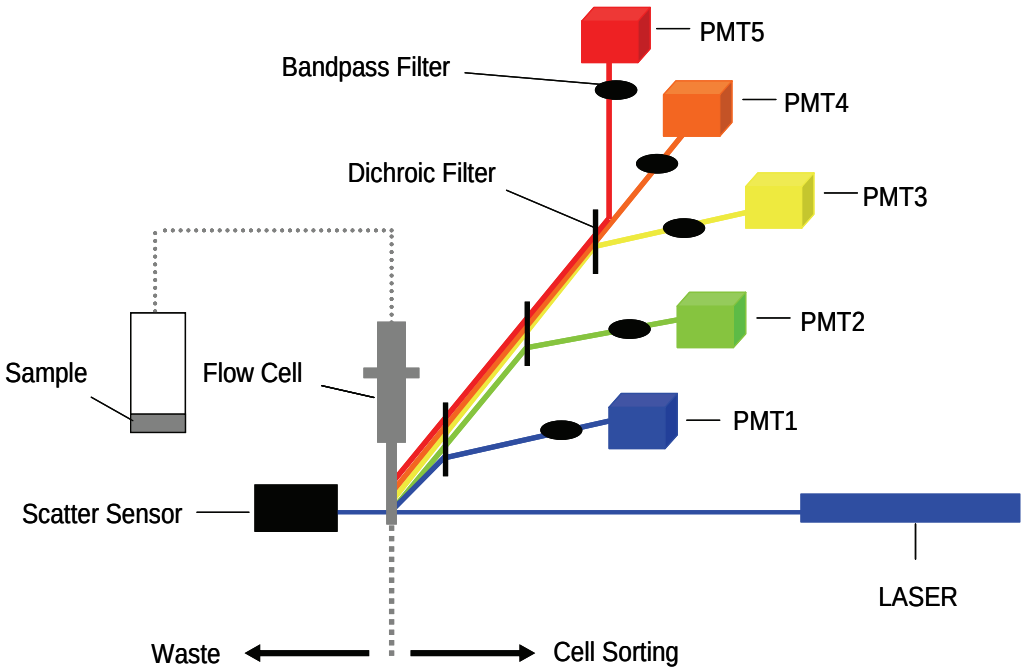

Figure 2.2 Generalised view of the major components of a flow cytometer. The fluidic system is shown as a grey dotted line running through the flow cell. The filters are shown as black ellipses for band pass filters and black lines for dichroic filters and photomultiplier tubes (PMT) are shown as coloured cubes (adapted from Shapiro, 2003).

nm or 633 nm) (Shapiro, 2003). As a cell passes through the beam, the laser light is scattered in different directions. Scattered light is filtered using two different types of filter:

Dichroic filters allow light of long wavelengths to pass through them while short wavelengths of light are reflected. A dichroic filter of 500 nm separates scattered light by reflecting it towards one detector, whilst the fluorescent light is

transmitted to another detector (Shapiro, 2003).

Band pass filters only allow light of a specific wavelength, or narrow band of wavelengths, to pass through. In this way fluorescence from a single cellular component or added fluorophore can be isolated and quantified. The filtered light signal is detected by photodetectors which detect light of specific wavelengths; blue (488 nm), green (525 nm), orange (575 nm), red (635 nm) and also by photomultiplier tubes which amplify its signal so it can be analysed by the computer. Flow cytometry can be used to measure parameters of cells using light scatter patterns and fluorophores to measure cell physiology (Shapiro, 2003).

Light scattering occurs when the incident light of the laser interacts with a cell. Light is scattered as forward angle light scattering (FALS) between 0.5° to 5°, and can give a rough estimation of cell size, and as right angle light scattering (RALS) at 90° which can determine the presence of the internal granular structure of a cell (Shapiro, 2003).

Cells can be labelled with a fluorophore which will absorb light of a specific wavelength emitted by the laser. Provided the absorbed light is of a wavelength that is shorter or equal to the wavelength of the emitted light the fluorophore will reach an excited state during which an electron will be raised to a higher energy level. The difference in wavelength between absorption and emission is known as the Stokes shift and typically lasts only for a few nanoseconds (Shapiro, 2003). Table 2.2 shows some of the parameters measurable with a flow cytometer.

Parameter	Measurement technique
Internal structural cellular parameter (no fluorophore)	
Cell size	Electronic (DC) impedance, extinction, small angle light scattering, image analysis
Cell shape	Pulse shape analysis (flow), image analysis
Cytoplasmic granularity	Large angle light scattering, electronic (AC) impedance
Birefringence (e.g., of blood eosinophil granules)	Polarised light scattering, absorption
Haemoglobin, photosynthetic pigments, porphyrins	Absorption, fluorescence, multiangle light scattering
Internal functional cellular parameter (no fluorophore)	
Redox state	Fluorescence (endogenous pyridine and flavin nucleotides)
External structural cellular parameter (fluorophore)	
DNA content	Fluorescence (propidium, DAPI, Hoechst dyes)
DNA base ratio	Fluorescence (A-T and G-C preference dyes e.g., Hoechst333258 and chromycinA
Nucleic acid sequence	Fluorescence (labelled oligonucleotides)
Chromatin structure	Fluorescence (fluorochromes after DNA denaturation)
RNA content (single and double stranded)	Fluorescence (Acridine orange, pyronin Y)
Total protein	Fluorescence (covalent or ionic bonded acid dyes)
Basic protein	Fluorescence (acid dyes at high pH)
Surface / intracellular antigens	Fluorescence, scattering (labelled antibodies)
Surface sugars (lectin binding sites)	Fluorescence (labelled lectins)
Lipids	Fluorescence (Nile red)
External functional cellular parameter (fluorophore)	
Surface / intracellular receptors	Fluorescence (labelled ligands)
Surface charge	Fluorescence (labelled polyionic molecules)

Membrane integrity	Fluorescence (propidium, fluroscein diacetate [FDA], absorpsion or scattering (trypan blue)
Membrane fusion / turnover	Fluorescence (labelled long chain fatty acid derivatives)
Membrane organization (phospholipids, etc.)	Fluorescence (annexin V, merocyanine 540)
Membrane fluidity or microviscosity	Fluorescence polarization (diphenylhexatriene)
Membrane permeability (dye / drug uptake / efflux)	Fluorescence (anthracyclines, rhodamind 123, cyanines)
Endocytosis	Fluorescence (labelled microbeads or bacteria)
Generation number	Fluorescence (labelled lipophilic or covalently bonded tracking dyes)
Cytoskeletal organisation	Fluorescence (NBD-phallacidin)
Enzyme activity	Fluorescence, absorption (fluorogenic / chromogenic substrates)
Oxidative metabolism	Fluorescence (dichlorofluoroscein)
Sulphydryl groups / glutathione	Fluorescence (bimanes)
DNA synthesis	Fluorescence (anti-BrUdr antibodies, labelled nucleotides)
DNA degradation (as in apoptosis)	Fluorescence (labelled nucleotides)
"Structuredness of cytoplasmic matrix"	Fluorescence (fluroscein diacetate [FDA])
Cytoplasmic / mitochondrial membrane potential	Fluorescence (cyanines, rhodamine 123, oxonols)
"Membrane-bound" Ca^{2+}	Fluorescence (chlortetracycline)
Cytoplasmic [Ca^{2+}]	Fluorescence ratio (indo-1), fluorescence (fluo-3)
Intracellular pH	Fluorescence ratio (BCECF, SNARF-1)
Gene expression	Fluorescence (reporter proteins)

Table 2.2 Cellular parameters measurable using flow cytometry (Shapiro, 2003).

Two of the fluorophores used in this study measure microbial viability as a function of cytoplasmic membrane potential; bis-(1, 3-dibutylbarbituric acid) trimethine oxonol ($DiBac_4(3)$) and 3, 3'-dihexyloxacarbocyanine iodide ($DiOC_6(3)$).

These charged fluorophores are sufficiently lipophilic to pass through the lipid bilayer and partition themselves across the cytoplasmic membrane in response to the potential gradient (Shapiro, 2003).

$DiBac_4(3)$ is a lipophilic anionic oxonol with an excitation wavelength of 490 nm often referred to as Bis-oxonol although this could describe a number of other compounds which are also oxonols (Figure 2.3). Due to its negative charge it is excluded from the cytoplasmic membrane if the cytoplasmic membrane potential is maintained (Shapiro, 2003). However a reduction in cytoplasmic membrane potential allows $DiBac_4(3)$ to bind to intracellular macromolecules and emit green fluorescence (Deere *et al*., 1995).

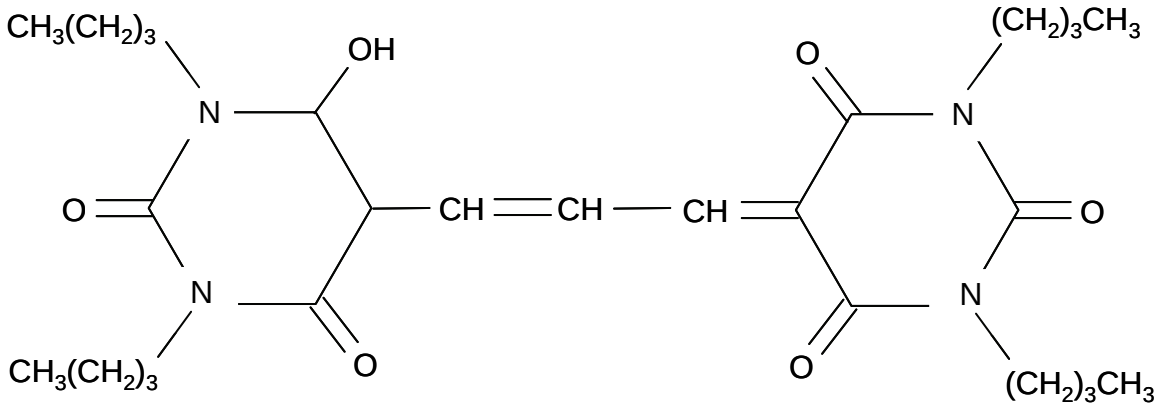

Figure 2.3 Bis-(1, 3-dibutylbarbituric acid) trimethine oxonol ($DiBac_4(3)$) (Shapiro, 2000).

$DiOC_6(3)$ is a lipophilic cationic carbocyanine dye with an excitation wavelength of 484 nm. $DiOC_6(3)$ is described as a slow response dye. Due to its positive charge it concentrates inside cells which can maintain a cytoplasmic

membrane potential and emits green fluorescence (Shapiro, 2003) (Figure 2.4). Carbocyanine dyes can inhibit respiration and can be toxic at high concentrations (Miller *et al*., 1978).

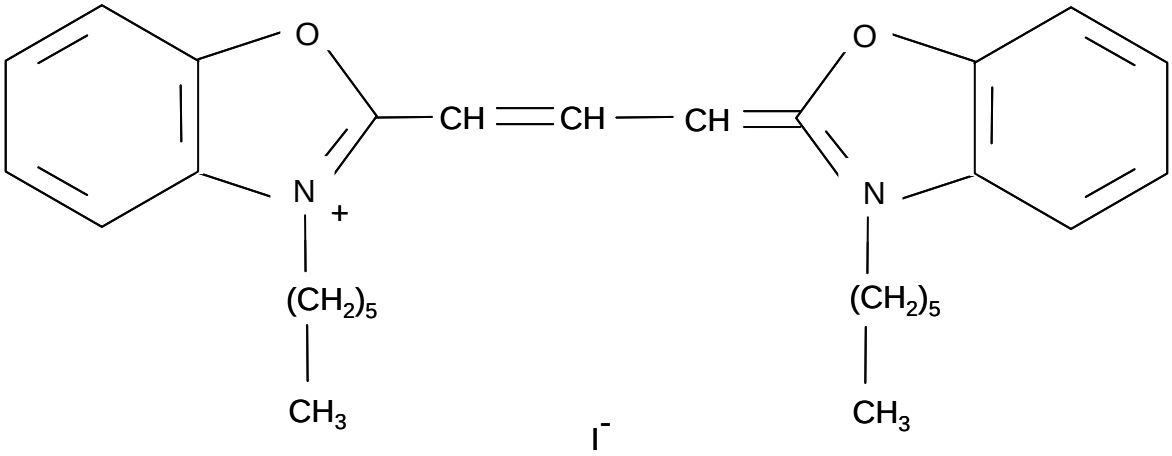

Figure 2.4 3, 3'-dihexyloxacarbocyanine iodide ($DiOC_6(3)$) (Shapiro, 2000).

REDOX sensor green reagent is a relatively new product and information regarding its chemistry and mode of action is limited. It is known to be a fluorogenic dye which emits green fluorescence when modified by energy dependent reductase enzymes located in the bacterial electron transport chain (Gray *et al*., 2005). REDOX sensor green reagent measures microbial cell viability as a product of metabolic activity within the cell, although there is some contention about whether reductase enzymes remain active even after a cell loses its cytoplasmic membrane integrity and has lost viability.

Propidium Iodide (PI) contains a phenanthridinium ring and a propyl group with a quaternary ammonium as its N-alkyl group giving it a double positive charge and as such cannot enter the cytoplasmic membrane of viable cells (Shapiro, 2003), (Figure 2.5). It is commonly used to detect dead or dying cells whose cytoplasmic membrane integrity is compromised. Inside a cell it is a powerful intercalating agent of double stranded nucleic acids and fluoresces red with a maximum excitation wavelength of 535 nm (Shapiro, 2003). It is commonly used in addition to the above green fluorescent stains so that polarised, de-polarised and permeablised cells can be identified within a microbial population (Hewitt *et al*., 1998, 2001, 2004).

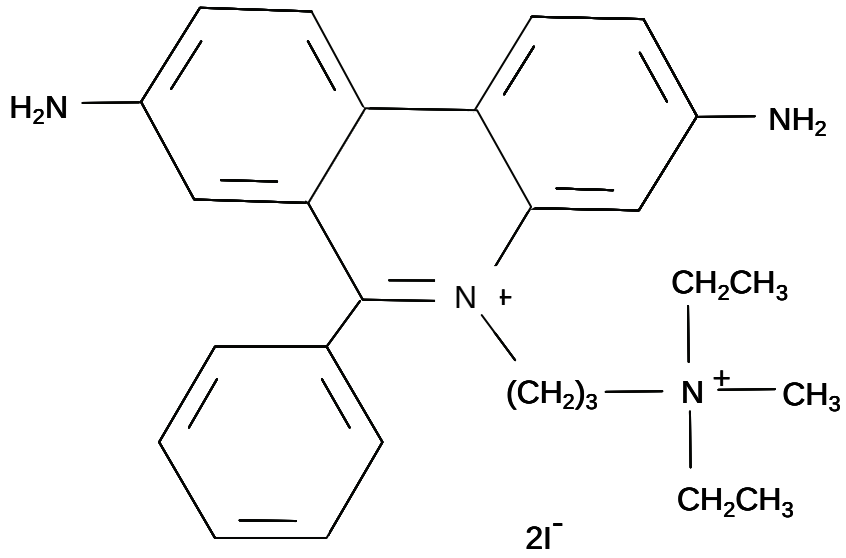

Figure 2.5 Phenanthridinium, 3,8-diamino-5-[3-(diethylmethylammonio) propyl]-6-phenyl-, di-iodide (Propidium Iodide) (Shapiro, 2000).

Cells that have been interrogated in the flow cell emerge in the stream of sheath fluid and can either be discarded as waste or sorted and further analysed. The stream of fluid exiting the flow cell is broken into droplets because a stream of fluid emerging from an orifice is hydrodynamically unstable, if the system has been finely calibrated each droplet will contain a single cell. As each of the droplets is forming it is given a positive, negative or neutral charge by a voltage pulse. The charged and uncharged droplets are then passed between two high voltage charged deflecting plates which can deflect the droplets to the left or right of the original stream (Shapiro, 2003). The charge given to each droplet is controlled by circuitry which gives each droplet a charge based on the parameters chosen by the user. Sorting is accomplished by selecting a specific parameter on the computer such as fluorescence intensity or light scattering properties. Droplets of interest are deposited in a collection vessel or on to a plate whilst the remaining droplets are collected as waste. Figure 2.6 shows the principles of droplet sorting.

There are several reasons why flow cytometry is advantageous to the study of cells. It allows real time analysis of cells during an experiment or process allowing at line modifications to be made if required saving time and money. It is a high throughput technique allowing analysis of tens of thousands of cells per second (Shapiro, 2003). Cells can be counted rapidly with the use of ratiometric counting beads. With the ever increasing number of fluorophores available more and more cellular characteristics can be analysed. Cells can be sorted and

analysed in further detail. Despite this flow cytometry is not as widespread a technique as one might expect and this could be due to a number of reasons. Firstly the equipment is very expensive, and secondly it is complicated and requires the operator to be highly trained.

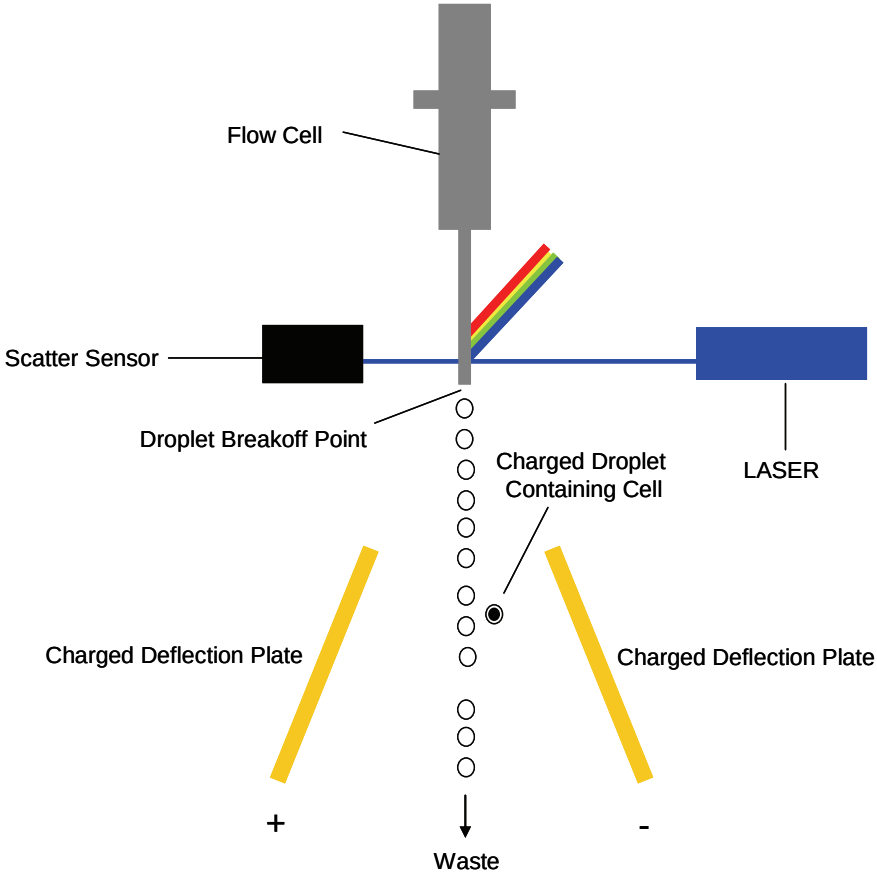

Figure 2.6 Schematic diagram of droplet cell sorting. The laser interacts with the cell occupying the flow cell and if the cell meets the criteria for sorting the flow stream is charged just before the break off point of the droplet containing the target cell. The charged droplet is then deflected by the charged deflection plates into a collection tube or plate (adapted from Shapiro, 2003).

2.9 Aims and Objectives of this study

Excellent product quality coupled with a high productivity and yield is the ultimate goal for any research and development programme leading to the large-scale production of microbial based products at the commercial scale. Product quality is directly linked to the batch to batch reproducibility of a process. This work aimed to investigate the cryopreservation of *B. licheniformis* cell banks used as inoculum for α-amylase producing 5 L batch fermentations. The quality of the inoculum is often overlooked, which is surprising since it can have a significant effect on overall process performance (Gnoth *et al*., 2007, Hornbæk *et al*., 2002, Hornbæk *et al*., 2004, Webb *et al*., 1993). The effect of the presence of various cryopreservants on final fermentation performance measured in terms of biomass and α-amylase concentration were investigated using optical density, dry cell weight, colony forming units, and multi-parameter flow cytometry. This work aimed to use multi-parameter flow cytometry to determine the physiological state of individual microbial cells, and to visualise how different sub-populations of microbial cells develop with time throughout the fermentation process. Multi-parameter flow cytometry was the ideal choice for measuring microbial physiology because it allowed measurements to be made in real time while the fermentation was in progress, it is a high throughput technique, different fluorophores can be used to provide detailed information about microbial cell physiology and microbial cells of specific interest can be sorted and analysed separately in more detail.

Chapter 3

Materials and Methods

3.1 Micro-organisms

3.1.1 *Bacillus cereus* NCTC11143

B. cereus NCTC11143 was obtained from the United Kingdom National Culture Collection (UKNCC) (Colindale, London). As a non-industrial strain it lacks robust growth characteristics and it is sensitive to slight changes in growth conditions leading to increased evidence of population heterogeneity when studied with multi-parameter flow cytometry. This makes it an excellent candidate to evaluate fluorescent dyes which are designed to measure microbial viability. It was plated onto nutrient agar plates (Oxoid, Basingstoke, Hampshire) made according to manufacturer's instructions and stored at 4 °C until required.

3.1.2 *Bacillus licheniformis* SJ4628

B. licheniformis SJ4628 was obtained from Novozymes A/S (Bagsvaerd, Denmark). It was stored as cell banks in 1.5 mL Eppendorf tubes and cultured by growing in the yeast malt broth described here as the medium for shake flask fermentation to an optical density of 1.0 at 600 nm (OD_{600nm}) followed by addition of glycerol to a final concentration of 20% v/v in 1 mL and stored at -

80 °C until required. For experiments using different cryopreservant chemicals cell banks were prepared with 25% v/v glycerol, 15% v/v DMSO, 20% v/v Tween 80 (concentrations determined from the shake flask experiments in Chapter 4). A cell bank was also prepared which contained no cryopreservant (1 mL cells in medium).

3.2 Media

3.2.1 *Bacillus cereus* NCTC11143

B. cereus NCTC11143 was cultured using nutrient agar and nutrient broth (Oxoid, Basingstoke, Hampshire) made according to the manufacturers instructions.

3.2.2 *Bacillus licheniformis* SJ4628

B. licheniformis SJ4628 was cultured using the following buffer and medium:

3.2.2.1 M9 Buffer

M9 buffer was prepared (composition in gL^{-1}: Na_2HPO_4, 6; NaCl, 5; KH_2PO_4, 3) and made up to 1 L with distilled water. 1 mL of 1 M $MgSO_4$ was added aseptically after autoclaving.

3.2.2.2 Yeast malt broth (YM broth)

YM broth was prepared (composition in gL^{-1}: yeast malt extract powder, 40; yeast extract powder, 20) and supplemented with 3mL of 2% polypropylene glycol 2025. The solution was made up to 1 L with distilled water before adjusting pH to 7.0 with 2 M NaOH and autoclaving.

3.2.2.3 Yeast malt agar (YM agar)

YM agar was prepared (composition in gL^{-1}: malt extract powder, 40; yeast extract powder, 20; M Lab agar powder, 20) and made up to 1 L with distilled water and heated to 100 °C until fully dissolved followed by autoclaving.

3.2.2.4 Batch medium

Batch medium was prepared (composition in gL^{-1}: glucose, 92.63; yeast extract powder*, 20; $NH_4 2HPO_4$*, 16; KH_2PO_4, 1.5; $MgSO_4.7H_2O$, 0.5; $CaCl.2H_2O$, 0.45; $MnSO_2.4H_2O$, 0.04; $ZnSO_4.7H_2O$, 0.02; $FeSO_4.7H_2O$, 0.02; $CuSO_4.5H_2O$, 0.01; $Na_2MoO_4.2H_2O$, 0.002) and supplemented with 3mL of polypropylene glycol 2025.

* Autoclave each of these separately to prevent the Maillard reaction and recombine with the other components aseptically once cool.

3.2.2.5 Fed batch medium

3.2.2.5.1 Additional feed

Additional feed for the fed batch fermentations was prepared (composition in gL^{-1}: glucose, 500; yeast extract powder*, 20; NH_42HPO_4*, 16; KH_2PO_4, 1.5; $MgSO_4.7H_2O$, 0.5; $CaCl.2H_2O$, 0.45; $MnSO_2.4H_2O$, 0.04; $ZnSO_4.7H_2O$, 0.02; $FeSO_4.7H_2O$, 0.02, $CuSO_4.5H_2O$, 0.01; $Na_2MoO_4.2H_2O$, 0.002).

* Autoclave each of these separately to prevent the Maillard reaction and recombine with the other components aseptically once cool.

3.2.2.5.2 Main fermentation medium

The main fermentation medium was prepared (composition in gL^{-1}: yeast extract powder*, 20; $NH_4 2HPO_4$*, 16; glucose, 5; KH_2PO_4, 1.5; $MgSO_4.7H_2O$, 0.5; $CaCl.2H_2O$, 0.45; $MnSO_2.4H_2O$, 0.04; $ZnSO_4.7H_2O$, 0.02; $FeSO_4.7H_2O$, 0.02; $CuSO_4.5H_2O$, 0.01; $Na_2MoO_4.2H_2O$, 0.002) and supplemented with 3 mL polypropylene glycol 2025.

* Autoclave each of these separately to prevent the Maillard reaction and recombine with the other components aseptically once cool.

3.3 Sterilisation

All media and apparatus were heat sterilised in an autoclave at 121 °C and 1 atm for 15 min when an aseptic environment was required.

3.4 Fermentation processes

3.4.1 Inoculum preparation

3.4.1.1 *Bacillus cereus* NCTC11143

The nutrient agar plate containing the stock culture was removed from the fridge (4 °C) and placed in a 37 °C incubator for at least 1 hour prior to inoculum preparation.

An inoculation loop was used to transfer 2 loops full of culture into 500 mL baffled Erlenmeyer shake flasks containing 50 mL of sterilised nutrient broth. The inoculated shake flasks were placed in a shaking incubator at 37 °C and 200 rpm for 16 hours.

3.4.1.2 *B. licheniformis* SJ4628

The bacterial stock was removed from the freezer (-80 °C) and defrosted at room temperature for 10 mins. The 1 mL of stock culture was then combined with 9 mL of M9 buffer in a 10 mL syringe and inverted to ensure mixing. 5 mL of culture was then injected into a 500 mL side arm flask (Figure 3.1) which contained 200 mL of YM agar. The flask was placed into an incubator at 37 °C for 16 hours. After 16 hours 20 mL of M9 buffer was injected into the flask and the magnetic stirrer bar was released onto the surface of the agar. The flask was then placed on a magnetic stirrer and stirred until well mixed. Culture was then removed from the flask using a syringe and used to inoculate additional shake

flasks. This procedure was modified from a standard operating protocol used by Novozymes A/S (Bagsværd, Denmark).

Figure 3.1 Side arm baffled 500 mL conical flask.

3.5 Shake flask fermentation

3.5.1 Shake flask geometry

All shake flask fermentations were carried out using 500 mL baffled Erlenmeyer shake flasks (Figure 3.2).

Figure 3.2 Baffled 500 mL Erlenmeyer shake flasks.

3.5.1.1 *B. cereus* NCTC11143

B. cereus NCTC11143 was grown in 500 mL baffled Erlenmeyer shake flasks containing 50 mL of nutrient broth and 1 mL of inoculum and shaken

in an incubator at 37 °C and 200 rpm. Each experiment was duplicated.

3.5.1.2 *Bacillus licheniformis* SJ4628

B. licheniformis SJ4628 was grown in 500 mL baffled Erlenmeyer shake flasks containing 50 mL of YM broth with 1 mL of inoculum and shaken in an incubator at 37 °C and 200 rpm. Each experiment was duplicated. For the shake flask experiments containing different cryopreservant chemicals the YM broth was supplemented by the correct concentration of glycerol (20% v/v or 25% v/v), DMSO (15% v/v) or Tween 80 (20% v/v).

3.6 Batch and fed batch fermentations

3.6.1 Bioreactor geometry

Laboratory scale bioreactors were used for each experiment (Electrolab, Tewksbury, UK). The main reactor vessel comprises a glass vessel (160 mm inside diameter and 300 mm high) with a 5 L total volume and 4 L working volume. The stainless steel lid of the reactor contains a drive motor connection, a temperature probe, a condenser air outlet, a cooling finger and addition ports for inoculum, media, acid, base and antifoam, as well as ports for pH and dissolved oxygen probes. Mixing is achieved by two six-flat bladed paddle type Rushton impellers (820 mm diameter) spaced 80 mm apart. The lowest impeller was located 80 mm from the bottom of the vessel.

Each bioreactor contains four 90° baffles (15 mm width) equally spaced around the vessel to prevent the formation of vortices. Air was supplied to the reactor through an “L” shaped air sparger located between the lowest impeller and the vessel bottom. Incoming air was passed through a 0.2 µm PTFE filter to ensure sterility. Air was added to the reactor at a ratio of 1:1 (1 $Lmin^{-1}$ of air to each litre of medium). The outgoing gases from the bioreactor were passed through a condenser to prevent water loss by evaporation and filtered through a 0.2 µm filter.

3.6.2 On-line measurement and control

The agitator speed (rpm), DOT (% saturation), pH, antifoam and temperature and feed addition were all controlled by the bioreactor computer. DOT was controlled above the 90% saturation level by increasing agitator speed as required. DOT was monitored with a DOT probe (Oxyprobe, Broadley-James, USA). The pH was controlled at 7.0 by addition of 2 M NaOH and 2 M H_3PO_4 on demand. The pH was monitored by a pH probe (FermProbe pH electrodes, Broadley-James, USA). Temperature was maintained at 37 °C by a heating jacket and monitored with a temperature probe inserted into a sealed pocket in the lid of the reactor which passes down to below the level of the medium. Cooling was achieved by a cooled cold finger tube. Foaming was prevented by adding 2% v/v polypropylene glycol 2025 for 2 seconds of every minute. All measured online parameters were recorded (Version lite plus 1.1, Electrolab, UK).

3.6.2.1 Batch fermentations

The inoculum for the batch fermentations were obtained from 3 h shake flask fermentations in YM broth. A 10% v/v inoculum with an optical density at 600 nm of 1.0 was added to the bioreactor aseptically.

3.6.2.2 Fed batch fermentations

An exponential feeding profile was calculated from the following equation (Strandberg *et al*., 1994):

$$F = \left(\frac{1}{s} \right) \times \left(\frac{\mu}{Y_{xs}} + m \right) \times X_0 \times e^{\mu t}$$

where F is the glucose solution feed rate (Lh^{-1}); s is the substrate concentration in the feed solution (gL^{-1}); μ is the desired specific growth rate (h^{-1}); Y_{xs} is the maximum biomass yield with a limiting substrate (gg^{-1}); X_0 is the initial amount of biomass at the start of feeding (g); m, is the maintenance coefficient ($gg^{-1}h^{-1}$); t is the time after feeding commences (h). In this way feed rate was increased every hour for 7 hours after which the feed rate was held constant for the remainder of

the fermentation. Following correspondence with Novozymes A/S (Bagsvaerd, Denmark) a value of 0.5 gg^{-1} was used for the yield coefficient (Y_{xs}) and a value of 0.04 $gg^{-1}h^{-1}$ as the maintenance coefficient (m).

3.7 Analytical techniques

3.7.1 Optical density (OD_{600nm})

Optical density was measured at 600 nm in a dual beam spectrophotometer (UV-VIS430, Kontron, UK) against a phosphate buffered saline (PBS) blank.

3.7.2 Viable count (Colony forming units per mL ($CFUmL^{-1}$))

The viable cell counts were obtained by serial dilutions of a sample in PBS and plated onto agar plates (Section 3.2). After 12 h incubation at 37 °C incubator plates within the range of 30-300 colonies were counted and $CFUmL^{-1}$ calculated.

3.7.3 Dry cell weight (DCW (gL^{-1}))

The dry cell weight (DCW (gL^{-1})) was measured by taking 4 Eppendorf tubes which had been dried for 24 h in an oven at 90 °C, and allowed to cool before weighing. A 1 mL sample of culture was pipetted into each Eppendorf tube and then they were centrifuged at 13000 rpm for 10 mins. The supernatant was poured away and the pellet washed in filter sterilised PBS and centrifuged again.

The PBS was poured away leaving just the pellet. The open Eppendorfs were dried for 24 h in an oven at 90 °C and allowed to cool before being re-weighed.

3.7.4 Multi-parameter flow cytometry

All flow cytometry results were analysed using a Coulter Epics Elite analyser or sorter (Coulter Electronics, High Wycombe, UK). An argon laser was used at 15 mW and 488 nm excitation. The sheath fluid that was used was azide free balanced electrolyte solution (Isoton II, Beckman Coulter, UK).

3.7.4.1 Cleaning of the flow cytometer

Optimal performance was achieved by copious cleaning of the flow cell. 5mL of each of the following were run through the equipment: 99.5% ethanol, sodium hypochlorite, Coulter clenz (Beckman Coulter, UK) followed by filter sterilised PBS solution.

3.7.4.2 Alignment of the flow cytometer

For accurate results it was essential that the beam of the laser was aligned and focused on the analysis point in the flow cell as the cells travel through it. A first coarse alignment was achieved by using 10 µm diameter Fluorocheck spheres (Beckman Coulter, UK) at a data rate of 500 particles per second. Fine alignment was then carried out with 0.5 µm diameter Flow check high intensity

green alignment grade particles (Polysciences Europe Gmbh, Germany) at a data rate of 1500 particles per second. The plot of forward angle light scatter (FALS) against right angle light scatter (RALS or PMT1) and photomultiplier tubes (PMT): PMT2, PMT3, PMT4 were used to check for normal distribution where a sharp and high signal was indicative of good alignment and the ½ CV (coefficient of variance) values were approximately the same value as stated by the manufacturer. All fluoro-spheres were stored at 4 °C and fresh beads used each time.

3.7.4.3 Fluorophores used for viability measurements

The green fluorescent dyes: Bis-oxonol dye bis-(1,3-dibutylbarbituric acid) trimethine oxonol ($DiBac_4(3)$), 3,3'-dihexyloxacarbocyanine iodide ($DiOC_6(3)$) and REDOX sensor green reagent and the red fluorescent counter stain Propidium Iodide (PI) were obtained from Molecular Probes UK and were used to measure cellular viability with flow cytometry and fluorescence microscopy. Stock solutions of each dye were prepared as follows; $DiBac_4(3)$, 1 $mgmL^{-1}$ in dimethyl sulphoxide (DMSO), $DiOC_6(3)$, 1 $mgmL^{-1}$ in DMSO, REDOX sensor green reagent was diluted straight from the vial supplied by the manufacturer and PI 1 $mgmL^{-1}$. Stock solutions were stored at -20 °C until required and then defrosted before use. Working concentrations were prepared from the stock solutions by dilution with 0.2 µm filter sterilised phosphate buffered saline (PBS) solution to the following concentrations; $DiBac_4(3)$ 10 μgmL^{-1}, $DiOC_6(3)$, REDOX sensor

green reagent and PI 100 μgmL^{-1}. The optical filters were set up as standard for the Coulter Epics Elite analyser. The fermentation sample was diluted with 0.2 µm filter sterilised PBS as appropriate and the following volumes of dyes used in the following combinations: 20 µL of $DiBac_4(3)$ with 10 µL of PI, 20 µL of $DiOC_6(3)$ with 10 µL of PI and 1 µL of REDOX sensor green reagent with 10 µL of PI.

3.7.4.4 Analysis and data acquisition

10,000 events (particles) were obtained at a data rate of between 600-1,000 per second and the bacterial population of interest separated from background noise (particulate or electronic) by using the discrimination software. All data files were analysed using WinMDI (Joseph Trotter, Salk Institute for Biological Studies, La Jolla, California, USA) which can be downloaded from the following website: http://www.cyto.purdue.edu/flowcyt/software/Winmdi.htm

3.7.4.5 Flow cytometry controls

To ensure that the fluorophores used for flow cytometry were working optimally a series of control experiments were carried out which were ultimately compared with experimental data. A sample of cells during the exponential growth phase was heat treated at 60 °C for 30 seconds and then stained with a mixture of each of the following: $DiBac_4(3)$ and PI, $DiOC_6(3)$ and PI or REDOX

sensor green reagent and PI. Three physiological states could then be identified from the heat stressed bacterial populations; polarised cells, cells with a de-polarised cytoplasmic membrane and cells with a de-polarised and permeabilised cytoplasmic membrane. This method for generating positively stained controls were based on the method used for studying *Escherichia coli* W3110 cells (Hewitt *et al*., 1998).

For the shake flask experiments with cells grown in different concentrations of glycerol additional controls were required as the dead cell population for cells stained with $DiBac_4(3)$ and PI appeared in the lower right quadrant of the flow cytometry plot instead of in the top right quadrant (Figure 4.16 and 4.18) where it would normally be. Figure 3.3a to c shows the control experiments which were prepared by taking a sample of exponentially growing cells and heat treating them at 60 °C for 1 minute to ensure that they are fully killed. The dead cells were then mixed in equal volume with a sample of exponentially growing healthy cells. The cell mixture was then treated with 30% v/v glycerol.

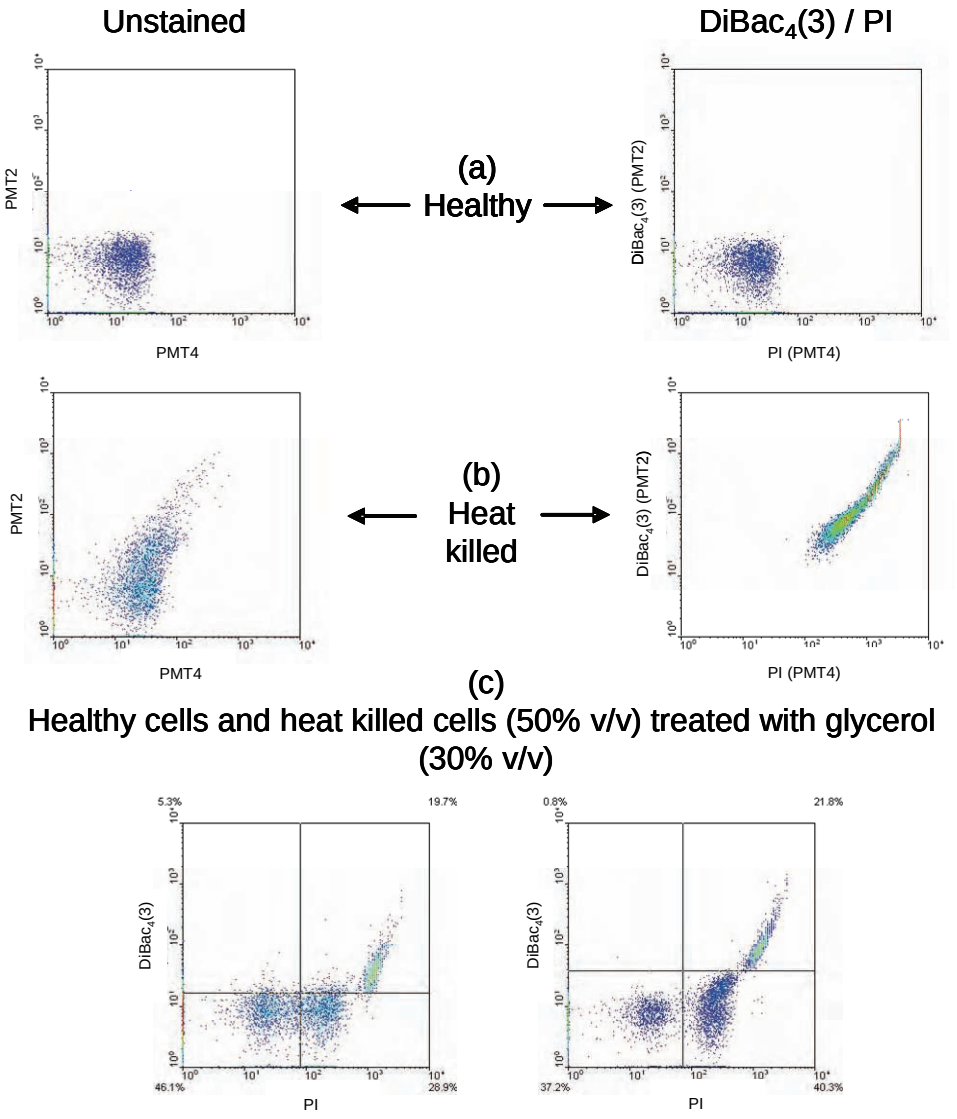

Figure 3.3 Control samples for the shake flask experiments containing different concentrations of glycerol. (a) Healthy cells unstained and stained with $DiBac_4(3)$ /PI. (b) Heat killed cells unstained and stained with $DiBac_4(3)$ /PI. (c) A 50% v/v mixture of healthy and heat killed cells treated with 30% v/v glycerol. The heat killed cells appear closer to the top right quadrant and the cells killed with 30% v/v glycerol are closer to the bottom right quadrant indicating the effect of glycerol on $DiBac_4(3)$ / PI.

3.7.5 High Pressure Liquid Chromatography (HPLC) analysis

All HPLC results were analysed using a Cecil CE4200 ultraviolet (UV) analyser and a Cecil 4700 refractive index (RI) analyser (Cecil Instruments, Cambridge, UK). The UV samples were detected at 210 nm. An Aminex BIO-RAD HPX87H column was used (BIO-RAD, Hemel Hempstead, UK). The mobile phase was degassed 0.005 M sulphuric acid made using filter sterile distilled water with a flow rate of 1.2 $mLmin^{-1}$ and an operating temperature of 60 °C.

3.7.5.1 Cleaning of the HPLC machine

To prevent the build up of sulphuric acid crystalline deposits the HPLC column was disconnected and the HPLC machine was flushed through with sterilised distilled water for at least 20 mins after use. Before running samples mobile phase was run through the column and the HPLC machine until a stable baseline was achieved.

3.7.5.2 Analysis and data acquisition

Standard solutions of 1.0 M, 0.5 M, 0.25 M and 0.125 M concentration were prepared of compounds known to be produced during microbial fermentative metabolism; lactic acid, ethanol, formate, acetate, malic acid, succinic acid, propionic acid, acetone, acetoin, 2,3-butandiol, isopropanol, pyruvic acid and glucose as the principal carbon source. The peaks generated from these

standards were analysed using Powerstream chromatography analysis software (Cecil Instruments, Cambridge, UK) and calibration curves produced. Samples from the fermentation were centrifuged at 4,000 rpm for 15 mins and the supernatant decanted and frozen at -20 °C for analysis. Later samples were defrosted at room temperature and filtered using a 0. 2 µm filter before being run to remove as much sediment as possible from the samples and avoid blocking the column. The peaks generated by the samples were then analysed by the Powerstream software and compared to the calibration curves of the standards.

3.7.6 α-amylase assay

Samples from the fermentation were centrifuged at 4,000 rpm for 15 mins and the supernatant decanted and frozen at -20 °C for analysis. Samples were defrosted at room temperature and the α-amylase concentration was determined with an AMYL analytical kit (Roche, Burgess Hill, UK), according to the manufacturers instructions.

Chapter 4

Results and Discussion

Shake Flask Fermentation

4.1 Growth and physiological characterisation of *Bacillus cereus* NCTC11143 and *Bacillus licheniformis* SJ4628 during shake flask fermentations.

Differences exist between shake flasks and stirred tank bioreactors of any size; oxygen transfer, pH control, nutrient gradients, shear forces and the effects of sterilisation are all difficult to mimic in a shake flask. However, they are easy to prepare, they can be run in large numbers and are cheaper than larger bioreactors, making them an ideal choice for testing the ability of fluorescent dyes for measuring microbial physiology.

The aim of the work in this chapter was to determine the growth and physiological characteristics of *B. cereus* NCTC11143 and *B. licheniformis* SJ4628 during shake flask fermentations, and to evaluate three fluorescent dyes used in multi-parameter flow cytometry for determining microbial viability, namely $DiBac_4(3)$, $DiOC_6(3)$ and REDOX sensor green reagent all counter stained with PI. For all the analyses in this thesis reproductively viable cells are taken to be cells which are able to reproduce under specific conditions

and are detected as colony forming units per mL ($CFUmL^{-1}$). The results for flow cytometry are expressed as percentage numbers in which the cells and are grouped as polarised, de-polarised and permeablised with respect to the integrity of their cytoplasmic membrane. Each population of cells appears in a different location on a density plot for each of the three fluorophores. Figure 4.1a to c shows where a given population of cells should have appeared according to the manufacturer's information (Molecular Probes UK). Both $DiBac_4(3)$ and $DiOC_6(3)$ measure viability with respect to cytoplasmic membrane polarisation, and REDOX sensor green reagent with respect to the activity of enzymes in the respiratory chain (Gray *et al*., 2005). Propidium Iodide measures permeability of the cytoplasmic membrane (Shapiro, 2003).

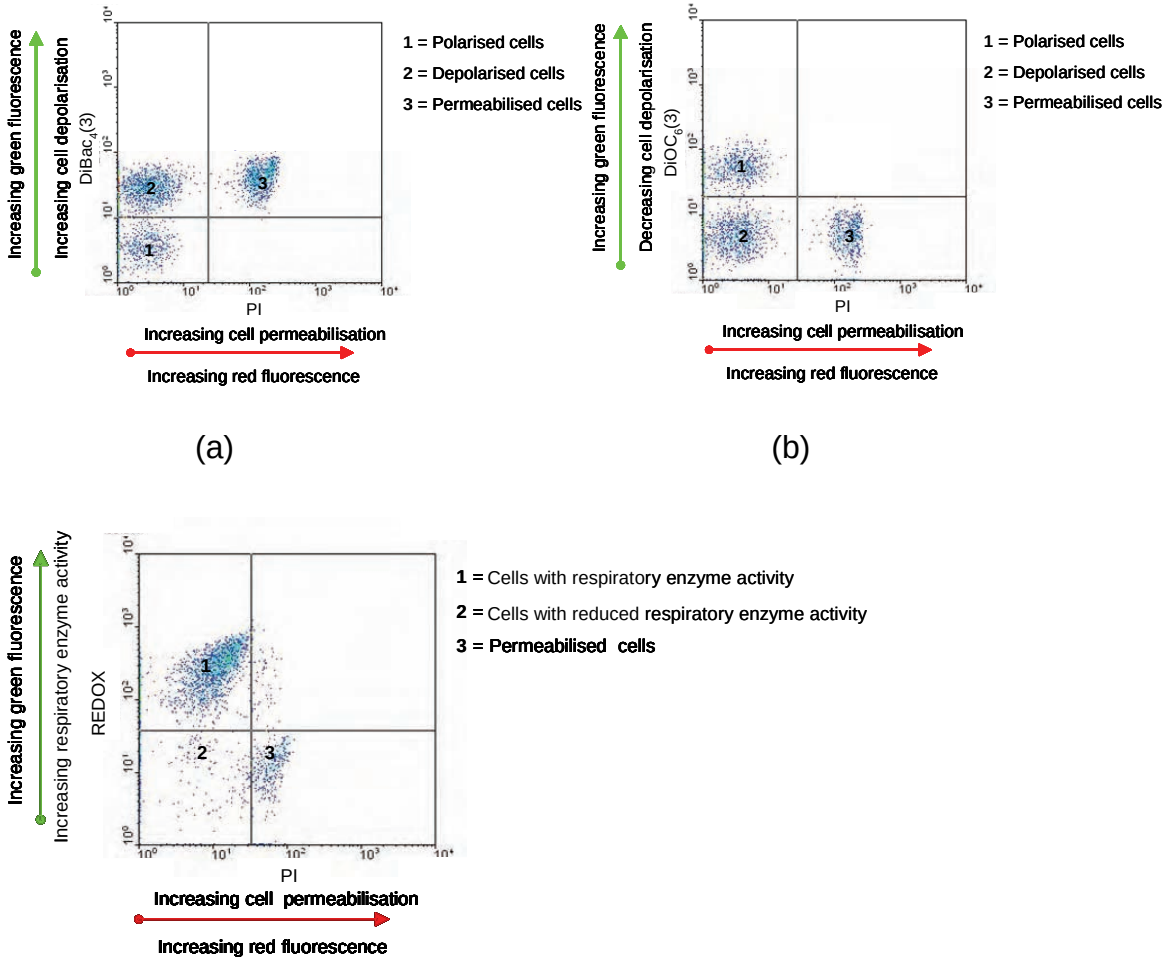

Figure 4.1 Density plot showing how cells stained with each of the three fluorescent dyes should appear according to the manufactures information (Molecular Probes UK); (a) $DiBac_4(3)$ and PI, (b) $DiOC_6(3)$ and PI and (c) REDOX sensor green reagent and PI. According to the manufacturers instructions only populations 1 and 3 are detectable with REDOX sensor green reagent and PI, population 2 has been labelled here as it is clear from this work that more than two populations are detectable with REDOX and PI.

All shake flask experiments were accurately reproduced three times using the methods outlined in Chapter 3.

4.1.1 *Bacillus cereus* NCTC11143 growing in nutrient broth

One of the aims for this work was to determine the physiological effects of cryopreservation on microbial fermentation performance using multi-parameter flow cytometry. Work carried out by Talsania (2007) demonstrated the high levels of population heterogeneity displayed by *B. cereus* NCTC11143 when grown in nutrient broth. These shake flask experiments with *B. cereus* NCTC11143 aimed to make use of these high levels of population heterogeneity to evaluate three fluorophores $DiBac_4(3)$, $DiOC_6(3)$ and REDOX sensor green reagent) combined with propidium iodide, and to select a suitable combination with which to conduct further studies.

Reproducible measurements of OD_{600nm}, DCW (gL^{-1}), $CFUmL^{-1}$ and pH were taken (Figure 4.2a and b). Multi-parameter flow cytometry was used to monitor the physiological state of cells during the course of the fermentation (Figure 4.3a to d and 4.4).

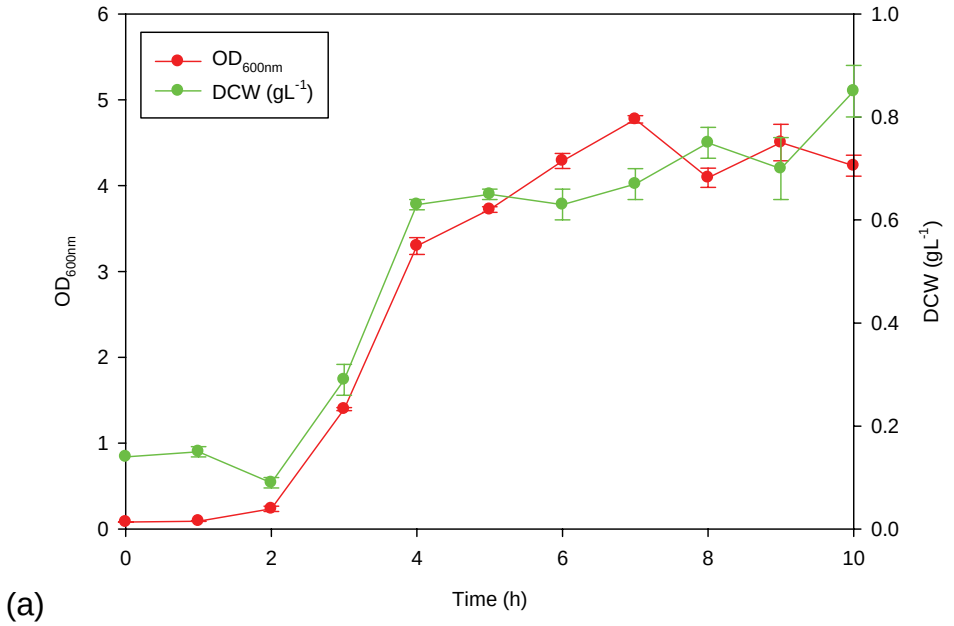

(a)

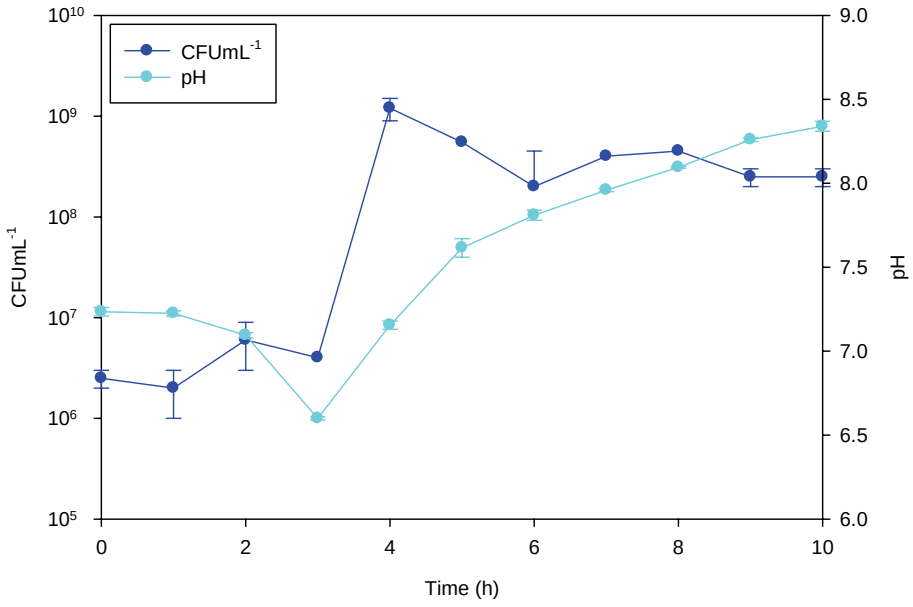

(b)

Figure 4.2 Time course of *Bacillus cereus* NCTC11143 during shake flask fermentation in nutrient broth at 37 °C and 200 rpm agitation speed. Profiles of (a) OD_{600nm} and DCW (gL^{-1}) and (b) pH and $CFUmL^{-1}$ are shown and error bars represent the range of data collected from three replicate experiments.

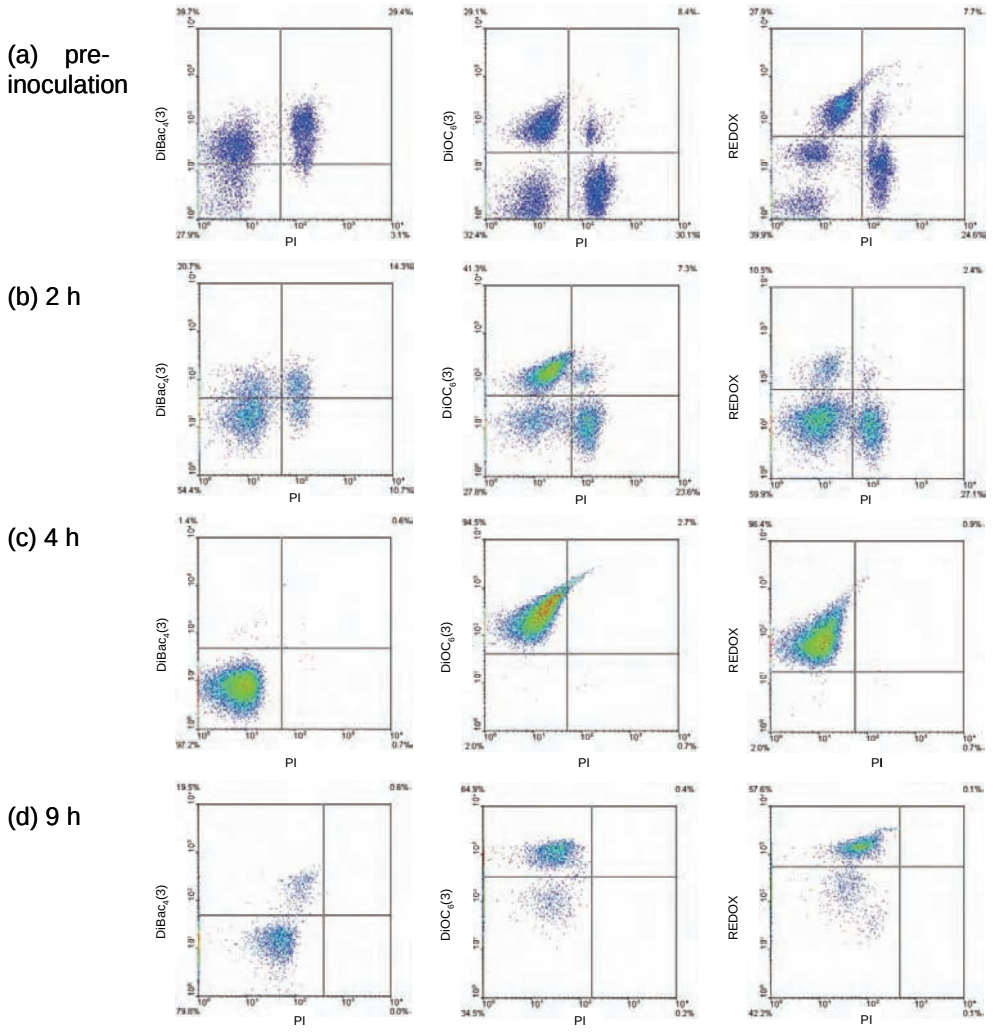

Figure 4.3 Flow cytometry of *Bacillus cereus* NCTC11143 during shake flask fermentation in nutrient broth at 37 °C and 200 rpm agitation speed: (a) Pre inoculation, (b) 2 h, (c) 4 h, and (d) 9 h. Results are shown for each of the three combinations of fluorophore $DiBac_4(3)$/PI, $DiOC_6(3)$/PI and REDOX sensor green reagent/PI.

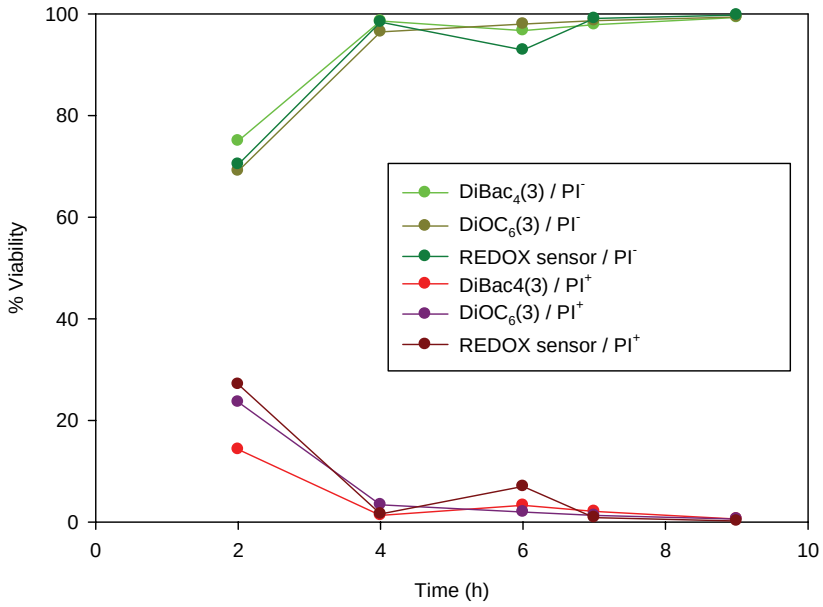

Figure 4.4 Flow cytometry of *Bacillus cereus* NCTC11143 during shake flask fermentation in nutrient broth at 37 °C and 200 rpm agitation speed. Profiles of PI^- (green) and PI^+ (red) cells are shown for three fluorophore combinations; $DiBac_4(3)$/PI, $DiOC_6(3)$/PI and REDOX sensor green reagent/PI.

Following a 2 hour lag phase the mean specific growth rate (μ) was calculated as 0.37 h^{-1} using the optical density data for the 3 and 4 h time points. At 4 hours, the maximum value for $CFUmL^{-1}$ (1.2 $x10^9$ cells) and dry cell weight (gL^{-1}) (1.33 gL^{-1}) was observed and the optical density readings started to increase more gradually. After 7 hours, the stationary phase has commenced as seen by a decrease in OD_{600nm} after this time point. The maximum optical density measurement was recorded as 4.77. The 4 h point may have represented the start of oxygen limitation through mass transfer within the shake flask or nutrient limitation. The pH showed an initial decline from pH 7.0 down to pH 6.5 at 3 h followed by a gradual rise to pH 8.4 at 10 h. This initial decline in pH was probably because the nitrogen source in the complex medium was being metabolised; this was followed by an increase which may have represented oxidative de-amination of amino acids which releases ammonia into the medium (Robinson *et al*., 1991). During the fermentation dissolved oxygen was not measured, and because *B. cereus* NCTC11143 is a facultative aerobe fermentation process performance may have been affected.

Figure 4.3a to d and 4.4 show the flow cytometry data obtained during the shake flask fermentation of *B. cereus* NCTC11143. Only one set of flow cytometry data is shown here and it was representative of each of the three shake flask experiments performed. All flow cytometry data are expressed as log scale density plots with percentages of cells appearing at the corners of each quadrant. Figure 4.4 shows changes in microbial viability throughout the

fermentation. Percentage PI^- cells includes both polarised and de-polarised cells for $DiBac_4(3)$ and $DiOC_6(3)$ as well as cells with respiratory enzyme activity for REDOX sensor green reagent, percentage PI^+ cells represents permeablised cells. Each fluorophore used for these experiments was interpreted to give information about the physiological state of a population of cells. The pre-inoculation culture and 2 hour sample during the lag phase showed high levels of population heterogeneity for each dye. At 4 hours, a single population with a polarised cytoplasmic membrane and respiratory enzyme activity was visible which concurred with the fermentation data as the point at which the cells were at their maximum $CFUmL^{-1}$. Towards the end of the fermentation, there was a shift towards multiple populations. Despite the different chemistry of $DiBac_4(3)$, $DiOC_6(3)$ and REDOX sensor green reagent (Section 2.8) they all gave similar results for the number of PI^- and permeablised cells at each of the time points sampled. The large degree of population heterogeneity shown by *B. cereus* NCTC11143 at the beginning and end of the shake flask fermentation could be due to a number of different factors (Section 2.7) and it prompted a series of flow cytometry assisted cell sorting (FACS) experiments. Figures 4.5a to c to 4.7 show the results for these experiments.

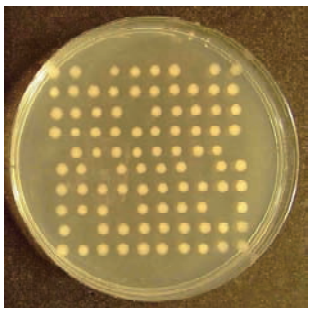

(a) Unstained

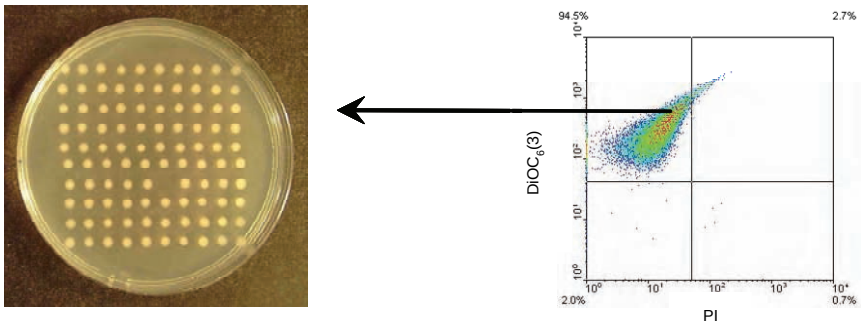

(b) $DiOC_6(3)$

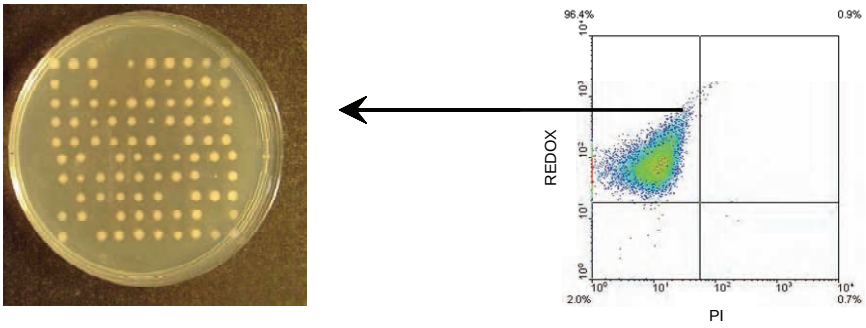

(c) REDOX

Figure 4.5 Flow cytometry and cell sorting of *Bacillus cereus* NCTC11143 after 4 h with (a) no staining (positive control) and fully polarised and actively respiring populations stained with (b) $DiOC_6(3)$ and (c) REDOX sensor green reagent.

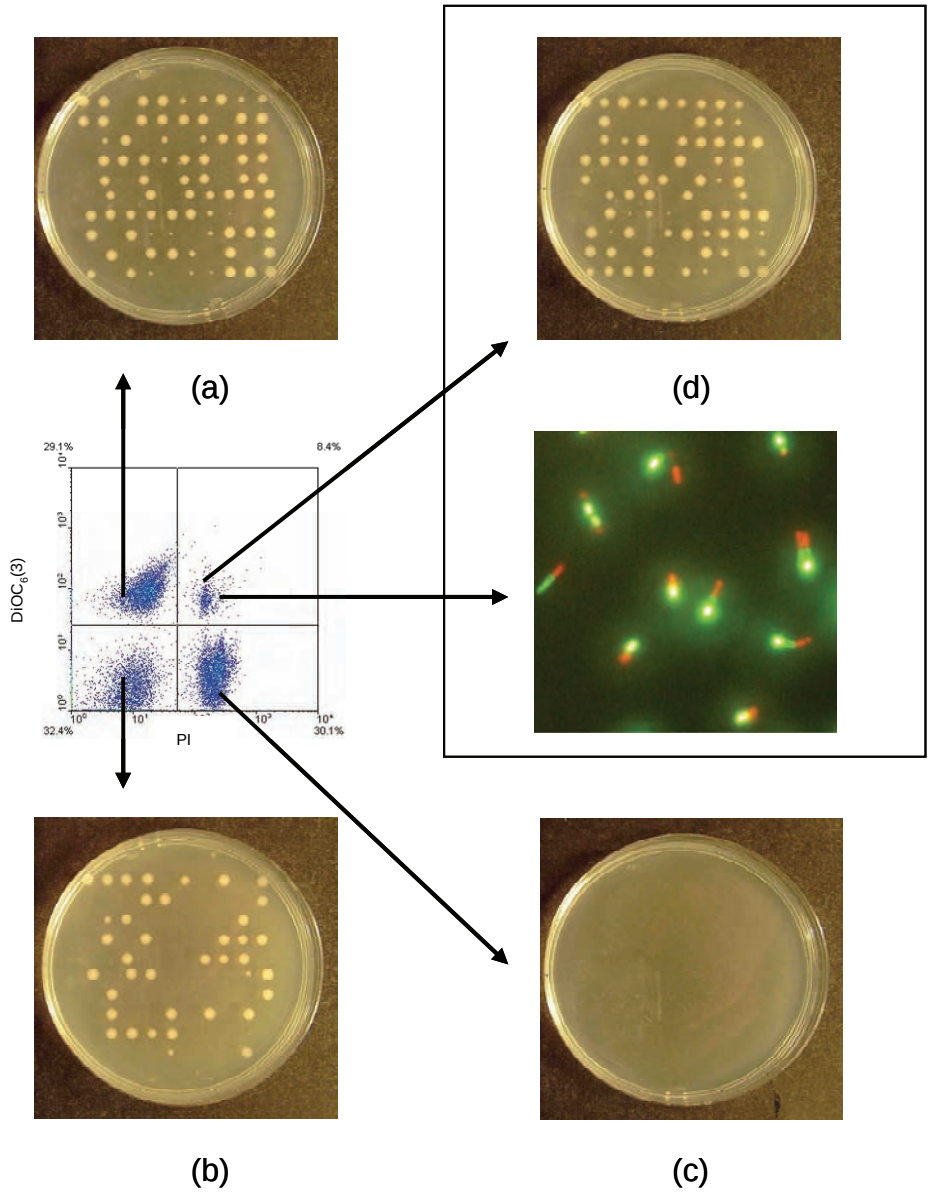

Figure 4.6 Flow cytometry and cell sorting of a sample of *Bacillus cereus* NCTC 11143 taken prior to inoculation and stained with $DiOC_6(3)$ and PI; (a) polarised, (b) de-polarised, (c) permeablised, (d) “doublets” a combination of polarised and permeablised cells joined together, as seen in the fluorescence microscope image with polarised cells shown in green ($DiOC_6(3)$) and permeablised cells shown in red (PI).

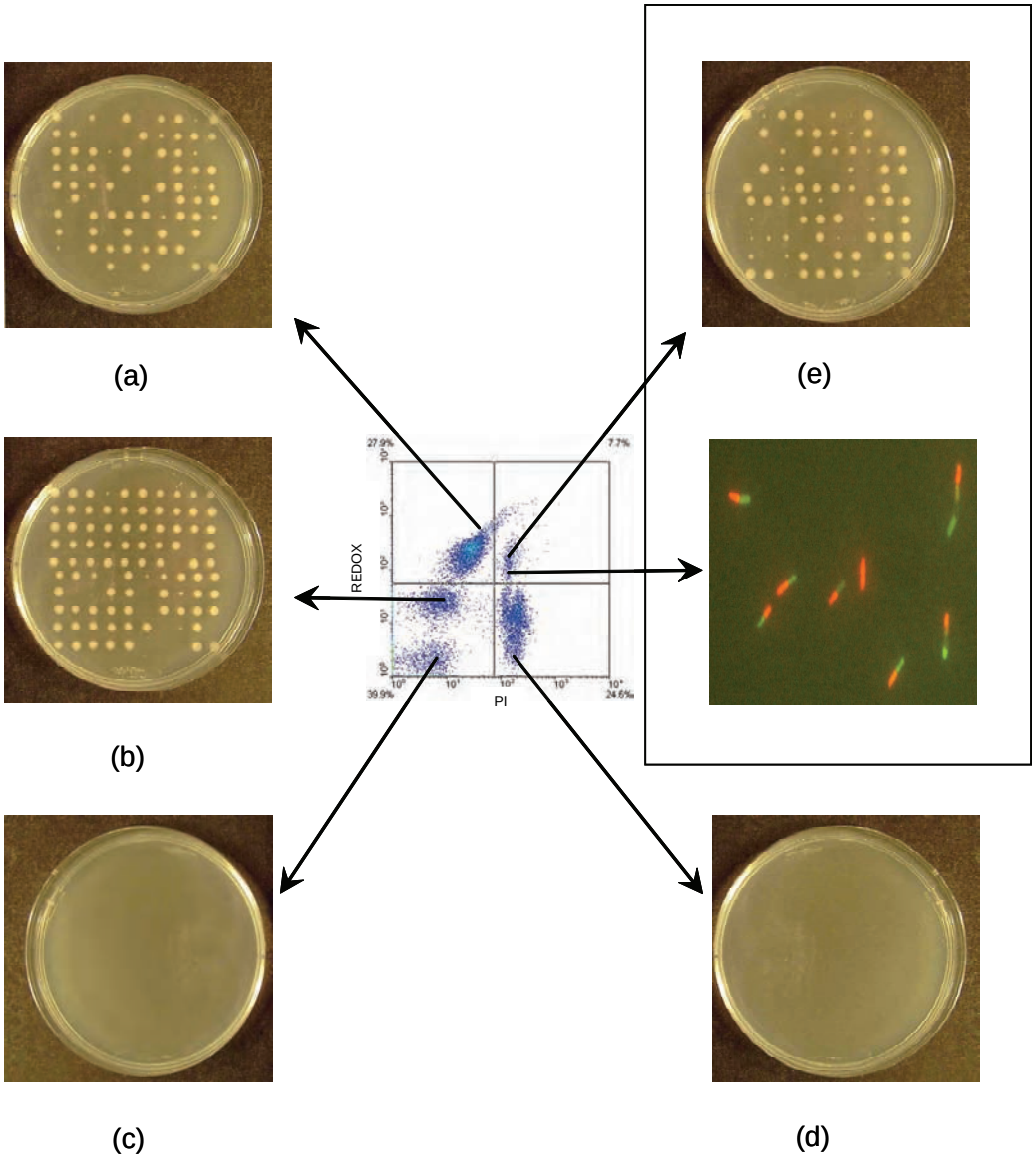

Figure 4.7 Flow cytometry and cell sorting of a sample of *Bacillus cereus* NCTC 11143 taken prior to inoculation and stained with REDOX sensor green reagent and PI; (a) actively respiring, (b) reduced respiratory activity, (c) cell debris, (d) permeablised, (e) “doublets” a combination of actively respiring and permeablised cells joined together, as seen in the fluorescence microscope image with actively respiring cells shown in green (REDOX sensor green reagent) and permeablised cells shown in red (PI).

Figure 4.5a shows FACS onto nutrient agar plates of an unstained population of cells (positive control) in which 90% of the cells remained reproductively viable, a polarised population stained with $DiOC_6(3)$ (Figure 4.5b) in which 99% of the cells remained reproductively viable and an actively respiring population stained with REDOX sensor green (Figure 4.5c) reagent in which 89% of cells remained reproductively viable. Each plate showed similar levels of reproductive growth characteristics when compared to the unstained plate. Cells stained with $DiOC_6(3)$ and PI (Figure 4.5b) had clearly remained reproductively viable which contradicts previous findings that $DiOC_6(3)$ is toxic to microbial cells (Miller *et al*., 1978).

Figure 4.6a to d shows the *B. cereus* NCTC11143 pre-inoculation sample stained with $DiOC_6(3)$ and PI and each sub-population has been sorted onto a nutrient agar plate using FACS. The top left quadrant (Figure 4.6a) represented the polarised population of cells which demonstrated a good amount of reproductive growth when grown on the agar plate, with 72% of cells able to undergo reproductive growth. The bottom left quadrant (Figure 4.6b) represented the de-polarised population of cells and this was demonstrated as a reduced amount of reproductive growth on the agar plate, with 39% of cells able to undergo reproductive growth. The bottom right quadrant (Figure 4.6c) represented the permeablised cells and this was demonstrated with the lack of colonies on the agar plate. The top right quadrant (Figure 4.6d) was representative of a sub-population in which the cells appeared to be somewhere

between polarised and permeablised with 68% of the cells able to undergo reproductive growth. To investigate this unusual population further fluorescence microscopy was employed (Figure 4.6d) and it was seen that in fact it consists of polarised and permeablised cells stuck together as ‘doublets’.

Figure 4.7a to e shows the *B. cereus* NCTC11143 pre-inoculation sample stained with REDOX sensor green reagent and propidium iodide and as before the sub-populations have been sorted onto nutrient agar plates. The REDOX sensor green reagent showed the formation of an actively respiring population in the top left quadrant (Figure 4.7a), which contained 66% of cells able to undergo reproductive growth on the agar plate. A population with reduced respiratory activity was present in the bottom left quadrant (Figure 4.7b), which contained 88% of cells able to undergo reproductive growth on the agar plate. The second population in the bottom left quadrant (Figure 4.7c) which did not demonstrate reproductive growth may have been representative of cell debris which had a low level of green fluorescence. The population in the bottom right quadrant (Figure 4.7d) was representative of the permeablised cell population and as such demonstrated no reproductive growth when sorted onto nutrient agar. The population in the top right (Figure 4.7e) demonstrated the population of “doublets” seen with the $DiOC_6(3)$ stain and was confirmed with the fluorescence microscopy picture (Figure 4.7e), 66% of cells plated were capable of reproductive growth. The results for cell sorting with the REDOX sensor green reagent and PI (Figure 4.7a to e) were of interest particularly as the manufacturer

reports that only an actively respiring and a permeablised population should be detectable (Figure 4.1c) (Gray *et al*., 2005). Cell sorting experiments using the $DiBac_4(3)$ fluorophore with PI have previously been performed by Nebe-von-Caron *et al*. (2000) and demonstrated that it was only the permeablised cells which did not demonstrate reproductive growth on an agar plate. Interestingly the results of the FACS experiments (Figures 4.5a to c to 4.7) demonstrated that not only were the cells showing population heterogeneity in terms of the integrity and polarisation of their cytoplasmic membranes, but also in their rates of reproductive growth when plated onto nutrient agar. This is seen by the range of different sized colonies present on the agar plates and may represent differences in length of lag phases or in different specific growth rates.

Due to its non industrial nature, *B. cereus* NCTC 11143 demonstrated low levels of growth and final biomass when grown in a shake flask. However, it was an excellent candidate for comparing $DiBac_4(3)$, $DiOC_6(3)$ and REDOX sensor green reagent in combination with PI for measuring microbial viability as it demonstrated high levels of population heterogeneity.

These results have shown that despite the different chemical properties of $DiBac_4(3)$, $DiOC_6(3)$ and REDOX sensor green reagent in combination with PI, similar readings of microbial viability have been measured for the organism *B. cereus* NCTC11143.

4.1.2 *Bacillus licheniformis* SJ4628 growing in yeast malt broth with and without cryopreservants

Section 4.1.1 demonstrated that $DiBac_4(3)$, $DiOC_6(3)$ and REDOX sensor green reagent in combination with PI gave similar results for measuring microbial viability for the organism *B. cereus* NCTC11143. The aim of the work in this section was to evaluate the same three fluorophores in combination with PI for measuring microbial viability of *B. licheniformis* SJ4628, when grown in yeast malt broth. Once a suitable combination of fluorophores was selected they were used to measure viability of *B. licheniformis* SJ4628 when grown in different concentrations of cryopreservants.

4.1.2.1 Yeast malt broth alone

Figure 4.8a shows OD_{600nm} and dry cell weight (gL^{-1}), Figure 4.8b the $CFUmL^{-1}$ and pH and Figure 4.8c the α-amylase activity data for the shake flask fermentations of *B. licheniformis* SJ4628. Multi-parameter flow cytometry was used to monitor the physiological state of cells during the course of the fermentation (Figure 4.9a to e and 4.10).

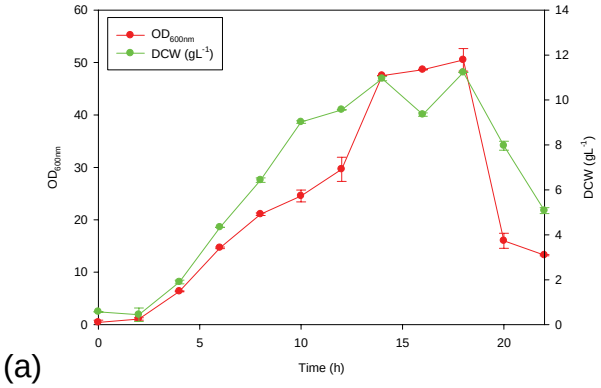

(a)

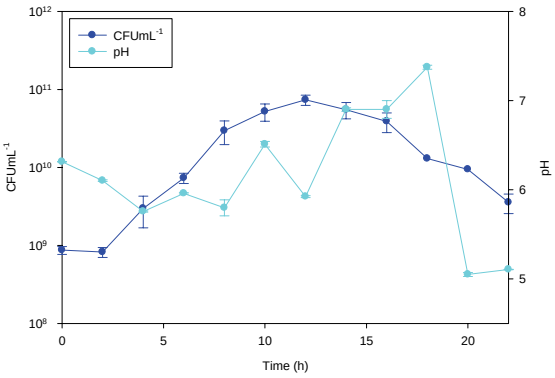

(b)

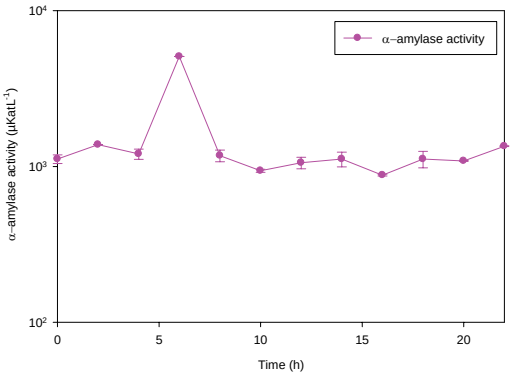

(c)

Figure 4.8 Time course of *Bacillus licheniformis* SJ4628 during shake flask fermentation in yeast malt broth at 37 °C and 200 rpm agitation speed. Profiles of (a) OD_{600nm} and DCW (gL^{-1}), (b) $CFUmL^{-1}$ and pH and (c) α-amylase activity are shown and error bars represent the range of data collected from three replicate experiments.

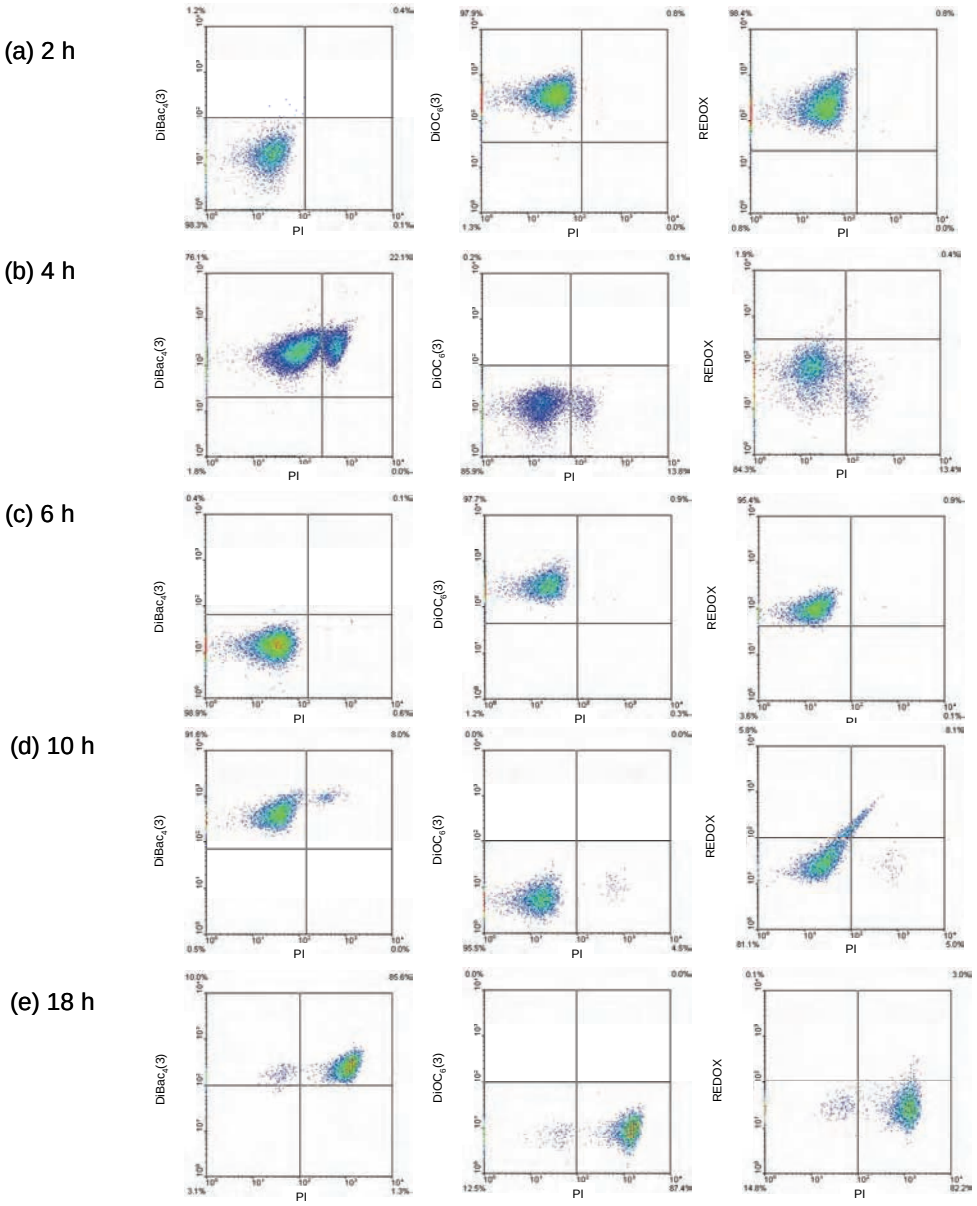

Figure 4.9 Flow cytometry of *Bacillus licheniformis* SJ4628 during shake flask fermentation in yeast malt broth at 37 °C and 200 rpm agitation speed: (a) 2 h, (b) 4 h, (c) 6 h, (d) 10 h, and (e) 18 h. Results are shown for each of the three combinations of fluorophore; $DiBac_4(3)$/PI, $DiOC_6(3)$/PI and REDOX sensor green reagent/PI.

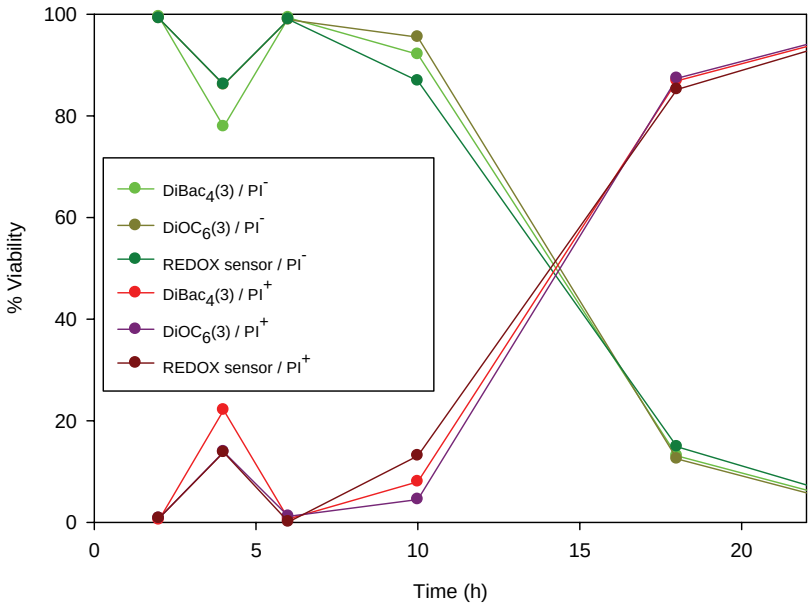

Figure 4.10 Flow cytometry of *Bacillus licheniformis* SJ4628 during shake flask fermentation in yeast malt broth at 37 °C and 200 rpm agitation speed. Profiles of PI- (green) and PI+ (red) cells are shown for three fluorophore combinations; DiBac4(3)/PI, DiOC6(3)/PI and REDOX sensor green reagent/PI.

Following a 2 hour lag phase, the mean specific growth rate (μ) was calculated as 0.28 h^{-1} from the optical density data at the 2 and 6 h time points. Optical density and dry cell weight (gL^{-1}) reached a maximum at 18 h and were 50.5 and 11.23 gL^{-1} respectively. The $CFUmL^{-1}$ data showed a steady increase up to 12 hours when the maximum $CFUmL^{-1}$ was recorded as 7.35 x 10^{10}. The pH varied throughout the fermentation from a starting value of 6.3 to a maximum recorded value of 7.4 at 18 h reflecting the changing metabolic activity of the culture. The fermentation profile for *B. licheniformis* SJ4628 (Figure 4.8a to c) differed greatly from that of *B. cereus* NCTC11143 (Figure 4.2a and b); the optical density readings reached 50 which was 10 times higher than *B. cereus* NCTC11143 and values were also higher for DCW (gL^{-1}) and $CFUmL^{-1}$. The pH fluctuated more dramatically in the fermentation of *B. licheniformis* SJ4628 possibly due to the production of different metabolic products and the effect of buffering. The α-amylase data showed that for most of the fermentation process the average yield was 1128 $\mu KatL^{-1}$ However, at the 6 h time point it rose sharply to 5074 $\mu KatL^{-1}$ The α-amylase results showed a large increase at the 5 h time point before returning to the baseline; this followed a rise in de-polarised, cells with reduced respiratory activity and permeablised cells at 4 h shown by the flow cytometry results (Figures 4.9a to e and 4.10) and may represent a survival response. α-amylase is referred to as a scavenger enzyme and is an extracellular enzyme that has no role in the internal metabolism of the cell; it is synthesised in response to changes in the availability of a carbon source and acts to produce an

easily metabolisible carbon source in order to maintain cellular growth (Priest *et al*., 1977). The decline in α-amylase production may also have been due to the presence of proteolytic enzymes in the broth. Figure 4.9a to e and 4.10 show the flow cytometry results for the shake flask fermentation of *B. licheniformis* SJ4628, although only one set of flow cytometry data is shown here it was representative of each of the three experiments performed. At 2 h, the total number of polarised and actively respiring cells for each of the 3 dyes was in good agreement and the cells were all PI^-. At 4 h, the cells became increasingly de-polarised with reduced respiratory activity and a permeablised cell population had developed, although this was not reflected in the $CFUmL^{-1}$ results in Figure 4.8b. For the remainder of the fermentation the cells remained PI^- until the 10 h time point at which the flow cytometry results showed the development of a de-polarised cell population, a population with reduced respiratory activity and a permeablised population. This concurred with the $CFUmL^{-1}$ data which showed a maximum value at 12 h. At 18 h, the flow cytometry data revealed a large permeablised cell population and this was in agreement with the optical density, $CFUmL^{-1}$ and DCW (gL^{-1}) data from Figure 4.8 which showed a sharp decrease from the 18 h time point. As with the *B. cereus* NCTC11143 flow cytometry shake flask data the results for each of the 3 dyes were in good agreement. However, *B. licheniformis* SJ4628 did not show the levels of population heterogeneity exhibited by *B. cereus* NCTC 11143, and it was therefore not necessary to do any additional cell sorting experiments. This reflected the highly robust nature of *B. licheniformis*

SJ4628 as an industrial production strain.

These experiments have shown that *B. licheniformis* SJ4628 shows good levels of growth and final biomass concentration when grown in a shake flask, and is able to produce α-amylase when grown in the medium selected. As an industrial production strain it demonstrated very little population heterogeneity compared to *B. cereus* NCTC 11143.

After reviewing the data for the two shake flask experiments $DiBac_4(3)$ dye was chosen to complete the rest of the flow cytometry experiments for a number of reasons: it is the most widely used dye in the laboratory where this work was carried out and as such is well understood; it is also inexpensive and reliable (Hewitt *et al*., (2001), Kochurunchitt (2007), Onyeaka *et al*., (2003)). Further experiments with $DiOC_6(3)$ showed it does not always give consistent results and the REDOX sensor green reagent is very expensive and not very much information exists about it in the literature.

4.1.2.2 Yeast malt broth containing different concentrations of glycerol

In section 4.1.2.1 $DiBac_4(3)$ with PI was chosen as the combination of fluorophores with which to measure microbial physiology. This section of work aimed to use $DiBac_4(3)$/PI to measure microbial physiology of *B. licheniformis* SJ4628 when grown in different concentrations of glycerol. These experiments had the overall aim of discovering the highest concentration at which glycerol is non-toxic to *B. licheniformis* SJ4628 so that it could be used for cell bank preparation for further experiments. When determining the correct concentration of cryopreservant to use that the highest concentration which is non-toxic to the cells is usually best (Simione., 1998).

Measurements of $CFUmL^{-1}$ (Figure 4.11) were used as a measure of reproductive growth and multi-parameter flow cytometry ($DiBac_4(3)$ and PI) was used to monitor the physiological status of cells during the course of the fermentation (Figure 4.12 to 4.17 and to 4.18a to f). As mentioned in Chapter 2 glycerol is one of the most widely used microbial cryopreservants (Hubálek., 2003) and is what Novozymes currently use to cryopreserve *B. licheniformis* SJ4628 at a concentration of 20% v/v. Early experiments which successfully cryopreserved cells relied upon glycerol, and this established it as an important cryoprotective agent (Polge *et al*., 1949).

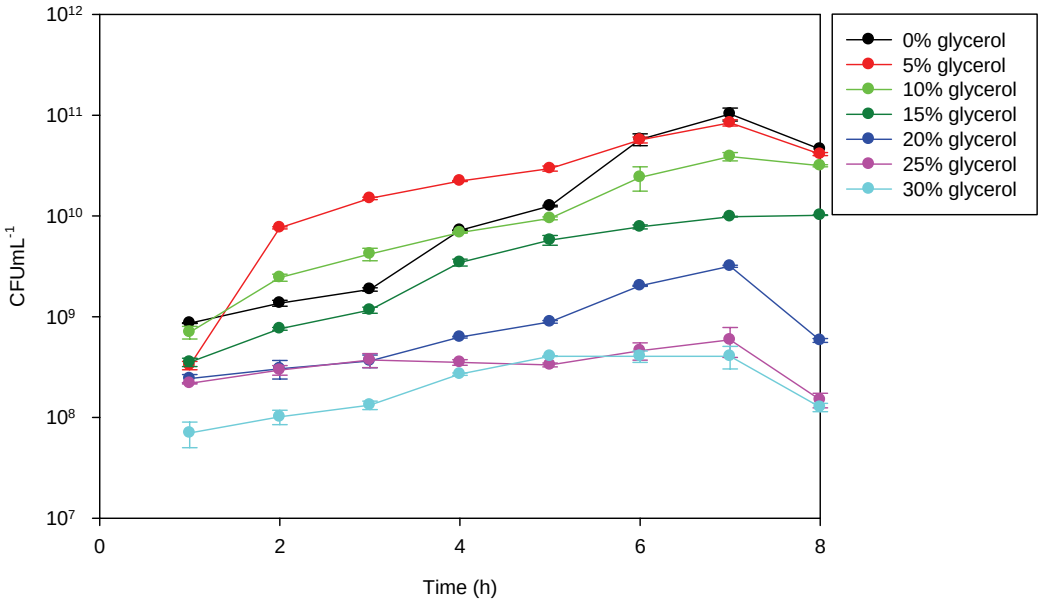

Figure 4.11 Time course of *Bacillus licheniformis* SJ4628 during shake flask fermentation in yeast malt broth containing different concentrations of glycerol (0 to 30% v/v), at 37 °C and 200 rpm agitation speed. Error bars represent the range of data collected from three replicate experiments.

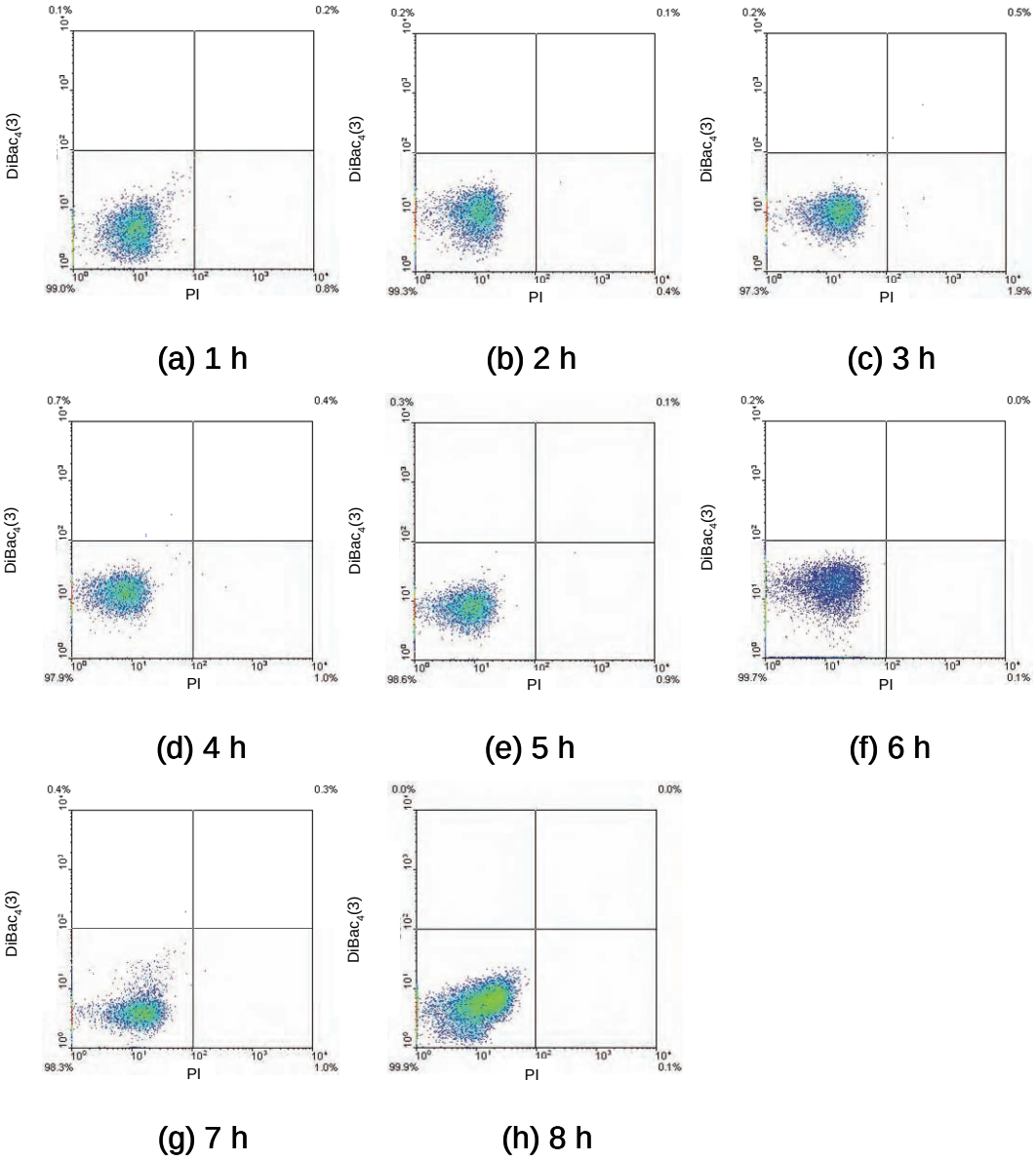

Figure 4.12 Flow cytometry of *Bacillus licheniformis* SJ4628 during shake flask fermentation in yeast malt broth containing 5% v/v glycerol, at 37 °C and 200 rpm agitation speed; (a) 1h, (b) 2h, (c) 3h, (d) 4h, (e) 5h, (f) 6h, (g) 7h, (h) 8h. Results are shown for the fluorophore combination; $DiBac_4(3)$/PI.

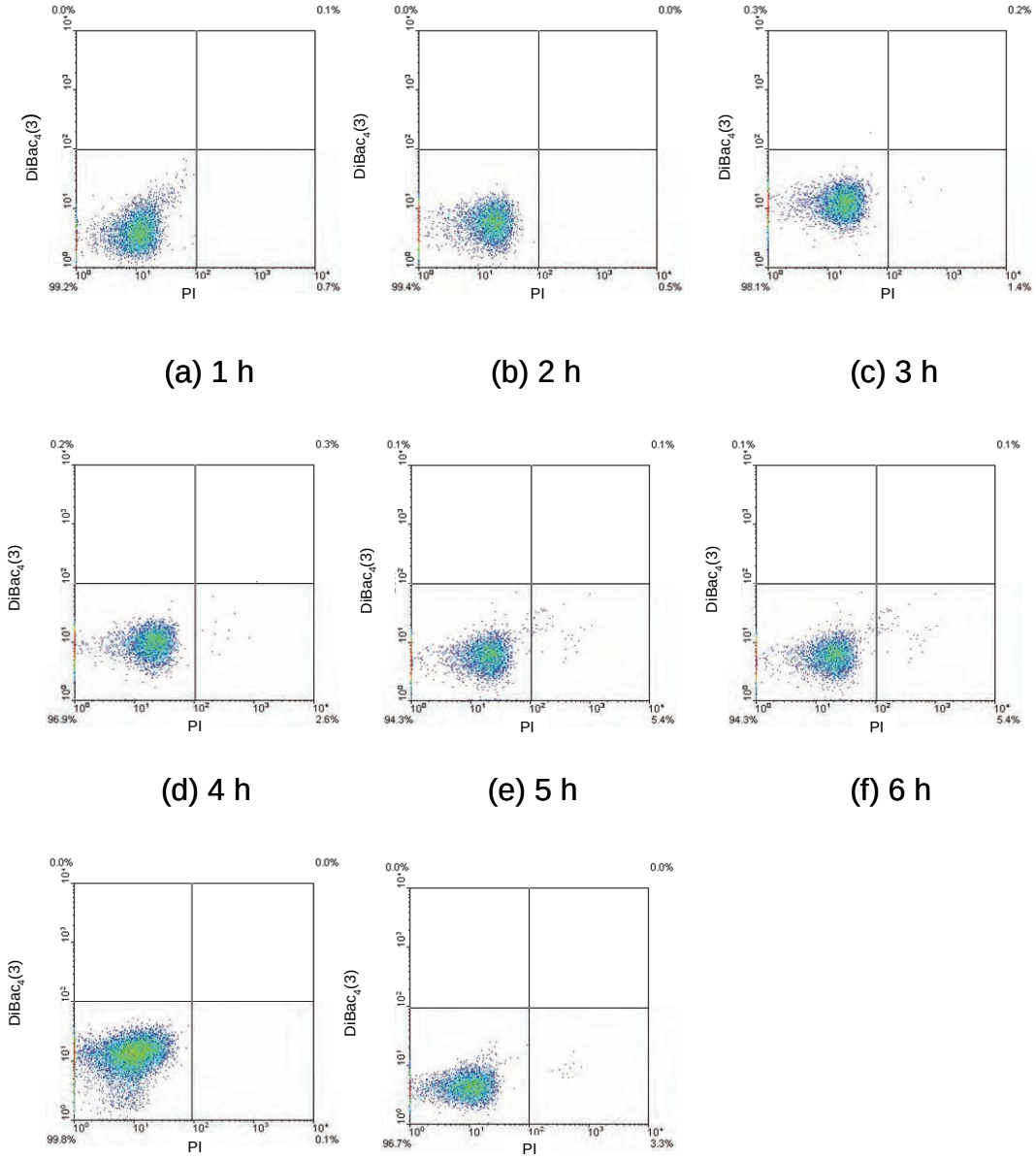

Figure 4.13 Flow cytometry of *Bacillus licheniformis* SJ4628 during shake flask fermentation in yeast malt broth containing 10% v/v glycerol, at 37 °C and 200 rpm agitation speed; (a) 1h, (b) 2h, (c) 3h, (d) 4h, (e) 5h, (f) 6h, (g) 7h, (h) 8h. Results are shown for the fluorophore combination; $DiBac_4(3)$/PI.

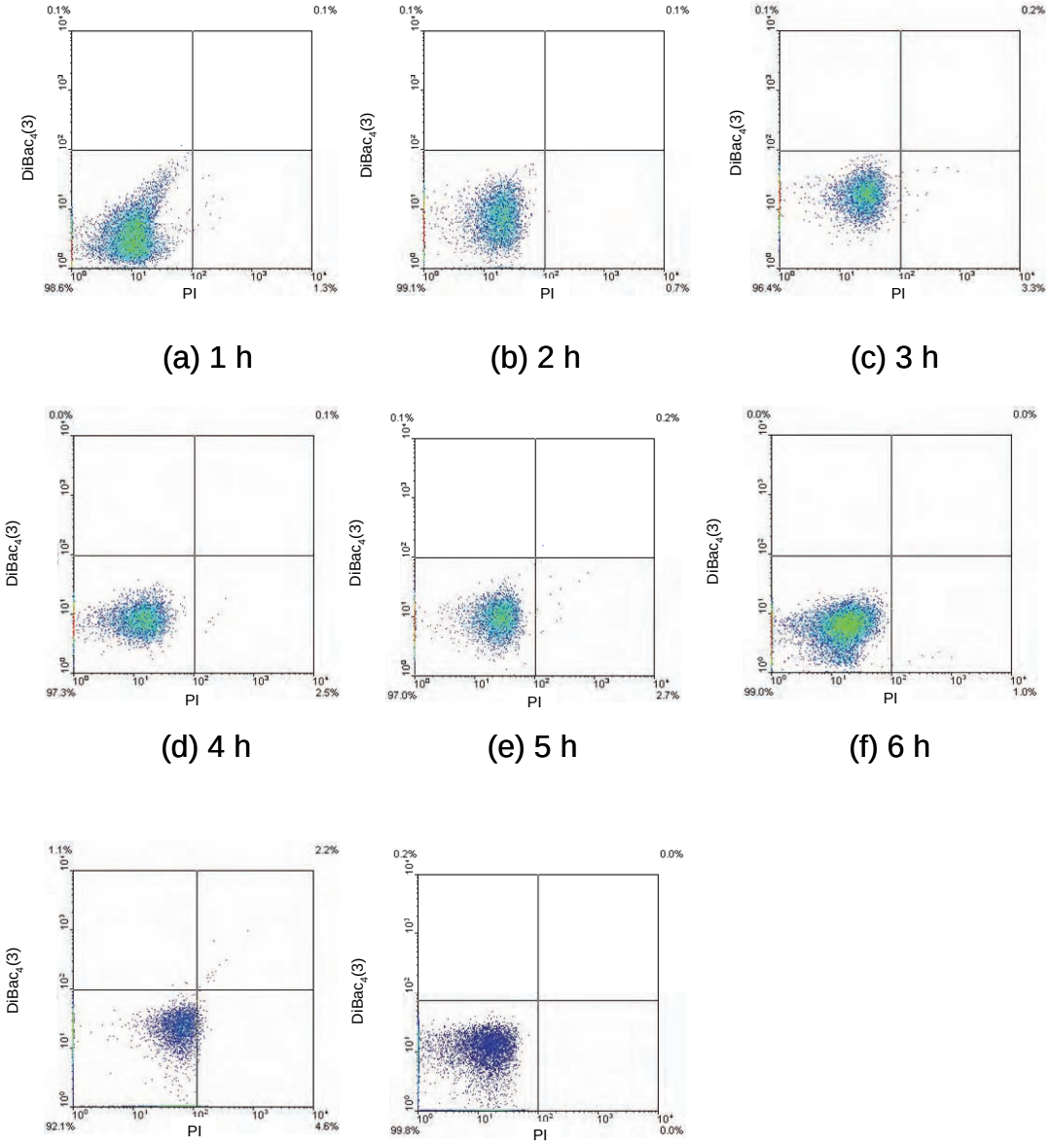

Figure 4.14 Flow cytometry of *Bacillus licheniformis* SJ4628 during shake flask fermentation in yeast malt broth containing 15% v/v glycerol, at 37 °C and 200 rpm agitation speed; (a) 1h, (b) 2h, (c) 3h, (d) 4h, (e) 5h, (f) 6h, (g) 7h, (h) 8h. Results are shown for the fluorophore combination; $DiBac_4(3)$/PI.

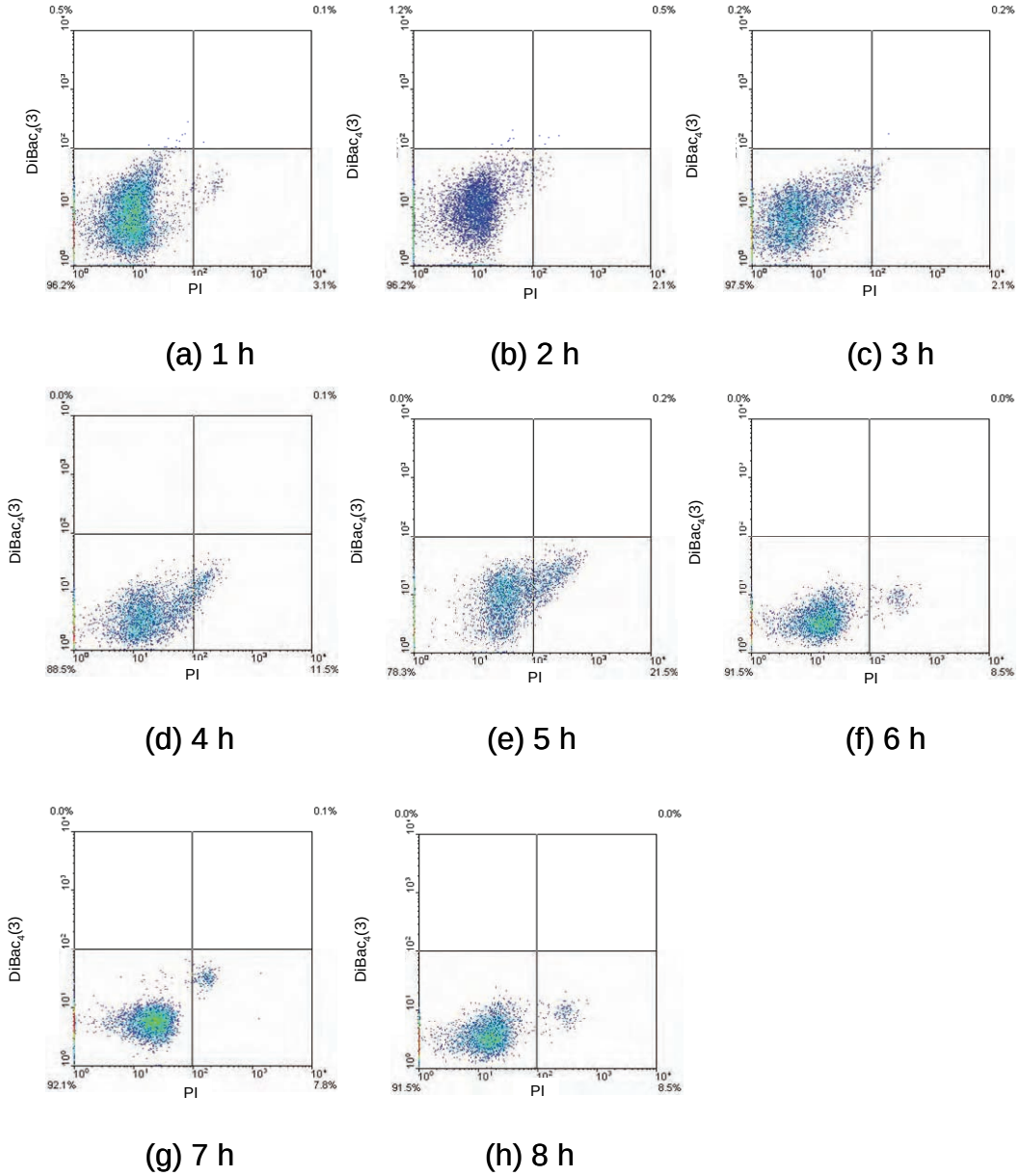

Figure 4.15 Flow cytometry of *Bacillus licheniformis* SJ4628 during shake flask fermentation in yeast malt broth containing 20% v/v glycerol, at 37 °C and 200 rpm agitation speed; (a) 1h, (b) 2h, (c) 3h, (d) 4h, (e) 5h, (f) 6h, (g) 7h, (h) 8h. Results are shown for the fluorophore combination; $DiBac_4(3)$/PI.

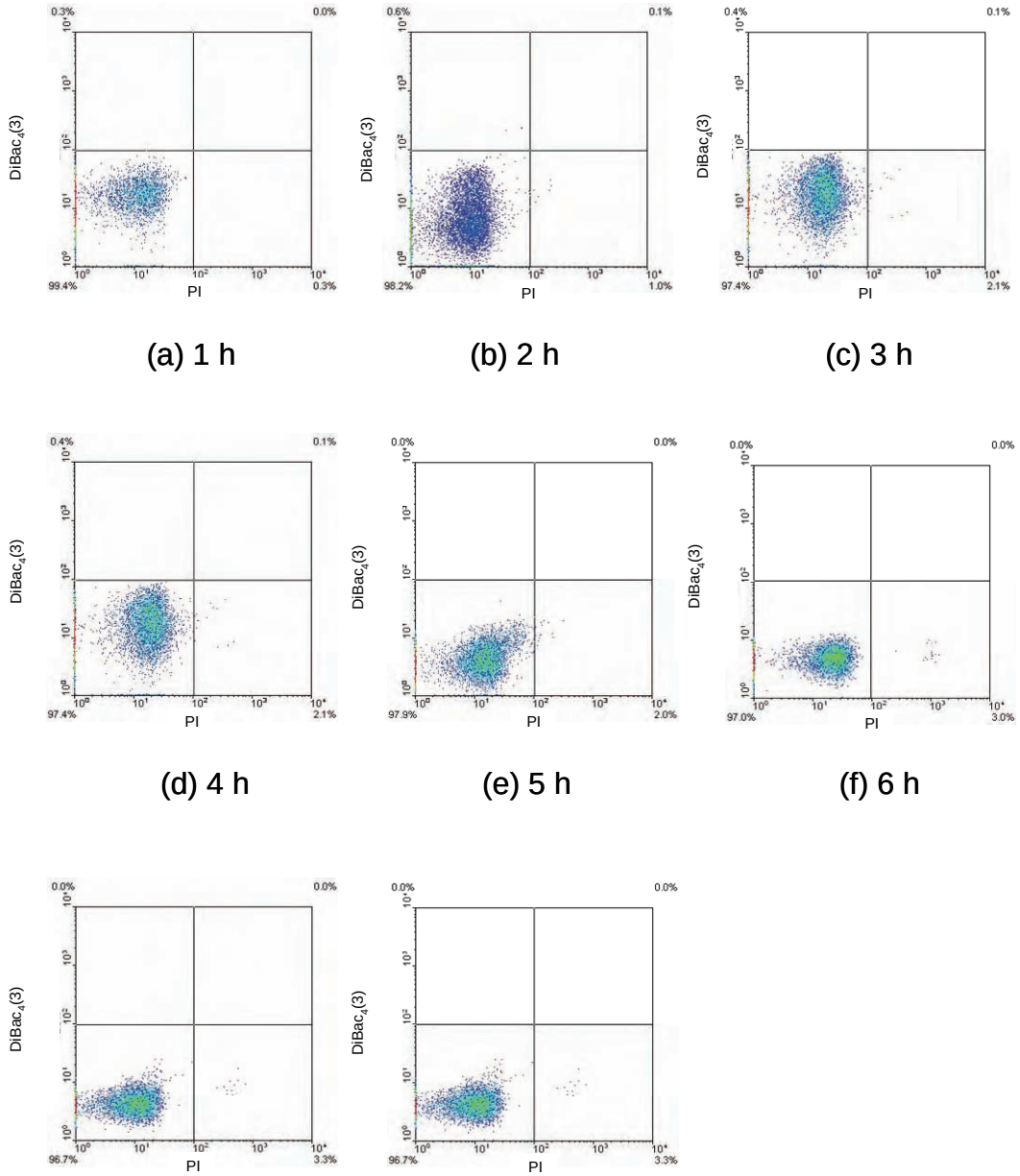

(a) 1 h (b) 2 h (c) 3 h

(d) 4 h (e) 5 h (f) 6 h

(g) 7 h (h) 8 h

Figure 4.16 Flow cytometry of *Bacillus licheniformis* SJ4628 during shake flask fermentation in yeast malt broth containing 25% v/v glycerol, at 37 °C and 200 rpm agitation speed; (a) 1h, (b) 2h, (c) 3h, (d) 4h, (e) 5h, (f) 6h, (g) 7h, (h) 8h. Results are shown for the fluorophore combination; $DiBac_4(3)$/PI.

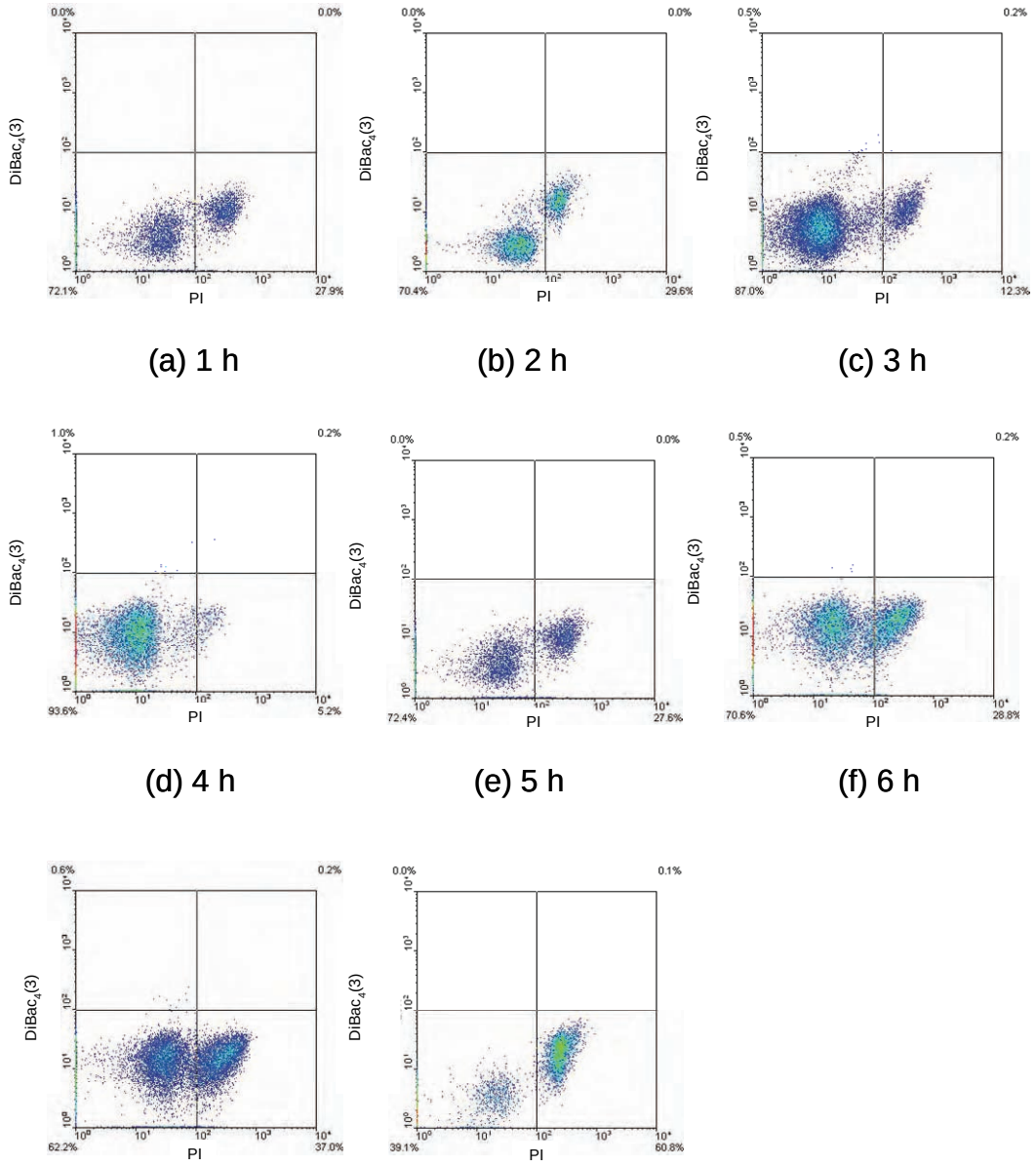

(a) 1 h (b) 2 h (c) 3 h

(d) 4 h (e) 5 h (f) 6 h

(g) 7 h (h) 8 h

Figure 4.17 Flow cytometry of *Bacillus licheniformis* SJ4628 during shake flask fermentation in yeast malt broth containing 30% v/v glycerol, at 37 °C and 200 rpm agitation speed; (a) 1h, (b) 2h, (c) 3h, (d) 4h, (e) 5h, (f) 6h, (g) 7h, (h) 8h. Results are shown for the fluorophore combination; $DiBac_4(3)$/PI.

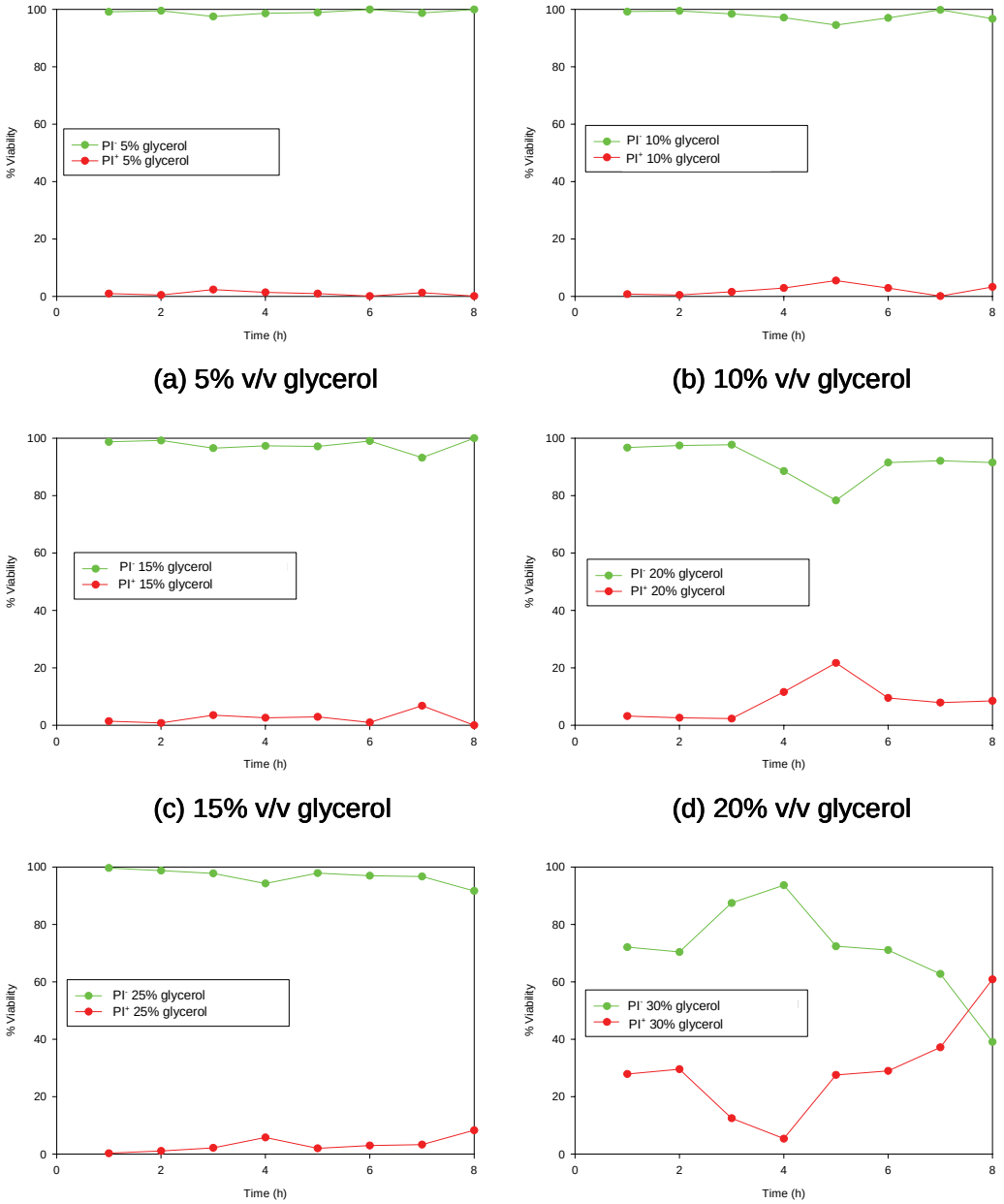

(a) 5% v/v glycerol (b) 10% v/v glycerol

(c) 15% v/v glycerol (d) 20% v/v glycerol

(e) 25% v/v glycerol (f) 30% v/v glycerol

Figure 4.18 Flow cytometry of *Bacillus licheniformis* SJ4628 during shake flask fermentation in yeast malt broth containing different concentrations of glycerol (0 to 30% v/v), at 37 °C and 200 rpm agitation speed. Profiles of PI^- (green) and PI^+ (red) cells are shown for fluorophore combination; $DiBac_4(3)$/PI.

Figure 4.11 shows the $CFUmL^{-1}$ results for the shake flask fermentations of *B. licheniformis* SJ4628 containing concentrations of 0% to 30% v/v glycerol. The 0% experiment represented the normal growth of *B. licheniformis* SJ4628 over the 8 h time course. Cells grown in 5% glycerol showed a slightly higher level of growth than in 0% glycerol presumably as they can metabolise the glycerol as a carbon source (Paulo da Silva *et al*., (2008). With further increases in the glycerol concentration from 10% to 30% there was a steady decline in the amount of reproductively viable cells. Figure 4.12a to h and Figure 4.18a showed that during the fermentation with 5% glycerol the cells remained polarised throughout the entire fermentation. Figure 4.13a to h and Figure 4.18b show that the cells grown in 10% glycerol remained polarised throughout the 8 h fermentation. Figure 4.14a to h and Figure 4.18c show that cells grown with 15% glycerol remained polarised during the fermentation. Figure 4.15a to h and Figure 4.18d show the cells grew well in 20% glycerol up to 4 h and then started to become permeablised. Figure 4.16a to h and Figure 4.18e show that cells grew well in 25% glycerol up to 6 h before a small proportion of the cells became permeablised. In Figure 4.17a to h and Figure 4.18f cells grown in 30% glycerol showed high levels of cellular permeablisation even from 1 h into the fermentation. The toxic effects could have been mediated by the ability of glycerol to enter the cytoplasmic membrane, and if present in sufficient quantities could cause disruption of the lipid bilayer and the functions it performs (Sikkema *et al*., 1995). The highly viscous nature of glycerol may also have coated the

outside of the cells and led to damaging effects at high concentrations presumably through the effect of osmosis. High concentrations of glycerol also appeared to affect the staining patterns of $DiBac_4(3)$ with the permeablised cell population appearing in the bottom right quadrant instead of the top right (Figure 4.1a shows were each population should appear). Further control experiments were conducted which involved mixing equal quantities of polarised cells and permeablised heat killed cells and then incubating them for 1 h in 30% v/v glycerol (Figure 3.3a to c in Chapter 3). The results revealed that the cells killed by heat appeared in the top right quadrant where as those killed by glycerol were in the lower right quadrant indicating that the glycerol affected the microbial cytoplasmic membrane and prevented the normal staining behaviour of $DiBac_4(3)$. It is also possible that the de-polarised population normally seen in the top left quadrant was undetected because of the changes in staining behaviour of $DiBac_4(3)$.

These experiments showed that 20% v/v glycerol which is the concentration currently used at Novozymes A/S for preparation of cell banks is not the highest concentration that is non-toxic to *B. licheniformis* SJ4628, 25% v/v is also non-toxic. Cell banks containing 20% v/v and 25% v/v glycerol were prepared for further study.

4.1.2.3 Yeast malt broth containing different concentrations of dimethyl sulphoxide (DMSO)

These experiments had the overall aim of discovering the highest concentration at which DMSO is non-toxic to *B. licheniformis* SJ4628 so that it could be used for cell bank preparation for further experiments.

Measurements of $CFUmL^{-1}$ (Figure 4.19) were used as a measure of reproductive growth and multi-parameter flow cytometry ($DiBac_4(3)$ and PI) was used to monitor the physiological status of cells during the course of the fermentation (Figure 4.20 to 4.23 and 4.24a to d). DMSO is also a widely used microbial cryopreservant (Chapter 2) and concentrations of 15% v/v or less are recommended (Hubálek., 2003), which agrees with the data reported in these experiments.

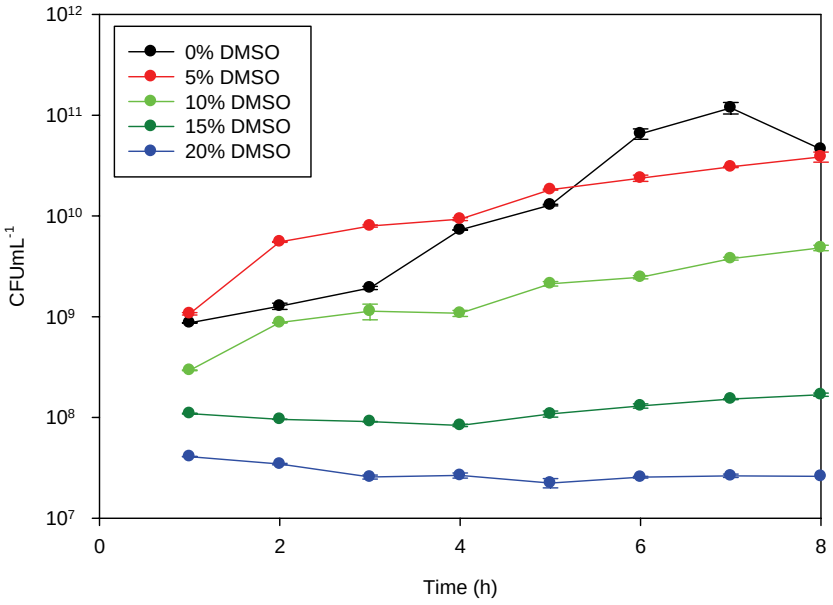

Figure 4.19 Time course of *Bacillus licheniformis* SJ4628 during shake flask fermentation in yeast malt broth containing different concentrations of DMSO (0 to 20% v/v), at 37 °C and 200 rpm agitation speed. Error bars represent the range of data collected from three replicate experiments.

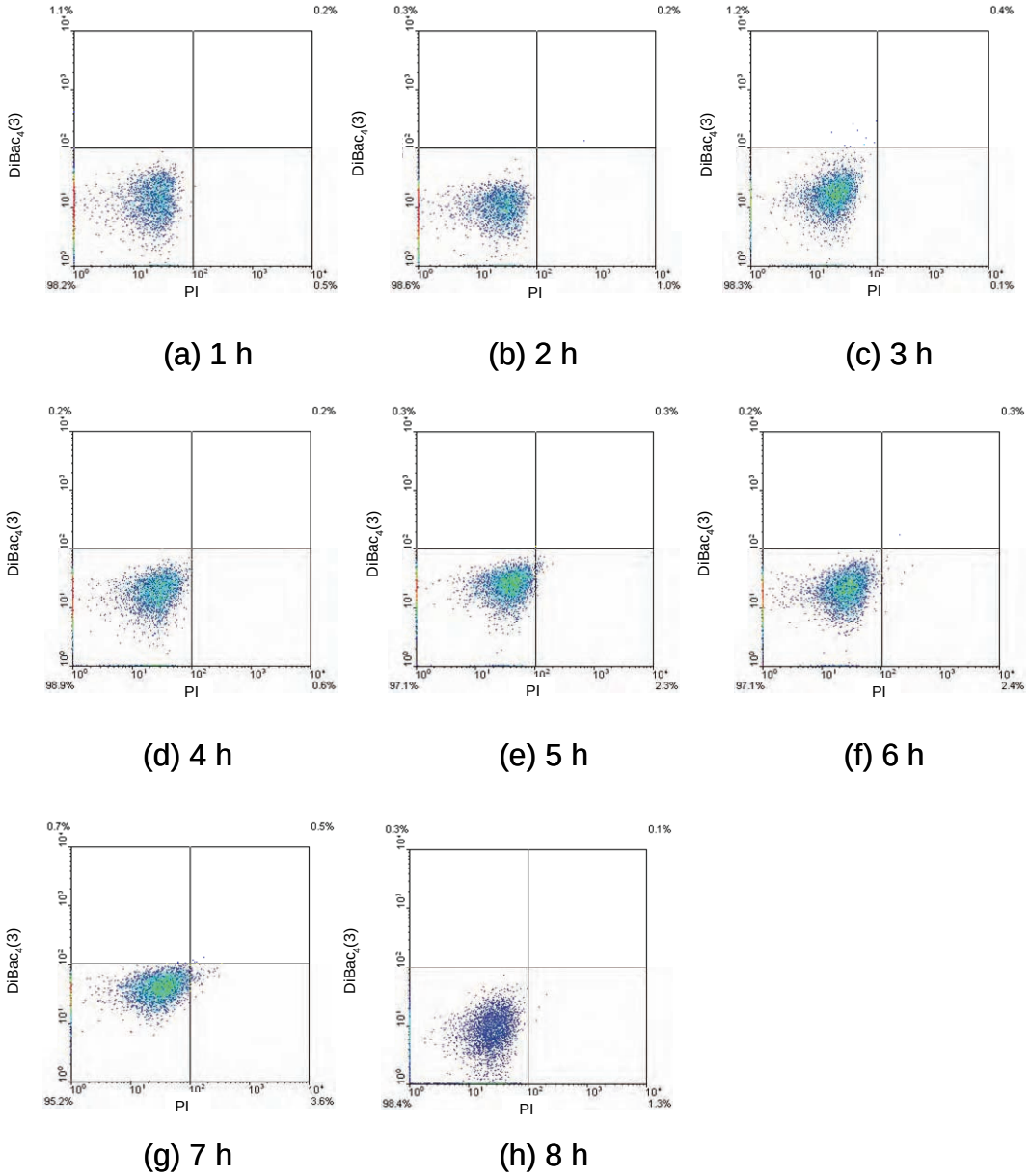

Figure 4.20 Flow cytometry of *Bacillus licheniformis* SJ4628 during shake flask fermentation in yeast malt broth containing 5% v/v DMSO, at 37 °C and 200 rpm agitation speed; (a) 1h, (b) 2h, (c) 3h, (d) 4h, (e) 5h, (f) 6h, (g) 7h, (h) 8h. Results are shown for the fluorophore combination; $DiBac_4(3)$/PI.

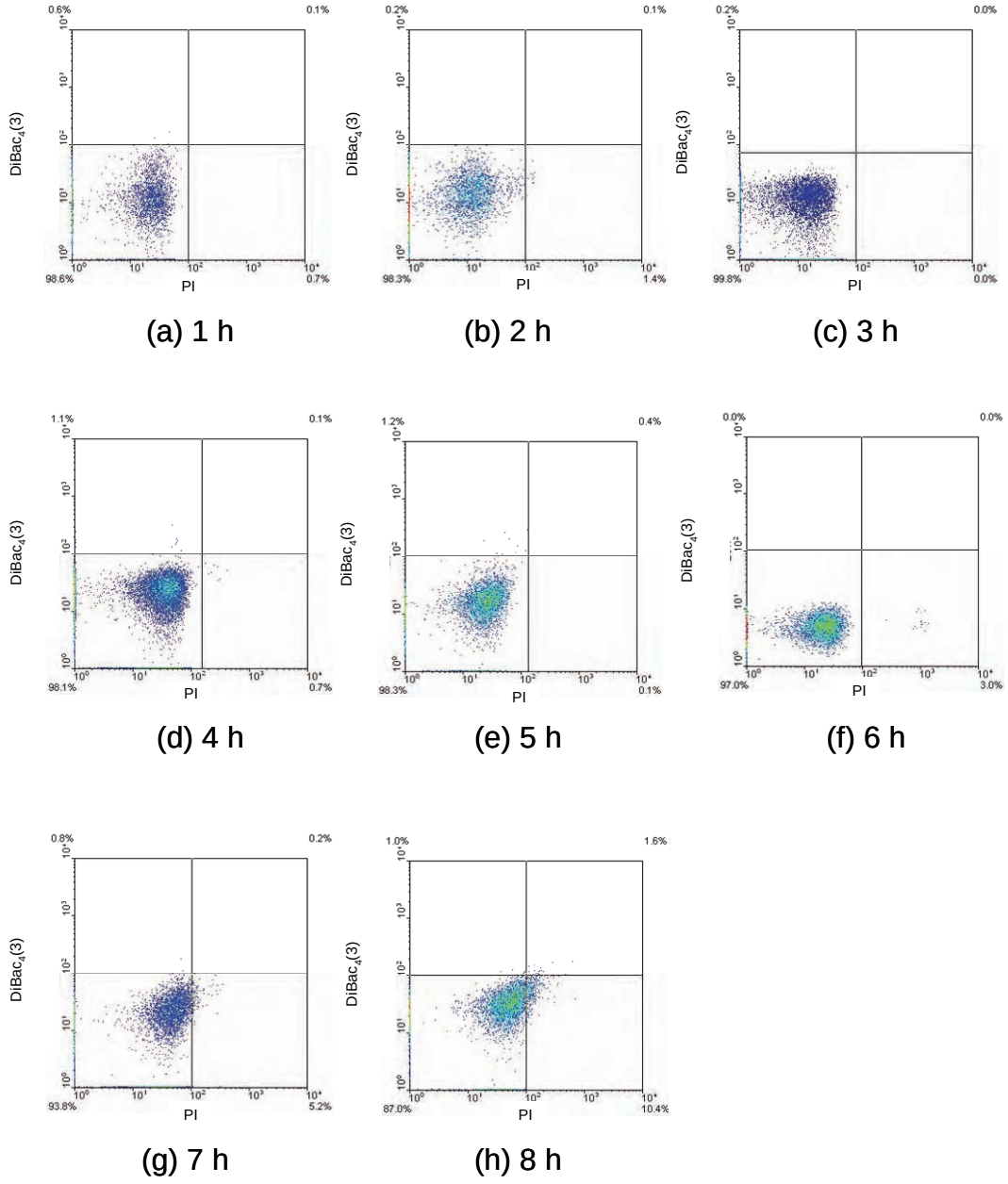

Figure 4.21 Flow cytometry of *Bacillus licheniformis* SJ4628 during shake flask fermentation in yeast malt broth containing 10% v/v DMSO, at 37 °C and 200 rpm agitation speed; (a) 1h, (b) 2h, (c) 3h, (d) 4h, (e) 5h, (f) 6h, (g) 7h, (h) 8h. Results are shown for the fluorophore combination; $DiBac_4(3)$/PI.

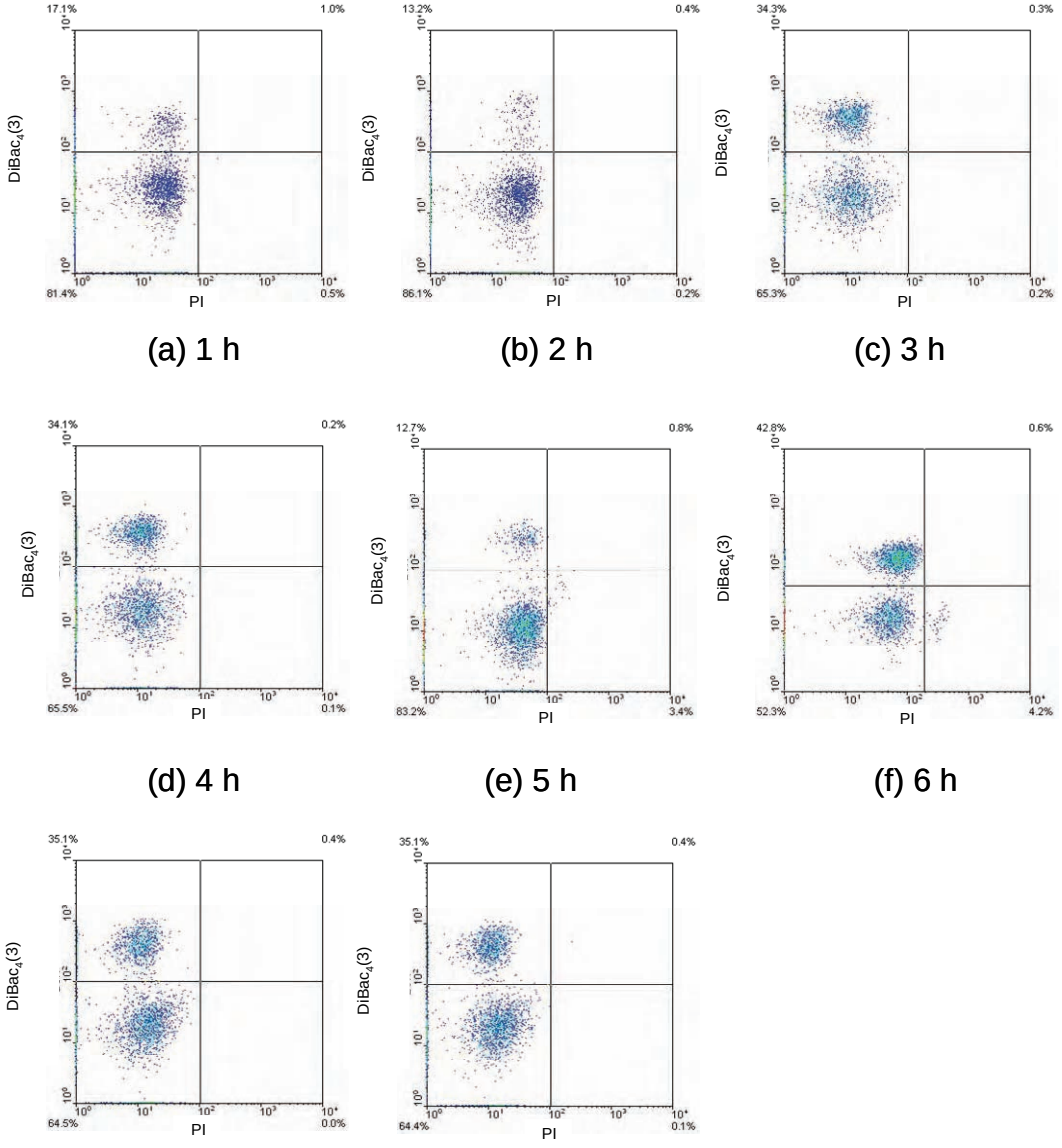

Figure 4.22 Flow cytometry of *Bacillus licheniformis* SJ4628 during shake flask fermentation in yeast malt broth containing 15% v/v DMSO, at 37 °C and 200 rpm agitation speed; (a) 1h, (b) 2h, (c) 3h, (d) 4h, (e) 5h, (f) 6h, (g) 7h, (h) 8h. Results are shown for the fluorophore combination; $DiBac_4(3)$/PI.

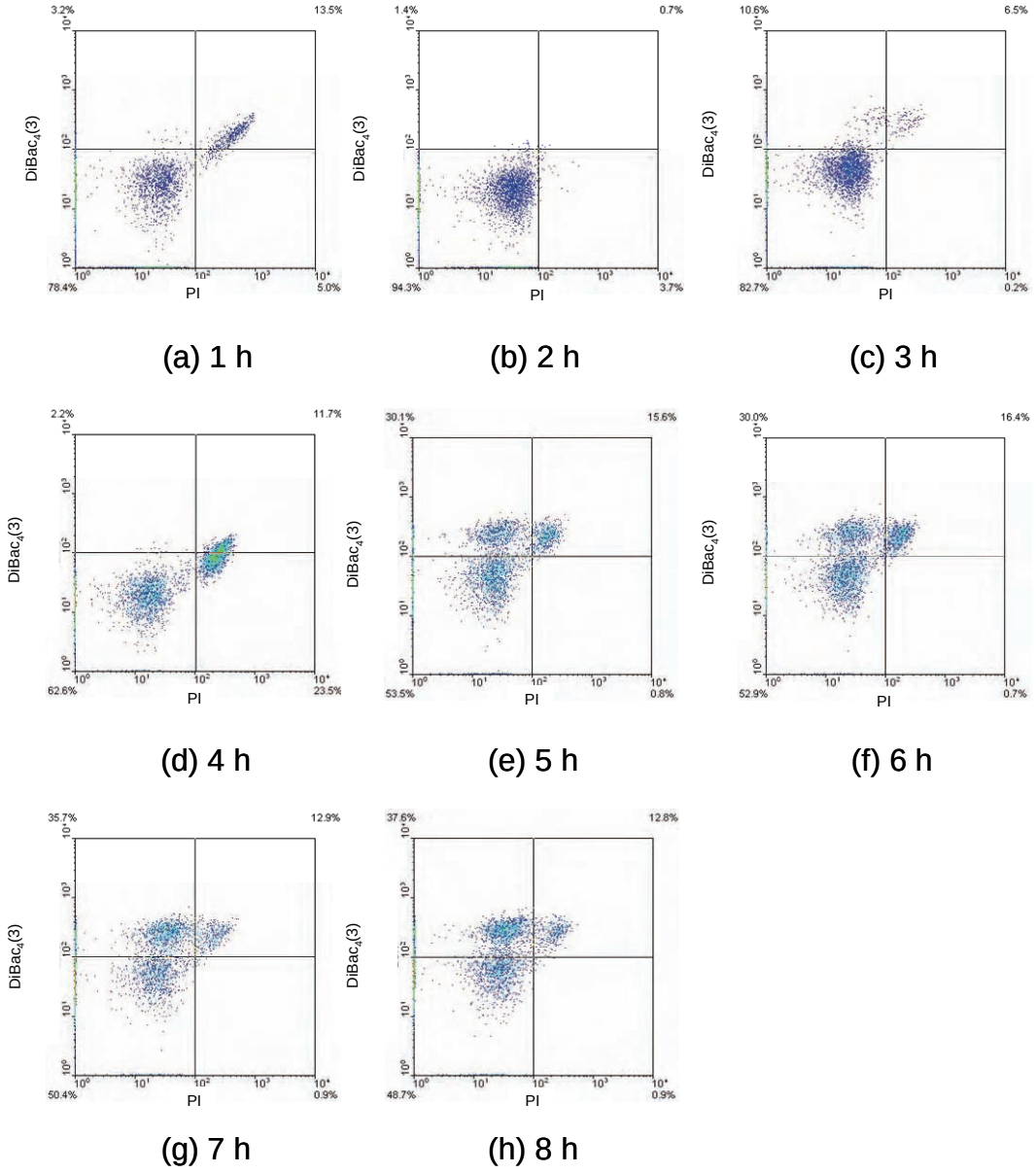

(a) 1 h (b) 2 h (c) 3 h

(d) 4 h (e) 5 h (f) 6 h

(g) 7 h (h) 8 h

Figure 4.23 Flow cytometry of *Bacillus licheniformis* SJ4628 during shake flask fermentation in yeast malt broth containing 20% v/v DMSO, at 37 °C and 200 rpm agitation speed; (a) 1h, (b) 2h, (c) 3h, (d) 4h, (e) 5h, (f) 6h, (g) 7h, (h) 8h. Results are shown for the fluorophore combination; $DiBac_4(3)$/PI.

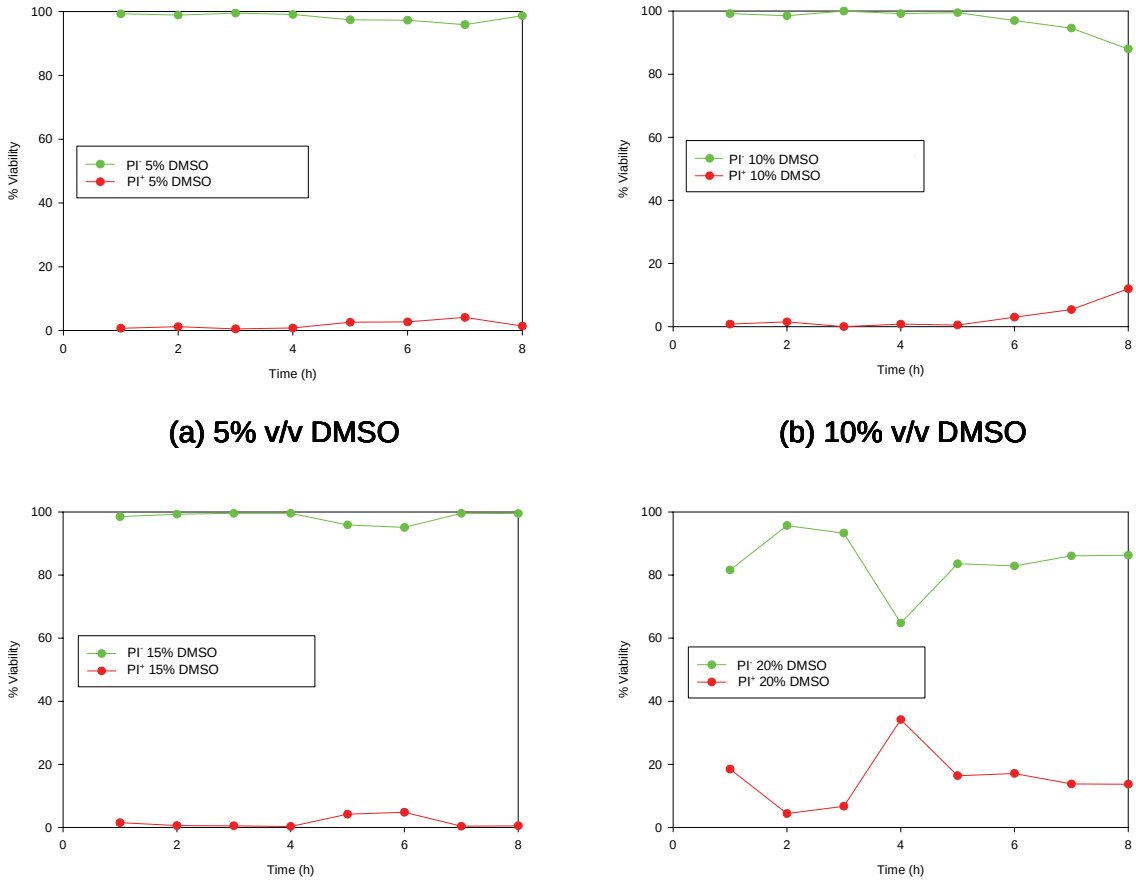

Figure 4.24 Flow cytometry of *Bacillus licheniformis* SJ4628 during shake flask fermentation in yeast malt broth containing different concentrations of DMSO (0 to 20% v/v), at 37 °C and 200 rpm agitation speed. Profiles of PI^- (green) and PI^+ (red) cells are shown for fluorophore combination; $DiBac_4(3)$/PI.

Figure 4.19 shows the $CFUmL^{-1}$ results for the shake flask fermentations of *B. licheniformis* SJ4628 containing concentrations of 0% to 20% v/v DMSO. The 0% experiment represents the normal growth of *B. licheniformis* SJ4628 over the 8 h time course. The cells grown in 5% DMSO showed a slightly higher level of growth than in 0% DMSO for 1 to 5 h presumably as they can metabolise DMSO to dimethyl sulphide and produce energy (Dworkin *et al*., 2006). With further increases in the DMSO concentration from 10% to 20% there was a dramatic decline in the amount of reproductively viable cells. Figure 4.20a to h and Figure 4.24a showed that during the fermentation with 5% DMSO the cells remained polarised throughout the entire fermentation. Figure 4.21a to h and Figure 4.24b showed that the cells grown in 10% DMSO remained polarised throughout the 8 h fermentation. Figure 4.22a to h and Figure 4.24c show that cells grown with 15% DMSO remained polarised during the fermentation but with an associated de-polarised population. Figure 4.23a to h and Figure 4.24d showed the cells grown in 20% DMSO contained a permeablised cell population 1 h into the fermentation and from 5 h show polarised, de-polarised and permeablised cell populations. Increasing concentrations of DMSO did not appear to affect the $DiBac_4(3)$ stain in the same way that glycerol does. The toxic effects of DMSO have been demonstrated by Gurtovenko *et al*., 2007 (Chapter 2) who demonstrated that at low concentrations DMSO causes lateral expansion and a reduction in the thickness of lipid membranes followed at higher concentrations by the formation of water pores

and water defects and increased thinning of the lipid bilayer. Finally, at high concentrations desorption of the lipid molecules from the membrane surface occurs and the bilayer structure completely disintegrates. The toxicity of DMSO may also have been mediated through the effects of osmosis leading to cellular dehydration.

From these experiments 15% v/v DMSO is the highest concentration which is non-toxic to *B. licheniformis* SJ4628 and was therefore chosen as the concentration with which to prepare cell banks and complete further experiments.

4.1.2.4 Yeast malt broth containing different concentrations of polyoxyethylene sorbitan monooleate (Tween 80)

These experiments had the overall aim of discovering the highest concentration at which Tween 80 is non-toxic to *B. licheniformis* SJ4628 so that it could be used for cell bank preparation for further experiments.

Measurements of $CFUmL^{-1}$ (Figure 4.25) were used as a measure of reproductive growth and multi-parameter flow cytometry ($DiBac_4(3)$ and PI) was used to monitor the physiological status of cells during the course of the fermentation (Figure 4.26 to 4.29 to 4.30a to d).

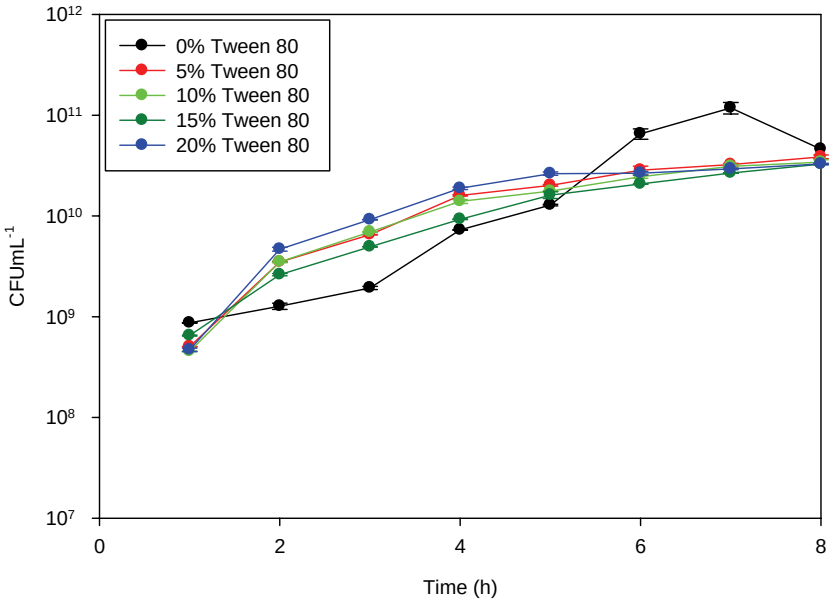

Figure 4.25 Time course of *Bacillus licheniformis* SJ4628 during shake flask fermentation in YM broth containing different concentrations of Tween 80, at 37 °C and 200 rpm agitation speed. Error bars represent the range of data collected from three replicate experiments.

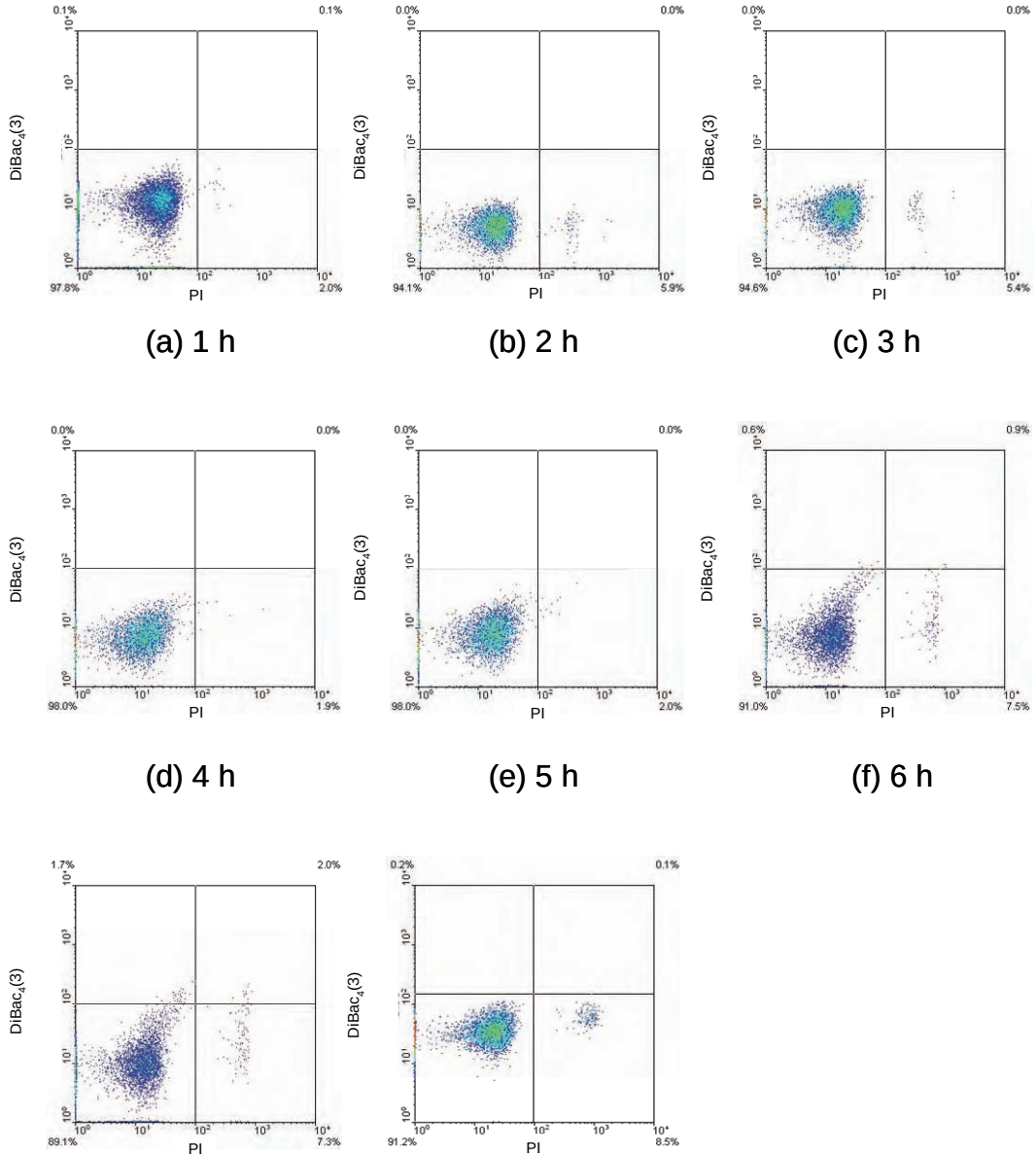

Figure 4.26 Flow cytometry of *Bacillus licheniformis* SJ4628 during shake flask fermentation in yeast malt broth containing 5% v/v Tween 80, at 37 °C and 200 rpm agitation speed; (a) 1h, (b) 2h, (c) 3h, (d) 4h, (e) 5h, (f) 6h, (g) 7h, (h) 8h. Results are shown for the fluorophore combination; $DiBac_4(3)$/PI.

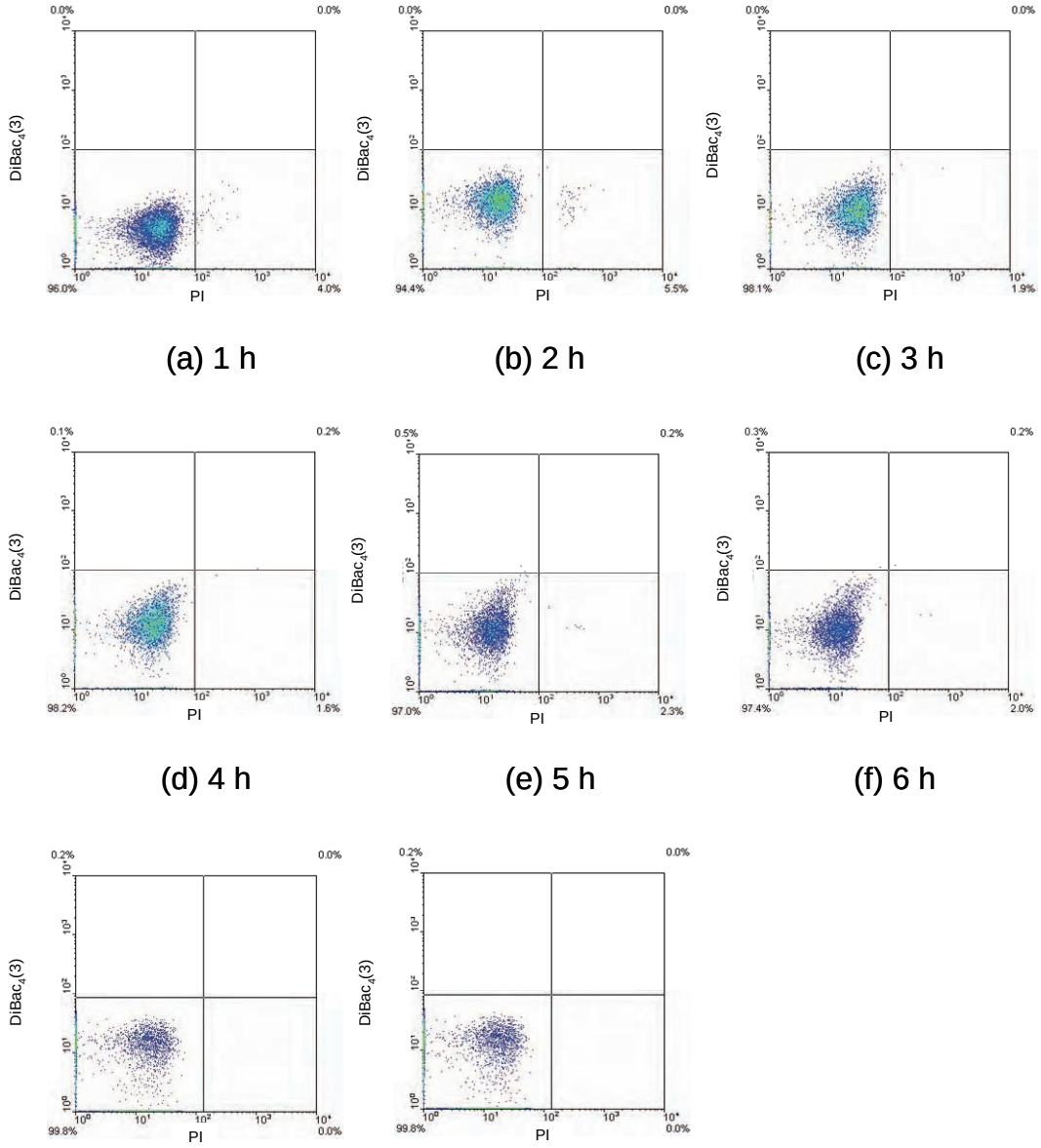

Figure 4.27 Flow cytometry of *Bacillus licheniformis* SJ4628 during shake flask fermentation in yeast malt broth containing 10% v/v Tween 80, at 37 °C and 200 rpm agitation speed; (a) 1h, (b) 2h, (c) 3h, (d) 4h, (e) 5h, (f) 6h, (g) 7h, (h) 8h. Results are shown for the fluorophore combination; $DiBac_4(3)$/PI.

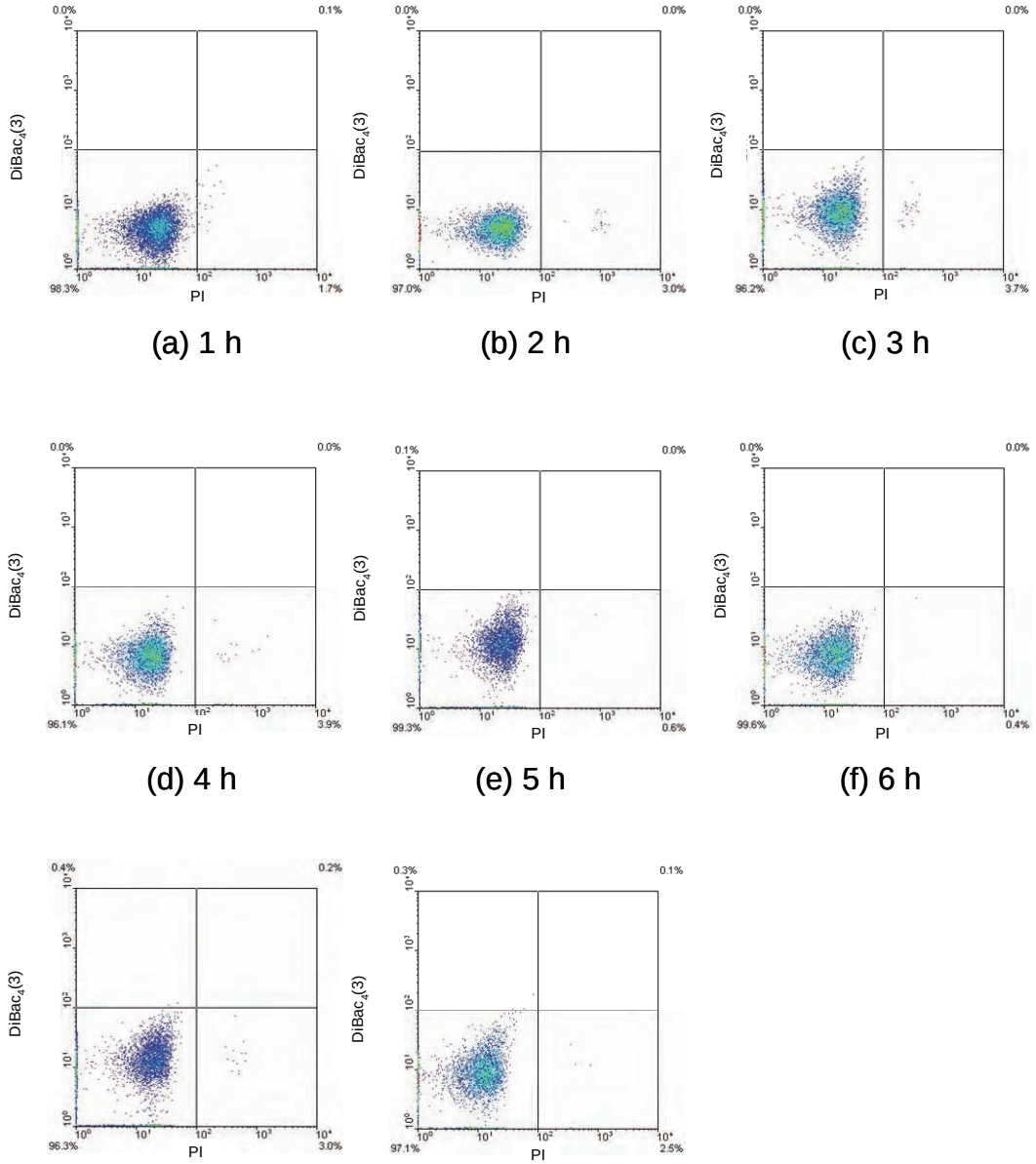

(a) 1 h (b) 2 h (c) 3 h

(d) 4 h (e) 5 h (f) 6 h

(g) 7 h (h) 8 h

Figure 4.28 Flow cytometry of *Bacillus licheniformis* SJ4628 during shake flask fermentation in yeast malt broth containing 15% v/v Tween 80, at 37 °C and 200 rpm agitation speed; (a) 1h, (b) 2h, (c) 3h, (d) 4h, (e) 5h, (f) 6h, (g) 7h, (h) 8h. Results are shown for the fluorophore combination; $DiBac_4(3)$/PI.

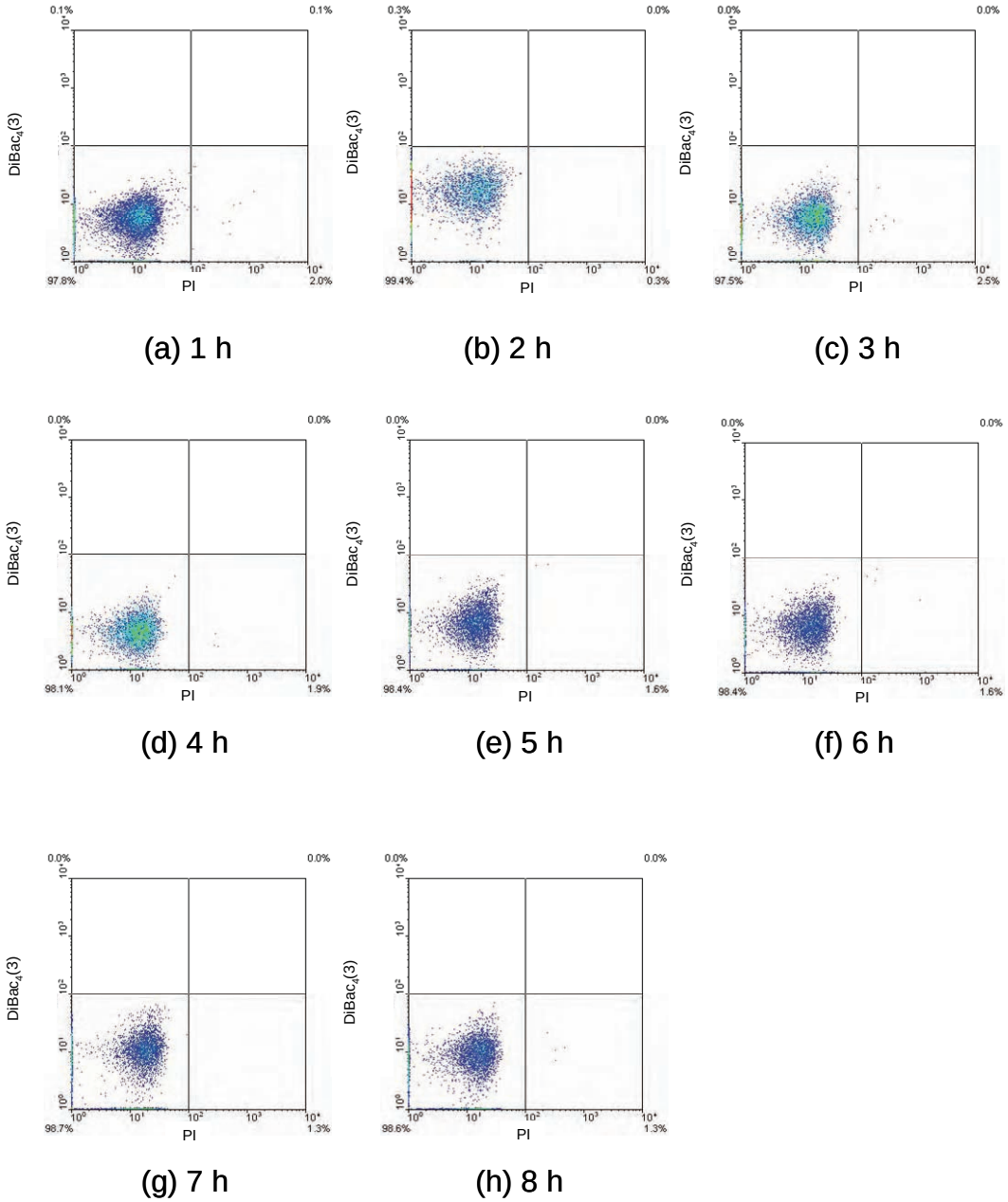

Figure 4.29 Flow cytometry of *Bacillus licheniformis* SJ4628 during shake flask fermentation in yeast malt broth containing 20% v/v Tween 80, at 37 °C and 200 rpm agitation speed; (a) 1h, (b) 2h, (c) 3h, (d) 4h, (e) 5h, (f) 6h, (g) 7h, (h) 8h. Results are shown for the fluorophore combination; $DiBac_4(3)$/PI.

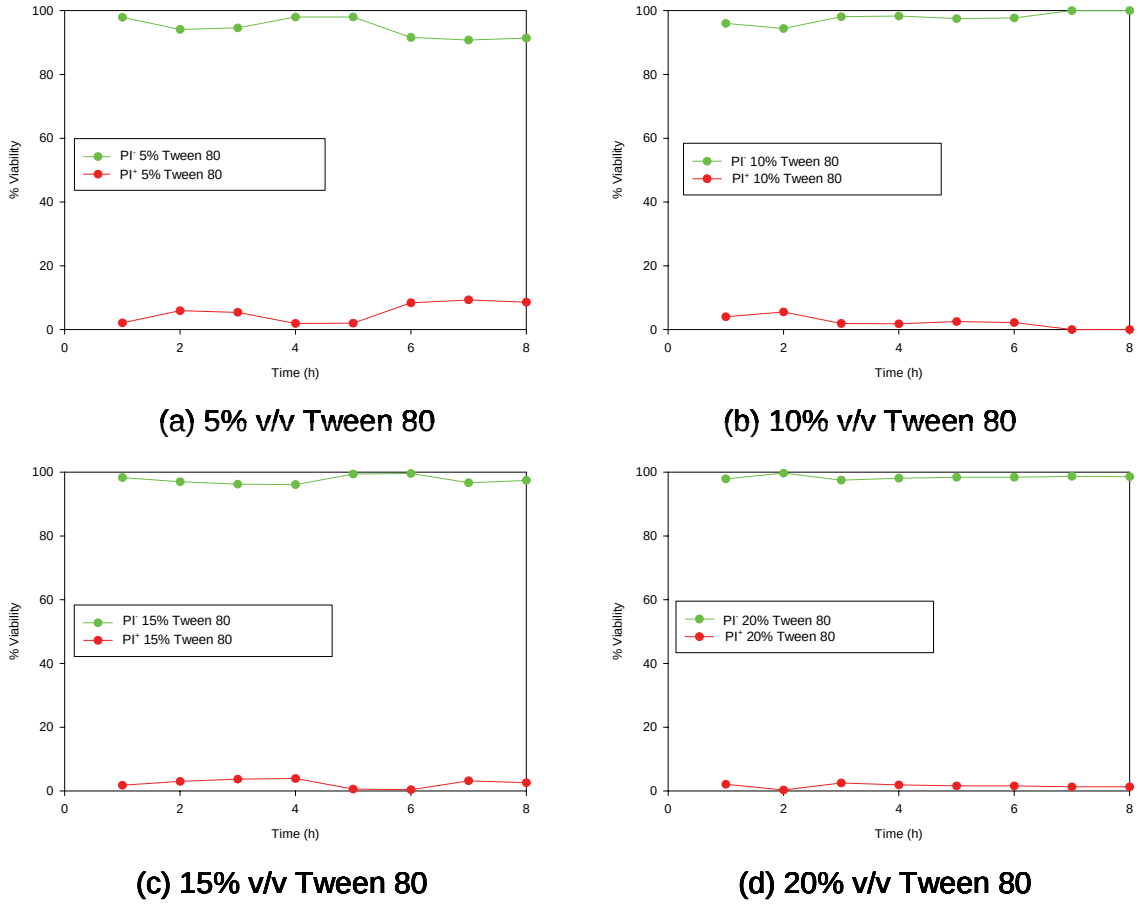

Figure 4.30 Flow cytometry of *Bacillus licheniformis* SJ4628 during shake flask fermentation in yeast malt broth containing different concentrations of Tween 80 (0 to 20% v/v), at 37 °C and 200 rpm agitation speed. Profiles of PI^- (green) and PI^+ (red) cells are shown for fluorophore combination; $DiBac_4(3)$/PI.

Figure 4.25 shows the CFUml^{-1} results for the shake flask fermentations of *B. licheniformis* SJ4628 containing concentrations of 0% to 20% v/v Tween 80. The 0% experiment represents the normal growth of *B. licheniformis* SJ4628 over the 8 h time course. The cells grown in 5% to 20% Tween 80 showed a slightly higher level of growth than in 0% Tween 80 for 1 to 5 h and very little difference in reproductive growth. Figure 4.26a to h and Figure 4.30a show that during the fermentation with 5% Tween 80 the cells remained polarised throughout the entire fermentation. Figure 4.27a to h and Figure 4.30b shows that the cells grown in 10% Tween 80 remained polarised throughout the 8 h fermentation. Figure 4.28a to h and Figure 4.30c show that cells grown with 15% Tween 80 remained polarised during the fermentation. Figure 4.29a to h and Figure 4.30d show the cells grown in 20% Tween 80 demonstrated also remained polarised during the 8 h fermentation. When determining the correct concentration of cryopreservant to use that the highest concentration which is non-toxic to the cells is usually best (Simione., 1998). However, in the case of Tween 80 a number of practical problems arose which have meant that, although concentrations higher than 20% may still be non-toxic to *B. licheniformis* SJ4628, these concentrations could not be used for these experiments for 2 reasons: firstly, Tween 80 is viscous (375-480 mPa.s) at 25 °C, and, secondly, it became increasingly difficult to pipette and because of its surfactant nature foaming became a large problem. As a large molecule (1310 gmol^{-1}) it is unlikely to be able to enter the cells and disrupt the lipid bilayer of the cytoplasmic

membrane in the same way as glycerol and DMSO and this may be why it was non-toxic. Increasing the concentration of Tween 80 from 5 to 20% v/v also had little effect on $CFUmL^{-1}$ values which also indicates that it was non-toxic. From these experiments it can be concluded that none of the concentrations of Tween 80 were toxic to *B. licheniformis* SJ4628 therefore the highest concentration tested (20% v/v) was used to prepare cell banks for further experiments.

4.1.3 *Bacillus licheniformis* SJ4628 growing in yeast malt broth after cryopreservation

4.1.3.1 All cryopreserved cell banks without an overnight incubation step

Based on the data from the shake flask experiments with *B. licheniformis* SJ4628 grown with different cryopreservants (Section 4.1.2) the following cells banks were prepared for the remainder of the work: 20% glycerol, 25% glycerol, 15% DMSO, 20% Tween 80 and no cryopreservant as a control. The inoculum was normally prepared from cells at an OD_{600nm} of 1.0 following an overnight incubation step on agar (Section 3.4.1.2) as this represents a homogeneous viable population of cells when analysed using multi-parameter flow cytometry ($DiBac_4(3)$/PI) (Figure 4.9a). Cells at this stage were approaching the end of the lag phase thereby decreasing the length of the lag phase experienced during an experiment. However, the cells had not yet reached a high enough cell density so that further growth in the bioreactor would be affected. The agar step is used by Novozymes A/S to ensure that each culture is at a similar cell density for inoculation and to remove the effects of different growth rates as cells recover from being frozen. These experiments were designed to defrost each cell bank and grow them up to OD_{600nm} 1.0 without the overnight incubation step on agar to determine if cryopreservation affects growth. All cells used for these experiments were defrosted for 10 minutes at room temperature (20 to 25 °C). Figure 4.31 shows the growth characteristics of each cell bank.

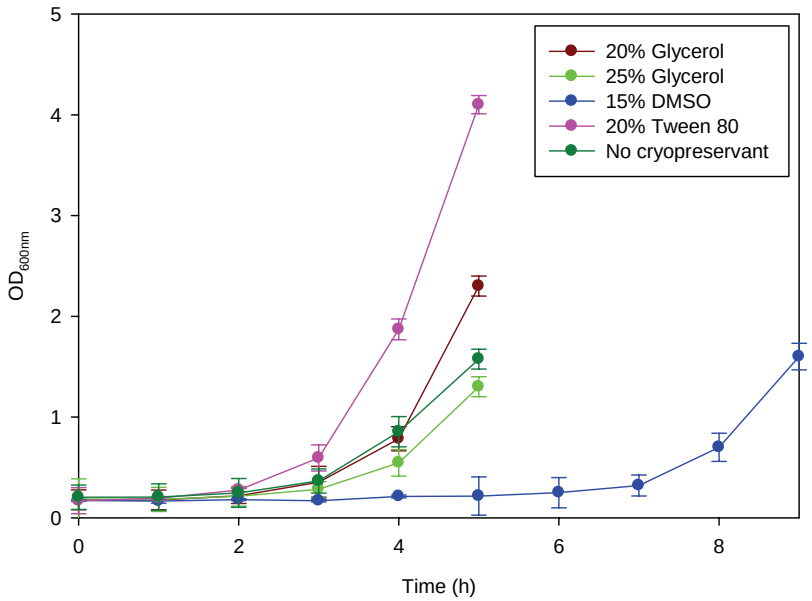

Figure 4.31 Time course of *Bacillus licheniformis* SJ4628 during shake flask fermentation in yeast malt broth, at 37 °C and 200 rpm agitation speed following cryopreservation with different treatments; 20% v/v glycerol, 25% v/v glycerol, 15% v/v DMSO, 20% v/v Tween 80 and no cryopreservant as a negative control. Error bars represent the range of data collected from three replicate experiments.

The results for growing each cell bank in a shake flask fermentation until the optical density at 600nm reached 1.0 revealed that cells cryopreserved with 20% Tween 80 recovered fastest and 15% DMSO took the longest. 20% glycerol, 25% glycerol and no cryopreservant cell banks took a similar length of time to grow to an optical density of 1.0. The differences in recovery times for each cell bank (Figure 4.31) was also observed in the physiological state of the cells during the fermentation measured by multi-parameter flow cytometry ($DiBac_4(3)$ and PI). The flow cytometry results for the fermentation of the cell bank cryopreserved with 20% v/v glycerol are shown in Figure 4.32a to e and 4.33.

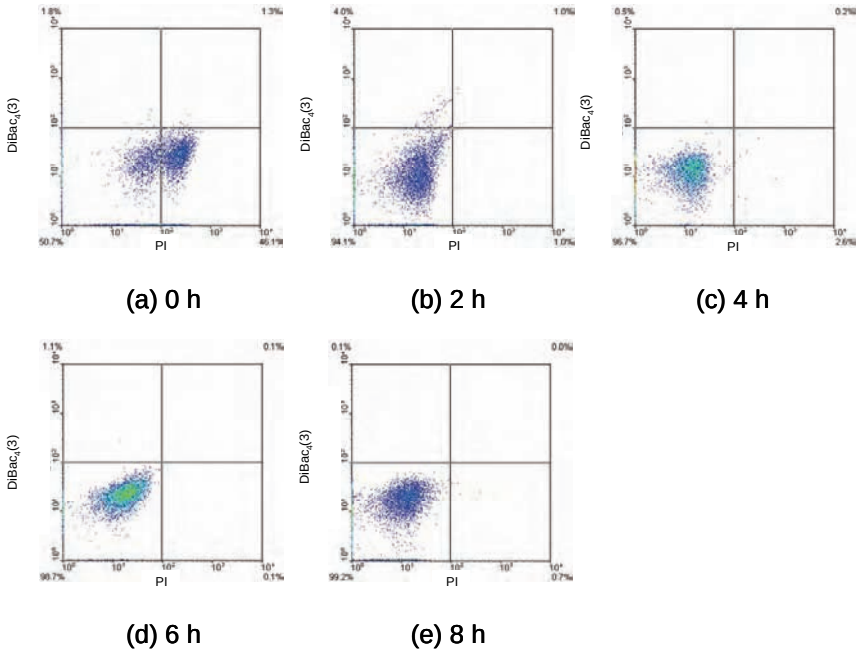

Figure 4.32 Flow cytometry of *Bacillus licheniformis* SJ4628 during shake flask fermentation in yeast malt broth, at 37 °C and 200 rpm agitation speed following cryopreservation with 20% glycerol; (a) 0h, (b) 2h, (c) 4h, (d) 6h, (e) 8h. Results are shown for the fluorophore combination; $DiBac_4(3)$/PI.

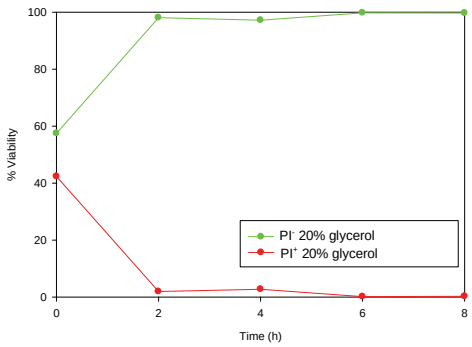

Figure 4.33 Flow cytometry of *Bacillus licheniformis* SJ4628 during shake flask fermentation in yeast malt broth following cryopreservation with 20% glycerol, at 37 °C and 200 rpm agitation speed. Profiles of PI^- (green) and PI^+ (red) cells are shown for the fluorophore combination; $DiBac_4(3)$/PI.

Figure 4.31 shows the sample cryopreserved with 20% glycerol took just over 4 h to reach the optical density of 1.0. Flow cytometry (Figure 4.32a to e and Figure 4.33) reveals that cells at the 0 h time point were split into two subpopulations with 50.7% of the cells polarised and 47.3% of the cells permeablised. By 2 h, they had recovered to being 100% polarised and remained polarised throughout the fermentation.

The flow cytometry results for the fermentation of the cell bank cryopreserved with 25% v/v glycerol are shown in Figure 4.34a to e and 4.35.

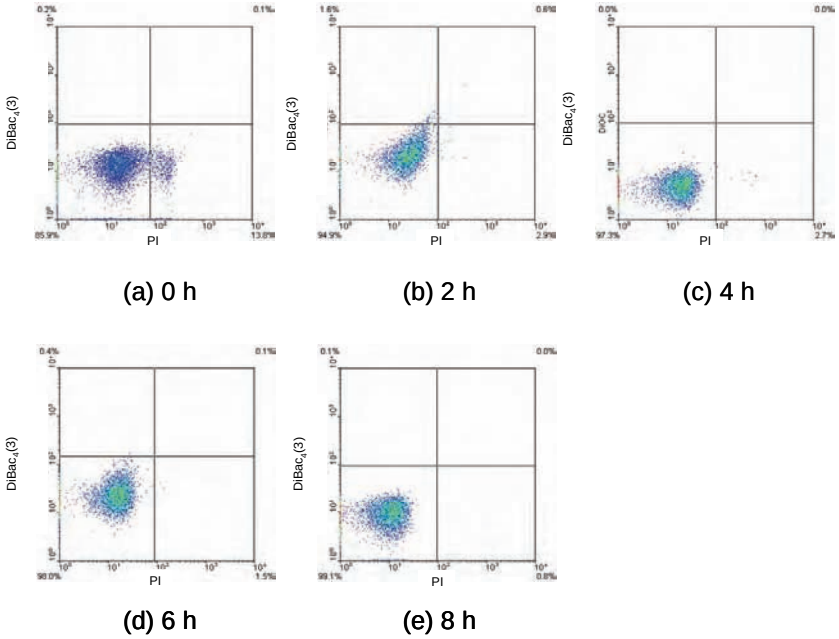

Figure 4.34 Flow cytometry of *Bacillus licheniformis* SJ4628 during shake flask fermentation in yeast malt broth, 37 °C and 200 rpm agitation speed following cryopreservation with 25% glycerol; (a) 0h, (b) 2h, (c) 4h, (d) 6h, (e) 8h. Results are shown for the fluorophore combination; $DiBac_4(3)$/PI.

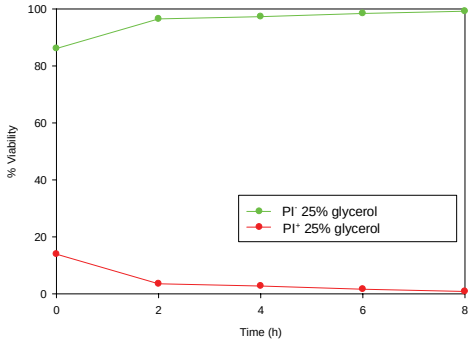

Figure 4.35 Flow cytometry of *Bacillus licheniformis* SJ4628 during shake flask fermentation in yeast malt broth following cryopreservation with 25% glycerol, at 37 °C and 200 rpm agitation speed. Profiles of PI^- (green) and PI^+ (red) cells are shown for the fluorophore combination; $DiBac_4(3)$/PI.

Figure 4.31 shows the sample cryopreserved with 25% glycerol took 5 h to reach the optical density of 1.0. Flow cytometry (Figure 4.34a to e and Figure 4.35) reveals that cells at the 0 h time point were split into two subpopulations with 85.9% of cells being polarised and 14% of cells being permeablised. By 2 h, they had recovered to being 100% polarised and remained polarised throughout the fermentation.

The cells preserved with 20% and 25% glycerol recovered faster than those cryopreserved with DMSO but not as well as those treated with Tween 80. Indicating that a 5% difference in glycerol concentration had little effect in protecting the cells. Interestingly, the samples preserved with glycerol recovered at about the same rate as cells cryopreserved in media only, suggesting that the yeast malt broth may protect cells during freezing.

The flow cytometry results for the fermentation of the cell bank cryopreserved with 15% v/v DMSO are shown in Figure 4.36a to e and 4.37.

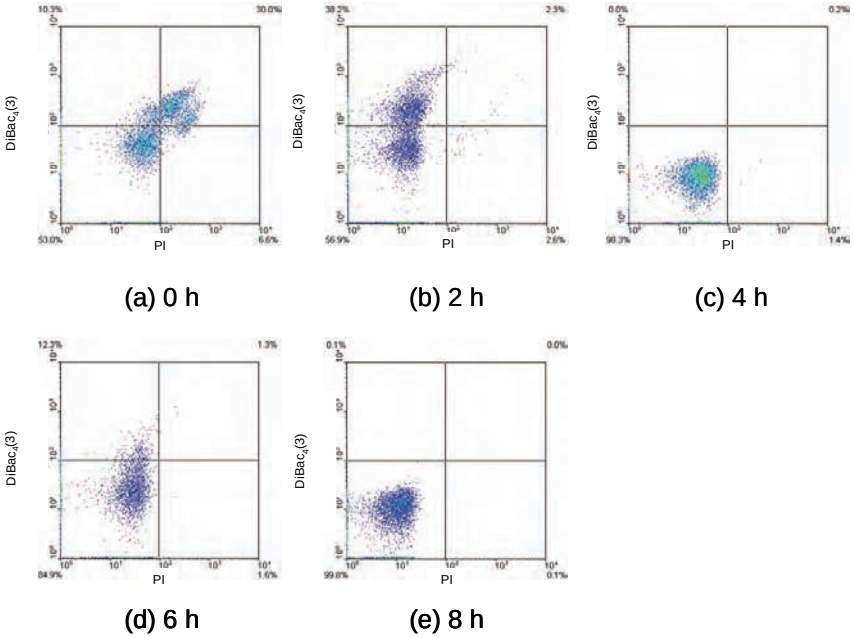

Figure 4.36 Flow cytometry of *Bacillus licheniformis* SJ4628 during shake flask fermentation in yeast malt broth, at 37 °C and 200rpm agitation speed following cryopreservation with 15% DMSO; (a) 0h, (b) 2h, (c) 4h, (d) 6h, (e) 8h. Results are shown for the fluorophore combination; $DiBac_4(3)$/PI.

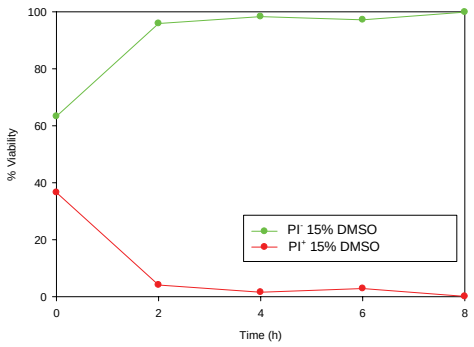

Figure 4.37 Flow cytometry of *Bacillus licheniformis* SJ4628 during shake flask fermentation in yeast malt broth following cryopreservation with 15% DMSO, at 37 °C and 200 rpm agitation speed. Profiles of PI^- (green) and PI^+ (red) cells are shown for the fluorophore combination; $DiBac_4(3)$/PI.

Figure 4.31 shows the sample cryopreserved with 15% DMSO took just over 8 h to reach the optical density of 1.0 and this was the longest time for each of the cell banks tested. Flow cytometry (Figure 4.36a to e and Figure 4.37) revealed that cells at the 0 h time point are split into several subpopulations with 53.0% of cells polarised, 10.3% of cells de-polarised and 36.6% of cells permeablised. By 2 h they showed subpopulations of 56.9% of cells polarised, 38.2% of cells de-polarised and 4.9% of cells permeablised. At 4 h the cells had become 100% polarised and remained polarised throughout the fermentation.

DMSO is known to be toxic to cell membranes at high concentrations because of its small size and its dual hydrophobic and hydrophilic nature (Section 2.2). It easily penetrates the lipid bilayer and also hydrogen bonds to water molecules inside the bilayer and replaces them. This can lead to unfavourable reactions with the polar head groups of the lipid bilayer by inducing dehydration (Sum *et al*., 2003). The unfavourable effects of DMSO are also temperature dependent, becoming more pronounced as temperature increases. This, coupled with a change from a hydrophilic to a hydrophobic nature means that DMSO loses its affinity to water and starts to bind to the lipid bilayer. DMSO has a larger molecular volume than water and its presence causes the lipid bilayer to expand and eventually disintegrate (Sum *et al*., 2003), a process which may have been triggered during thawing.

The flow cytometry results for the fermentation of the cell bank cryopreserved with 20% v/v Tween 80 are shown in Figure 4.38a to e and 4.39.

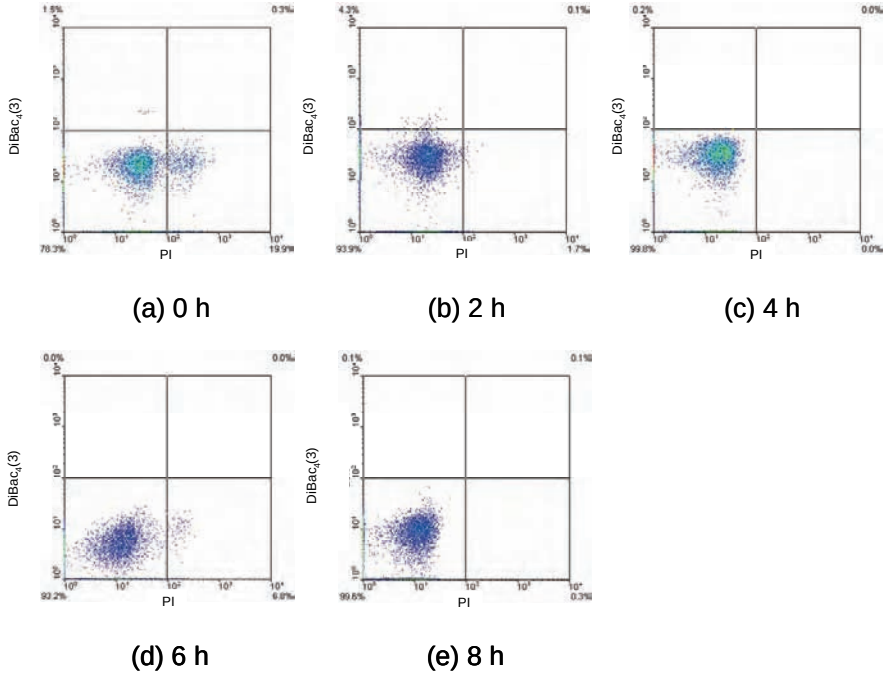

Figure 4.38 Flow cytometry of *Bacillus licheniformis* SJ4628 during shake flask fermentation in yeast malt broth, at 37 °C and 200 rpm agitation speed following cryopreservation with 20% Tween 80; (a) 0h, (b) 2h, (c) 4h, (d) 6h, (e) 8h. Results are shown for the fluorophore combination; $DiBac_4(3)$/PI.

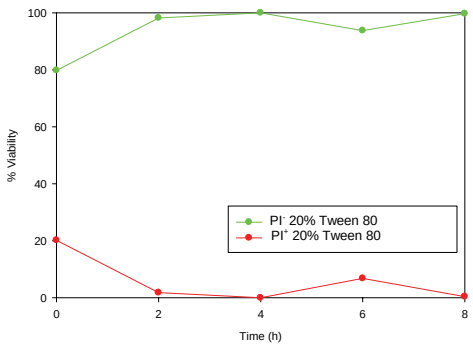

Figure 4.39 Flow cytometry of *Bacillus licheniformis* SJ4628 during shake flask fermentation in yeast malt broth following cryopreservation with 20% Tween 80, at 37 °C and 200 rpm agitation speed. Profiles of PI^- (green) and PI^+ (red) cells are shown for the fluorophore combination; $DiBac_4(3)$/PI.

Figure 4.31 shows the sample cryopreserved with 20% Tween 80 took just over 3 h to reach the optical density of 1.0. Flow cytometry (Figure 4.38a to e and Figure 4.39) revealed that cells at the 0 h time point were split into subpopulations with 78.3% of cells polarised and 20.2% of cells permeablised. By 2 h they had recovered to being 100% polarised and remained polarised throughout the fermentation.

Tween 80 is a large molecule compared to glycerol and DMSO and, therefore, provides a different type of protection to the frozen cells. Work done by Smittle *et al*. (1972) demonstrated that Tween 80 increases the success of cryopreserving *Lactobacillus bulgaricus* when conventional cryopreservant chemicals such as glycerol failed. Beal *et al*. (2001) demonstrated that *Streptococcus thermophilus* showed increased resistance to freezing when the ratio of unsaturated to saturated fatty acids in the cytoplasmic membrane was increased by addition of oleic acid (or Tween 80) to the freeze medium. They also noted that, although glycerol showed positive cryoprotective properties, it does not alter the fatty acid composition of the cytoplasmic membrane (Section 2.2). Oleic acid is a requirement for the formation of microbial cytoplasmic membranes (Endo *et al*., 2006) and its presence may have allowed *B. licheniformis* SJ4628 to repair any damage acquired during the freezing process and recover more quickly than in the presence of the other cryopreservant compounds. Studies by Endo and colleagues found that oleic acid was found to stimulate the growth of *Lactobacillus* species and it was incorporated into the

cytoplasmic membrane lipids where it added to the structural fatty acids already present in the cytoplasmic membrane (Endo *et al*., 2006). The oleic acid component of Tween 80 clearly not only helps to protect microbial cells from the damaging effects of freezing but also is necessary to repair any damage to the cytoplasmic membranes sustained during the freezing process. It is clearly an interesting compound which should be considered as a supplement to the medium of cells that experience cellular damage during bioprocessing.

The flow cytometry results for the fermentation of the cell bank cryopreserved with no cryopreservant are shown in Figure 4.40a to e and 4.41.

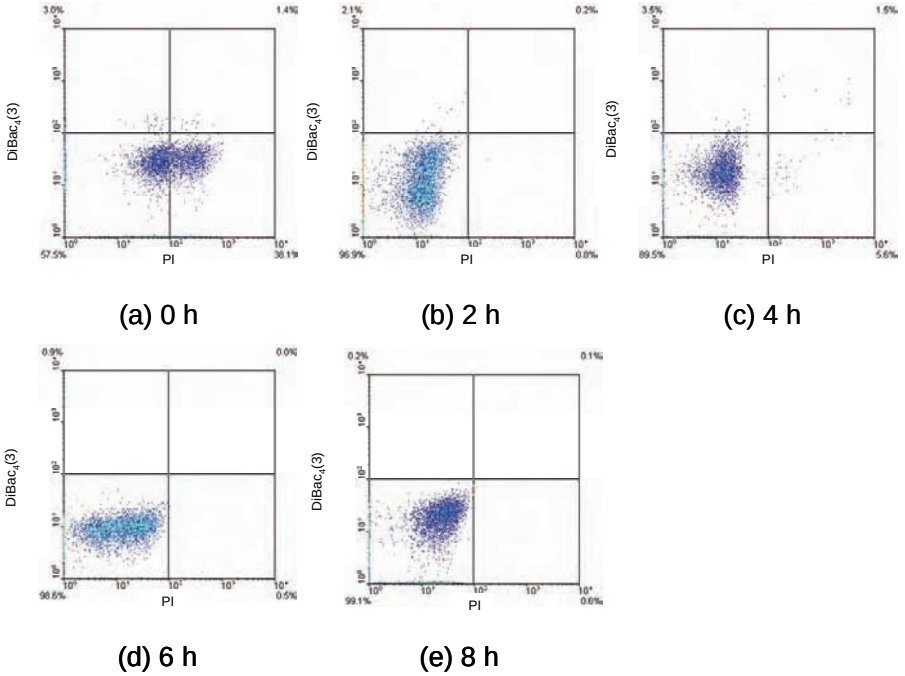

Figure 4.40 Flow cytometry of *Bacillus licheniformis* SJ4628 during shake flask fermentation in yeast malt broth, at 37 °C and 200 rpm agitation speed following cryopreservation with no cryopreservant; (a) 0h, (b) 2h, (c) 4h, (d) 6h, (e) 8h. Results are shown for the fluorophore combination; $DiBac_4(3)$/PI.

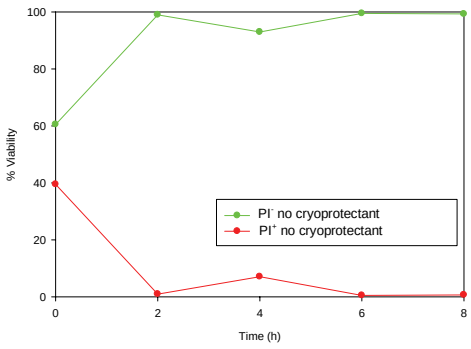

Figure 4.41 Flow cytometry of *Bacillus licheniformis* SJ4628 during shake flask fermentation in yeast malt broth following cryopreservation with no cryoprotectant, at 37 °C and 200 rpm agitation speed. Profiles of PI^- (green) and PI^+ (red) cells are shown for the fluorophore combinations; $DiBac_4(3)$/PI.

Figure 4.31 shows the sample cryopreserved with no cryopreservants took just over 4 h to reach the optical density of 1.0. Flow cytometry (Figure 4.40a to e and Figure 4.41) reveals that cells at the 0 h time point were split into several subpopulations with 57.5% of cells polarised, 3.0% of cells de-polarised and 39.5% of cells permeablised and that by 2 h they had recovered to being 100% polarised and remain polarised throughout the fermentation.

Cells cryopreserved with only the medium to protect them recovered at the same rate as cells cryopreserved in 20 and 25% glycerol indicating that components such as yeast and malt extract and polypropylene glycol in the medium can act as effective cryopreservants. This is supported by a number of studies which report that yeast extract is as good as glycerol at cryopreserving lactic acid bacteria, and is often included in freezing protocols. Malt extract is also used in cryopreservation protocols for lactic acid bacteria (Hubálek, 2003). Work done by Joannsen in 1972 who found that yeast and malt extracts were as successful at cryopreserving lactic acid producing bacteria as DMSO and glycerol (Johannsen, 1972). The media used for these experiments also contains very low concentrations of polypropylene glycol which may have helped to protect the cells as both propylene glycol and ethylene glycol have been shown to work as effective cryopreservants (Hubálek, 2003).

Despite the different lengths of time it took each cryopreserved cell bank to recover, they all did recover and grow to an OD_{600nm} of 1.0. This is supported by the work of Hornbæk and colleagues using the same organism that was used for

this project i.e. *B. licheniformis* SJ4628. They demonstrated cell populations displaying greater heterogeneity had longer lag phases than more homogenous populations (Hornbæk *et al*., 2004) (Section 2.3). From these results it can be concluded that any of the cryopreservation techniques described here could be used for *B. licheniformis* SJ4628. It would be costly for Novozymes A/S to switch to a new cryopreservation protocol if the existing protocol is sufficient. However, if they are experiencing difficulties with a particular cryopreservation protocol then Tween 80 may be an interesting alternative as it not only protects the cells during freezing but also helps them to recover after freezing.

Chapter 5

Results and Discussion

5 L Batch Fermentation

5.1 Growth and physiological characterisation of *Bacillus licheniformis* SJ4628 during 5 L batch fermentation

Microbial growth in a bioreactor has several advantages over shake flask fermentation; for example, increased control of pH and dissolved oxygen levels leading to shorter fermentation cycles due to increased growth of cells. However, rapid growth can lead to overflow metabolism which may impede growth due to build up of toxic chemicals; for example, ethanol in the yeast *S. cerevisiae* and acetate in *E. coli*.

The aim of the work described in this chapter was to determine the growth and physiology of *B. licheniformis* SJ4628 during 5 L batch fermentation and to use this information to calculate the feed rate for a 5 L fed batch process (Chapter 6) which was then used to test each of the different cell banks described in Chapter 4. The 5 L batch fermentation used 20% v/v glycerol as its cell bank as this is the standard used at Novozymes A/S.

5.1.1 *Bacillus licheniformis* SJ4628 growing in yeast malt broth with glucose as the carbon source

A series of three 5 L batch fermentations were performed. The robust nature of *B. licheniformis* SJ4628 as an industrial organism allowed easy duplication of each fermentation. Measurements of OD_{600nm}, DCW (gL^{-1}), $CFUml^{-1}$, pH, glucose concentration (gL^{-1}) and α-amylase activity ($\mu KatL^{-1}$) were recorded (Figure 5.1a to c). The following parameters were monitored during the course of the fermentation: agitation speed (rpm), temperature (°C), pH and dissolved oxygen (%). Figure 5.2 displays their status throughout the fermentation. Throughout the fermentation, samples were collected for HPLC analysis and Figure 5.3 showed the production of several metabolites (acetate, 2,3-butandiol and propionic acid). Multi-parameter flow cytometry ($DiBac_4(3)$ and PI) was used to monitor the physiological status of cells during the course of the fermentation (Figure 5.4a to e and 5.5).

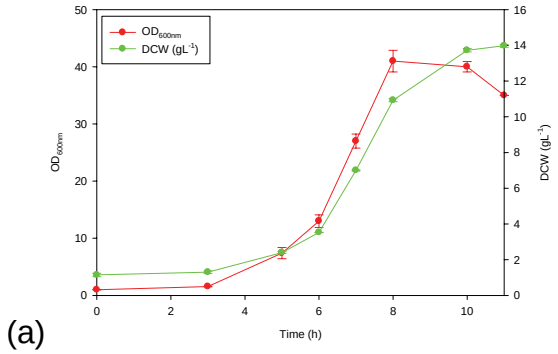

(a)

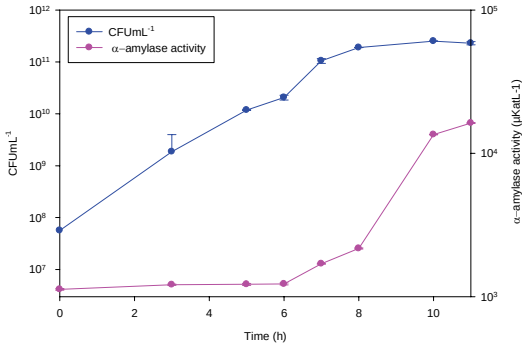

(b)

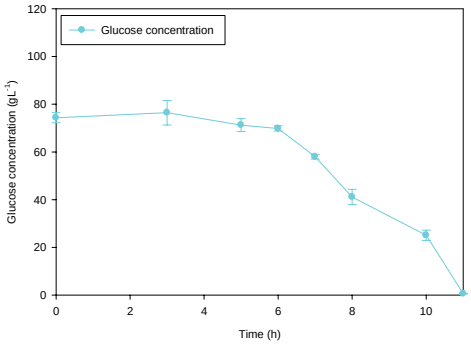

(c)

Figure 5.1 Time course of *Bacillus licheniformis* SJ4628 during 5 L batch fermentation in yeast malt broth supplemented with glucose. Profiles of (a) OD_{600nm} and DCW (gL^{-1}), (b) $CFUmL^{-1}$ and α-amylase activity and (c) glucose concentration are shown and error bars represent the range of data collected from three replicate experiments.

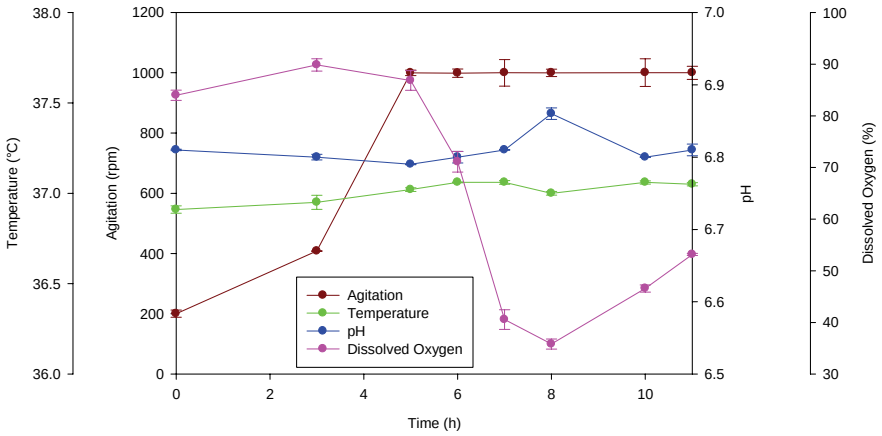

Figure 5.2 Environmental parameters measured during 5 L batch fermentation of *Bacillus licheniformis* SJ4628 in yeast malt broth supplemented with glucose. Profiles of agitation speed (rpm), temperature (°C), pH and dissolved oxygen (%) are shown and error bars represent the range of data collected from three replicate experiments.

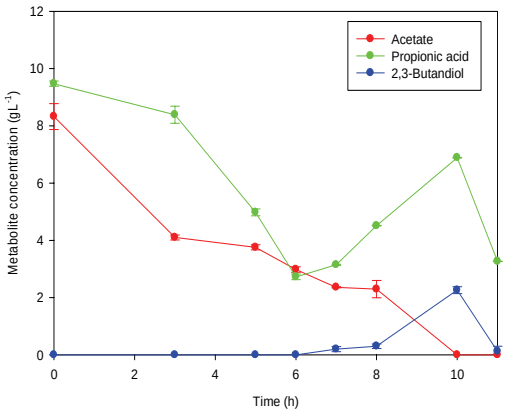

Figure 5.3 Metabolite concentration measured during 5 L batch fermentation of *Bacillus licheniformis* SJ4628 in yeast malt broth supplemented with glucose. Profiles of concentration (gL^{-1}) of acetate, propionic acid and 2,3-butandiol are shown and error bars represent the range of data collected from three replicate experiments.

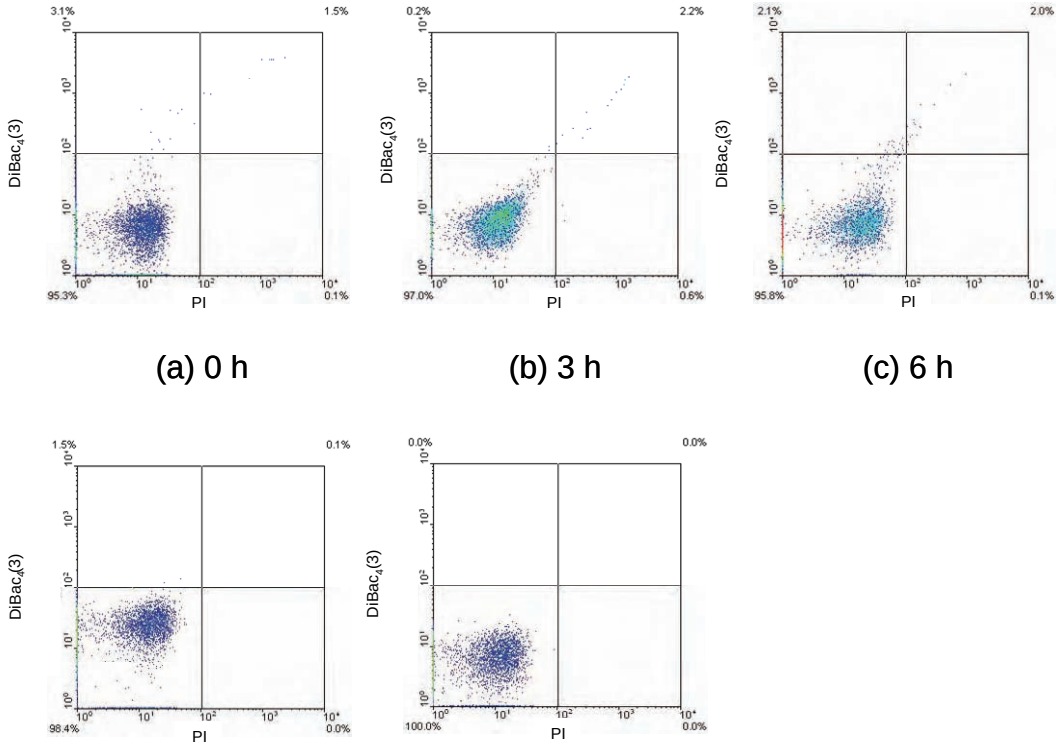

(a) 0 h (b) 3 h (c) 6 h

(d) 10 h (e) 11 h

Figure 5.4 Flow cytometry of *Bacillus licheniformis* SJ4628 during 5 L batch fermentation in yeast malt broth supplemented with glucose: (a) 0h, (b) 3h, (c) 6h, (d) 10h, (e) 11h. Results are shown for the fluorophore combination; $DiBac_4(3)$/PI.

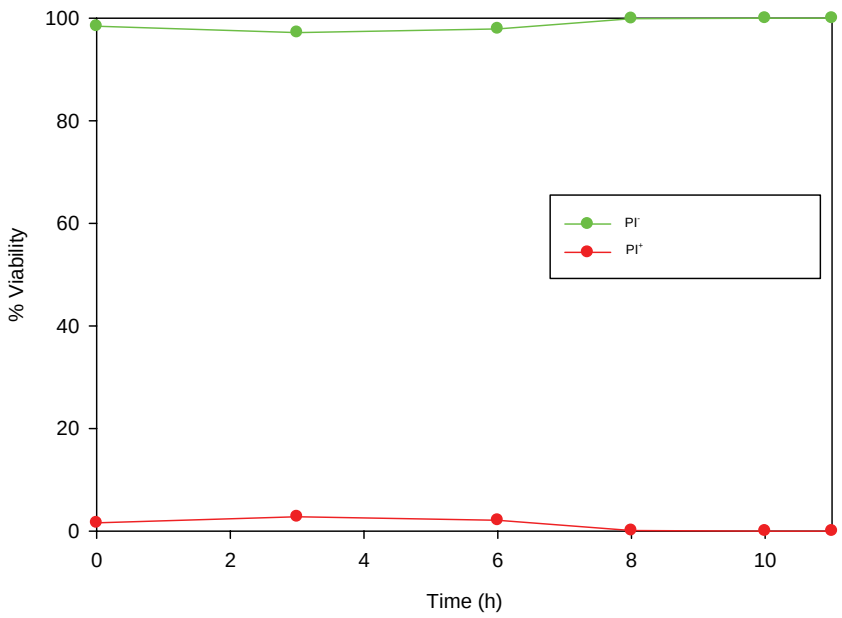

Figure 5.5 Flow cytometry of *Bacillus licheniformis* SJ4628 during 5 L batch fermentation in yeast malt broth supplemented with glucose. Profiles of PI^- (green) and PI^+ (red) cells are shown for the fluorophore combination; $DiBac_4(3)$/PI.

Figure 5.1a shows the OD_{600nm} and DCW (gL^{-1}), Figure 5.1b shows the $CFUml^{-1}$ and α-amylase activity and Figure 5.1c glucose concentration for the batch fermentation of *B. licheniformis* SJ4628. *B. licheniformis* SJ4628 showed a typical microbial fermentation profile during the 5 L batch fermentation with increased growth and α-amylase production when compared to the shake flask (Figure 4.8a to c). Following a 3 h lag phase, the mean specific growth rate (μ) was calculated as 0.25 h^{-1} using optical density data from the 6 and 8 h time points. The optical density, DCW (gL^{-1}) and $CFUml^{-1}$ showed a steady increase up to 5 h and then they increased dramatically to a maximum optical density at 8 h of 41; a maximum DCW (gL^{-1}) of 13.98 gL^{-1} appeared at 11 h and a maximum $CFUml^{-1}$ of 2.51 x 10^{11} at 10 h. Consumption of glucose closely followed the rapid growth of the cells, glucose concentration declined slowly for the first 6 h of the fermentation from 74.36 gL^{-1} at 0h to 69.87 gL^{-1} at 6 h and the declined more rapidly for the remainder of the process to a minimum of 0.57 gL^{-1} at 11 h. Production of α-amylase is controlled by catabolite repression of the *amyE* gene (Voigt *et al*., 2009) and this explains why α-amylase is produced later on in the fermentation when the glucose concentration began to fall. The α-amylase activity was very low for the first 6 h and then increased steadily to a maximum of 16250 $\mu KatL^{-1}$ at 11 h, this was 3 times the yield of α-amylase that was produced in the shake flask experiments. During the course of the fermentation, as Figure 5.2 shows, the pH remained between 6.8 and 6.9 and the temperature between 36.5 and 37.0 °C. The agitation rate started to increase

from the beginning of the fermentation to cope with the rapidly increasing growth of the culture until the maximum of 1000 rpm. This was mirrored by the gradual decline in dissolved oxygen between 5 and 8 h when the cells were growing rapidly, it was not possible to maintain the 90% dissolved oxygen concentration set point. Figure 5.3 shows the HPLC results for metabolite concentration during the fermentation. *B. licheniformis* SJ4628 produced three different metabolites: acetate, propionic acid and 2,3-butandiol. The concentration of acetate was at its highest at the beginning of the fermentation with a value of 8.33 gL^{-1} at 0 h and then gradually fell throughout the fermentation to 2.30 gL^{-1} at 8 h; from 10 h until the end of the fermentation the concentration of acetate was undetectable. Propionic acid concentration was at its maximum at the start of the fermentation with a value of 9.50 gL^{-1} at 0 h and then declined to a value of 3.15 gL^{-1} at 7 h. The concentration of propionic acid then increased to 6.89 gL^{-1} at 10 h before finally dropping to 3.27 gL^{-1} at 11 h. The concentration of 2,3-butandiol was undetectable until the 7 h time point where it measured 0.20 gL^{-1} and then showed a steady incline to its maximum of 2.26 gL^{-1} at 10 h before finally falling to 0.13 gL^{-1} at 11 h. The production of these metabolic products is affected by two important parameters measured during this experiment: glucose concentration and dissolved oxygen concentration. If excess glucose is present in the medium, it is not all used for energy production and cell growth, but is diverted into maintenance energy, overflow metabolism and futile energy cycles. The dissolved oxygen concentration is also known to have a profound effect on

cellular metabolism. In an environment with excess oxygen, glucose is completely oxidised to carbon dioxide and water via pyruvate, the citric acid cycle and oxidative phosphorylation. At lower than adequate oxygen concentrations, pyruvate is converted to organic metabolites. The concentration of acetate declined throughout the fermentation, indicating that both high concentrations of glucose and oxygen are required for its production. The concentration of propionic acid decreased up to the 6 h time point before it increased again. This trend closely followed the changes in dissolved oxygen concentration. The concentration of 2,3-butandiol was negligible up to 6 h when it started to increase in concentration; between 8 and 10 h the concentration increased sharply. This corresponded to low glucose and low dissolved oxygen concentrations. The relationship between dissolved oxygen concentration and metabolic product accumulation has been studied using the organism *B. subtilis* AJ1992 by Moes *et al*. (1984) and Amanullah *et al*. (2001b) who have shown that acetoin and 2,3-butandiol are produced during a specific range in dissolved oxygen concentration and that the effect is reversible. The production of 2,3-butandiol was shown to accumulate at low dissolved oxygen concentrations (below 1000 ppm) which agrees with the findings of this experiment. *B. licheniformis* is also capable of metabolising acetate and 2,3-butandiol as sole energy sources and contains genes which are homologous to isocitrate lyase and malate synthase of the glyoxylate shunt pathway, so it may be that acetate and 2,3-butandiol are being produced for use as a carbon source. *B. licheniformis* contains the genes for

acetate activation via acetyl coA synthetase (*acs* gene) and butanediol breakdown (*aco* and *acu* operons) (Voigt *et al*., 2009).

Figures 5.4a to e and 5.5 show the flow cytometry results during the course of the fermentation and reveal that the culture is predominantly polarised up to 6 h, although there are a small number of de-polarised and permeablised cells as the culture progresses through the lag phase. Throughout the course of the rest of the process, up to 11 h, the cells are fully polarised, indicating that as an industrial organism it has a robust nature and is well suited to being grown in laboratory culture conditions.

B. licheniformis SJ4628 grew well in the larger scale environment with an associated higher level of growth and biomass concentration and an increased production of α-amylase compared with the shake flask experiments. There was very little population heterogeneity and levels of overflow metabolism were very low further reflecting the industrial heritage of this organism.

Chapter 6

Results and Discussion

5 L Fed Batch Fermentation

6.1 Growth and physiological characterisation of *Bacillus licheniformis* SJ4628 during 5 L fed batch fermentation

Microbial growth in a bioreactor has several advantages over shake flask fermentation as mentioned in Chapter 5. Fed batch fermentation also has advantages over the batch process as it allows the carbon source, in this case glucose to be delivered to the cells in a controlled manner. The initial high levels of glucose used during a batch process may lead to lower yields of α-amylase as they cause carbon catabolite repression (Priest, 1977).

The aim of the work in this chapter was to determine the growth and physiology of *B. licheniformis* SJ4628 during 5 L fed batch fermentation using each of the different cell banks: 20% glycerol, 25% glycerol, 15% DMSO, 20% Tween 80 and no cryopreservant cell bank described in Chapter 4 and to determine if different cryoprotective compounds have an effect on overall process performance i.e. yield of α-amylase. The feed was started at 3 h and increased exponentially to 10 h and then kept constant until the end of the fermentation.

6.1.1 *Bacillus licheniformis* SJ4628 5 L fed batch fermentations following cryopreservation with and without cryopreservants

A series of duplicate 5 L fed batch fermentations were performed and due to the highly robust nature of *B. licheniformis* SJ4628 as an industrial production strain each fermentation was highly reproducible not only with each individual cell bank but also between all of the cell banks tested. Measurements of OD_{600nm} and DCW (gL^{-1}) (Figure 6.1a, 6.6a, 6.11a, 6.16a and 6.21a), $CFUml^{-1}$ and α-amylase activity ($\mu KatL^{-1}$) (Figure 6.1b, 6.6b, 6.11b, 6.16b and 6.21b) and glucose concentration (gL^{-1}) (Figure 6.1c, 6.6c, 6.11c, 6.16c and 6.21c) were taken throughout the fermentation. The following parameters were monitored during the course of the fermentation: agitation speed (rpm), temperature (°C), pH and dissolved oxygen (%) (Figure 6.2, 6.7, 6.12, 6.17 and 6.22). Production of metabolites was monitored using high pressure liquid chromatography (HPLC) (Figure 6.3, 6.8, 6.13, 6.18 and 6.23). Table 6.1 shows a comparison of the mean specific growth rates for each fermentation. Multi-parameter flow cytometry ($DiBac_4(3)$ and PI) (Section 2.8) was used to monitor the physiological status of cells during the course of the fermentation (Figure 6.4a to h, 6.9a to h, 6.14a to h, 6.19a to h, 6.24a to h and 6.5, 6.10, 6.15, 6.20, 6.25). Results are shown for fermentations with each different cell bank (Figure 6.1 to 6.25) and as a summary comparing fermentations with each cell bank (Figure 6.26 to 6.37 and Table 6.1).

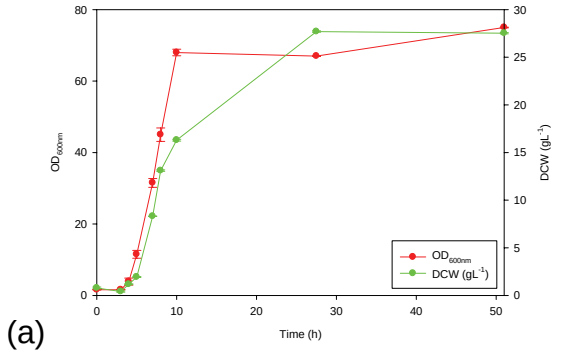

(a)

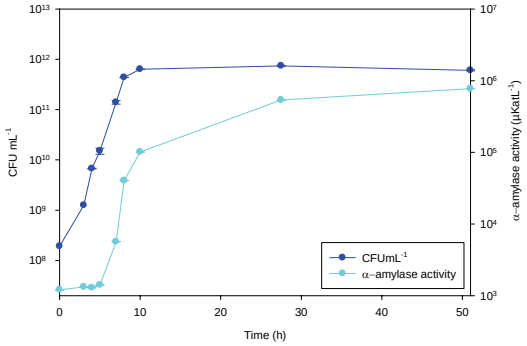

(b)

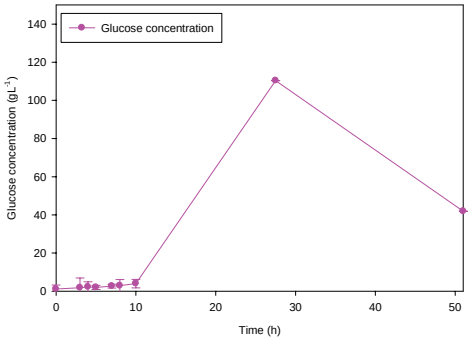

(c)

Figure 6.1 Time course of *Bacillus licheniformis* SJ4628 during 5 L fed batch fermentation in yeast malt broth with a glucose feed source, following cryopreservation with 20% v/v glycerol. Profiles of (a) OD_{600nm} and DCW (gL^{-1}), (b) $CFUmL^{-1}$ and α-amylase activity and (c) glucose concentration are shown and error bars represent the range of data collected from two replicate experiments.

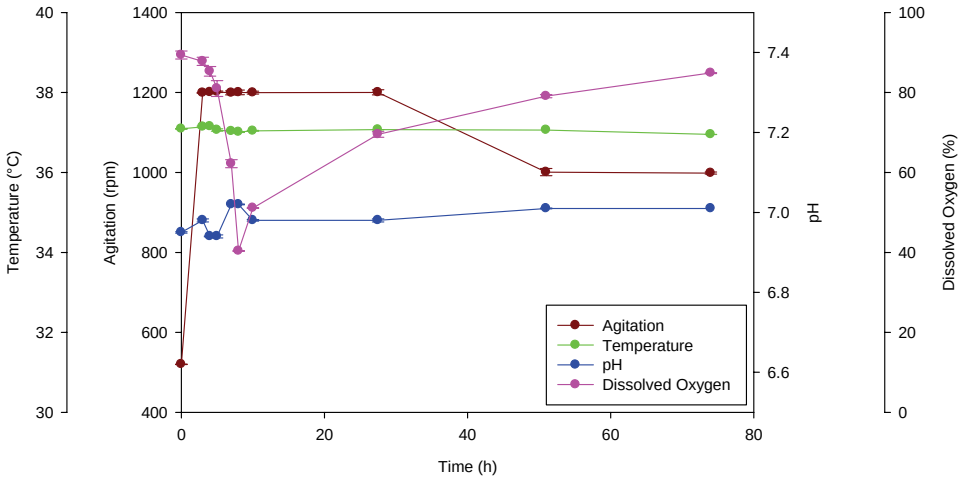

Figure 6.2 Environmental parameters measured during 5 L fed batch fermentation of *Bacillus licheniformis* SJ4628 in yeast malt broth with a glucose feed source, following cryopreservation with 20% v/v glycerol. Profiles of agitation speed (rpm), temperature (°C), pH and dissolved oxygen (%) are shown and error bars represent the range of data collected from two replicate experiments.

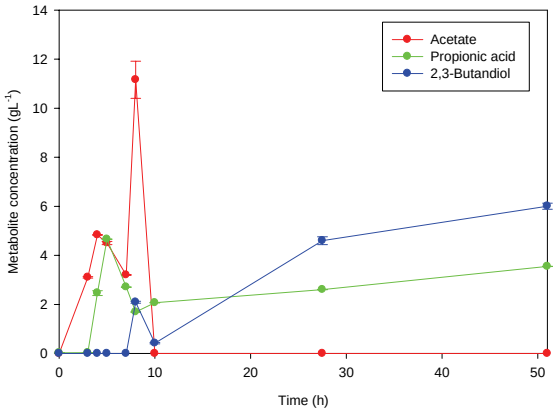

Figure 6.3 Metabolite concentration measured during 5 L fed batch fermentation of *Bacillus licheniformis* SJ4628 in yeast malt broth with a glucose feed source, following cryopreservation with 20% v/v glycerol. Profiles of concentration (gL^{-1}) of acetate, propionic acid and 2,3-butandiol are shown and error bars represent the range of data collected from two replicate experiments.

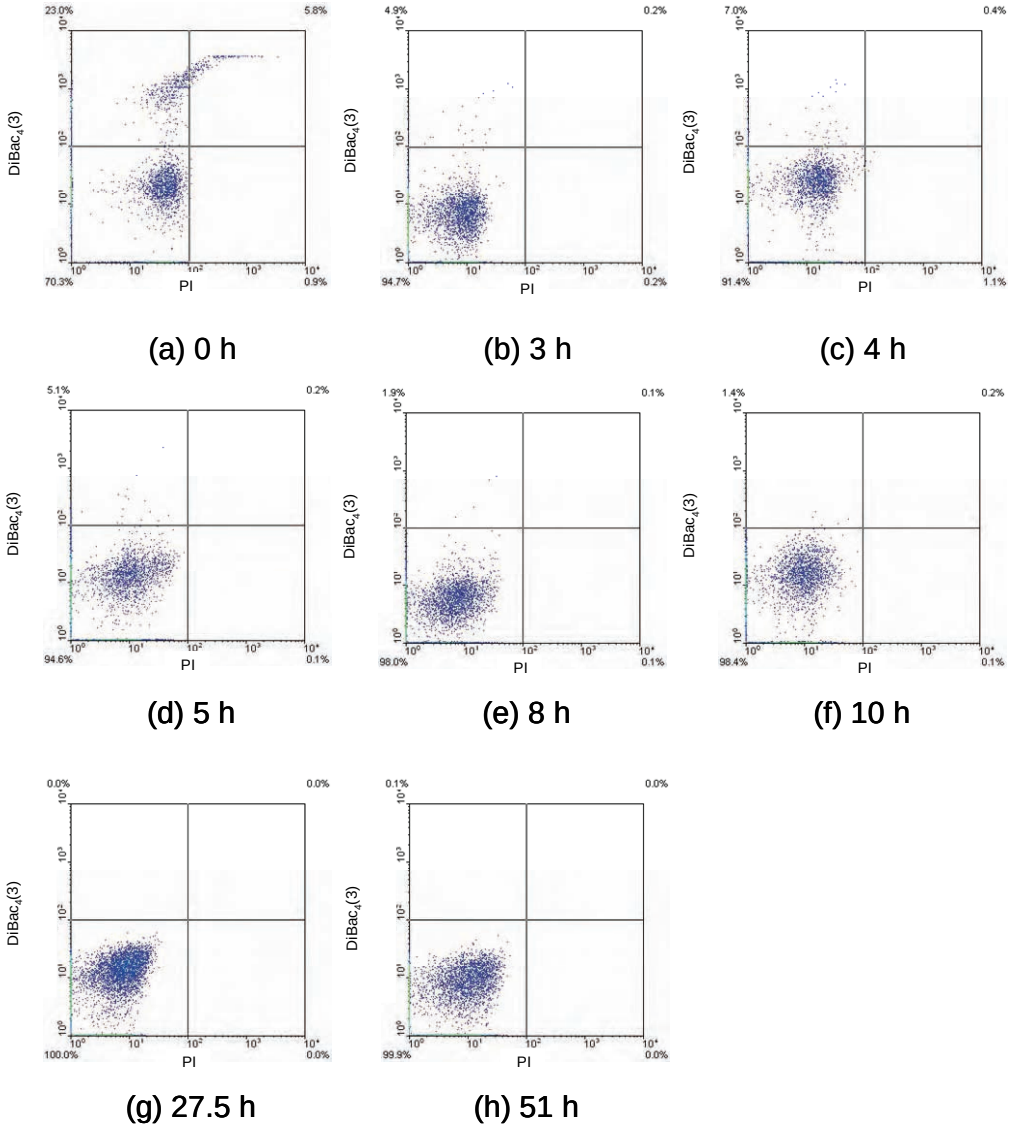

Figure 6.4 Flow cytometry of *Bacillus licheniformis* SJ4628 during 5 L fed batch fermentation in yeast malt broth with a glucose feed source, following cryopreservation with 20% v/v glycerol: (a) 0 h, (b) 3 h, (c) 4 h, (d) 5 h, (e) 8 h, (f) 10 h, (g) 27.5 h and (h) 51 h. Results are shown for the fluorophore combination; $DiBac_4(3)$/PI.

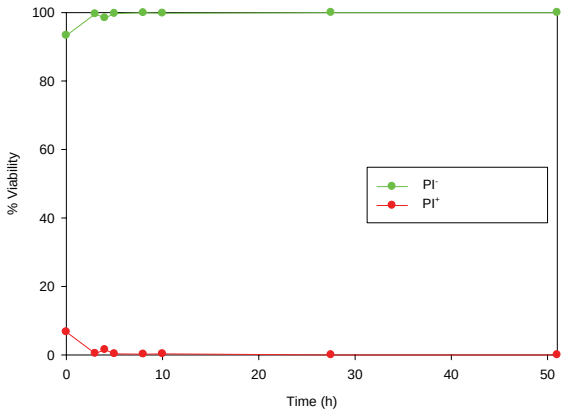

Figure 6.5 Flow cytometry of *Bacillus licheniformis* SJ4628 during 5 L fed batch fermentation in yeast malt broth with a glucose feed source, following cryopreservation with 20% v/v glycerol. Profiles of PI^- (green) and PI^+ (red) are shown for the fluorophore combination; $DiBac_4(3)$/PI.

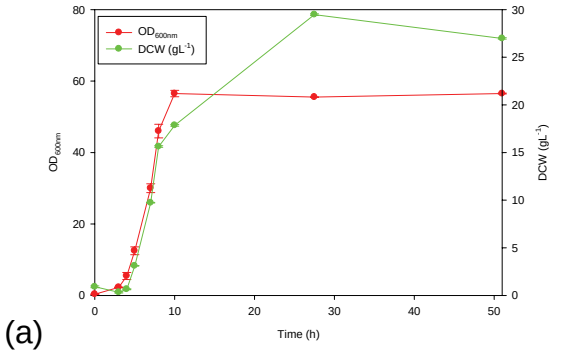

(a)

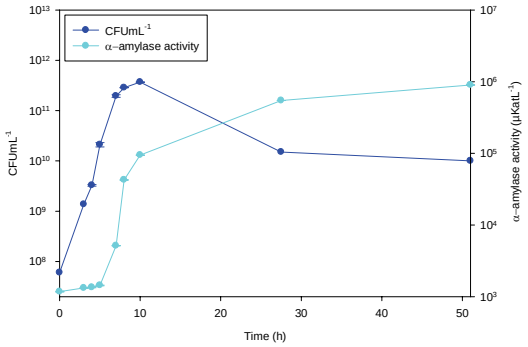

(b)

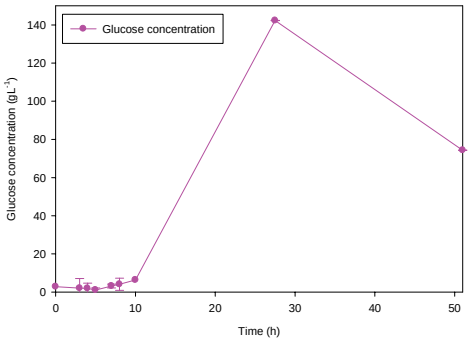

(c)

Figure 6.6 Time course of *Bacillus licheniformis* SJ4628 during 5 L fed batch fermentation in yeast malt broth with a glucose feed source, following cryopreservation with 25% v/v glycerol. Profiles of (a) OD_{600nm} and DCW (gL^{-1}), (b) $CFUmL^{-1}$ and α-amylase activity and (c) glucose concentration are shown and error bars represent the range of data collected from two replicate experiments.

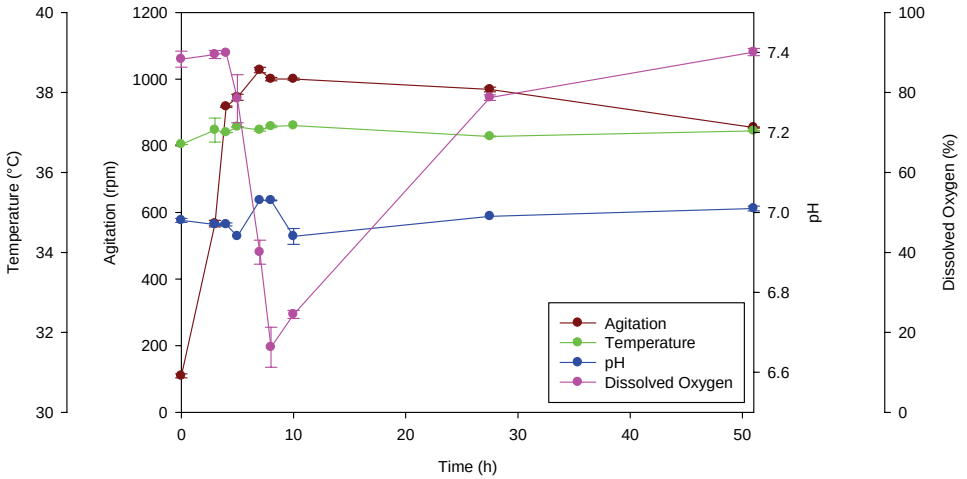

Figure 6.7 Environmental parameters measured during 5 L fed batch fermentation of *Bacillus licheniformis* SJ4628 in yeast malt broth with a glucose feed source, following cryopreservation with 25% v/v glycerol. Profiles of agitation speed (rpm), temperature (°C), pH and dissolved oxygen (%) are shown and error bars represent the range of data collected from two replicate experiments.

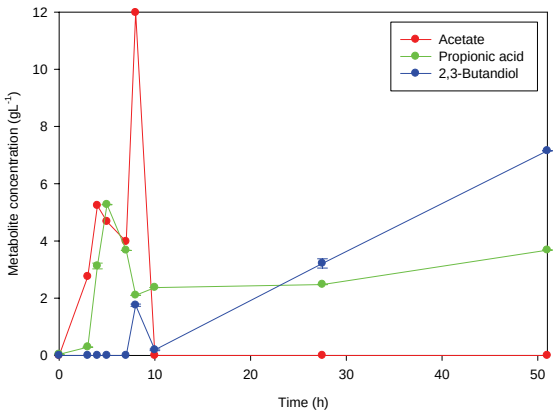

Figure 6.8 Metabolite concentration measured during 5 L fed batch fermentation of *Bacillus licheniformis* SJ4628 in yeast malt broth with a glucose feed source, following cryopreservation with 25% v/v glycerol. Profiles of concentration (gL^{-1}) of acetate, propionic acid and 2,3-butandiol are shown and error bars represent the range of data collected from two replicate experiments.

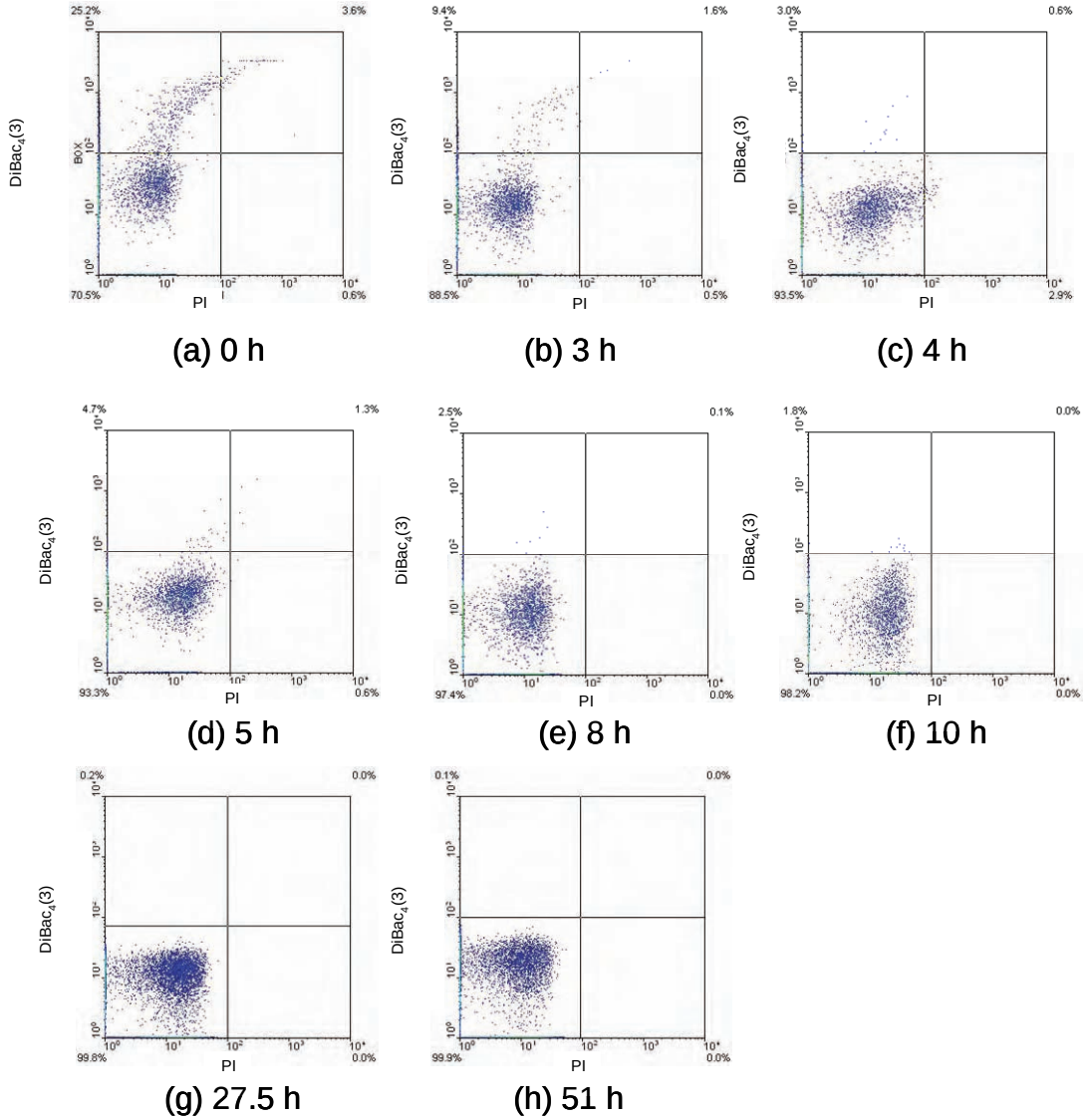

Figure 6.9 Flow cytometry of *Bacillus licheniformis* SJ4628 during 5 L fed batch fermentation in yeast malt broth with a glucose feed source, following cryopreservation with 25% v/v glycerol: (a) 0 h, (b) 3 h, (c) 4 h, (d) 5 h, (e) 8 h, (f) 10 h, (g) 27.5 h and (h) 51 h. Results are shown for the fluorophore combination; $DiBac_4(3)$/PI.

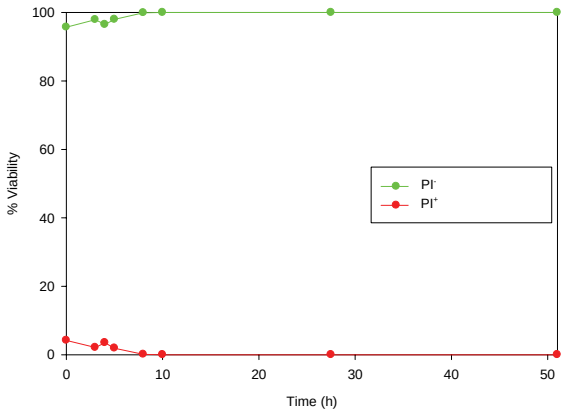

Figure 6.10 Flow cytometry of *Bacillus licheniformis* SJ4628 during 5 L fed batch fermentation in yeast malt broth with a glucose feed source, following cryopreservation with 25% v/v glycerol. Profiles of PI^- (green) and PI^+ (red) are shown for the fluorophore combination; $DiBac_4(3)$/PI.

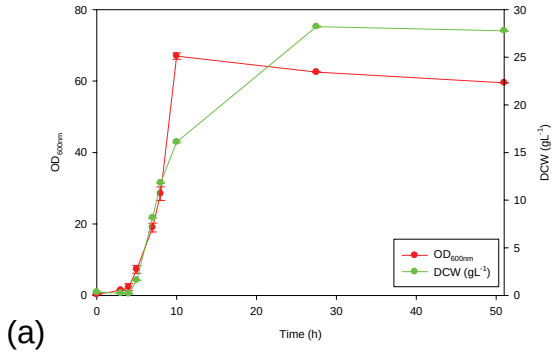

(a)

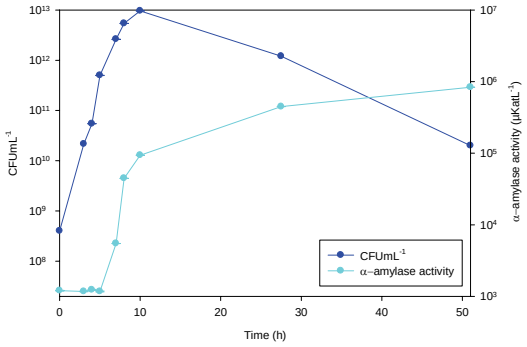

(b)

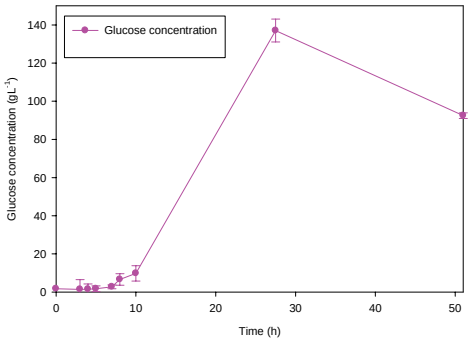

(c)

Figure 6.11 Time course of *Bacillus licheniformis* SJ4628 during 5 L fed batch fermentation in yeast malt broth with a glucose feed source, following cryopreservation with 15% v/v DMSO. Profiles of (a) OD_{600nm} and DCW (gL^{-1}), (b) $CFUmL^{-1}$ and α-amylase activity and (c) glucose concentration are shown and error bars represent the range of data collected from two replicate experiments.

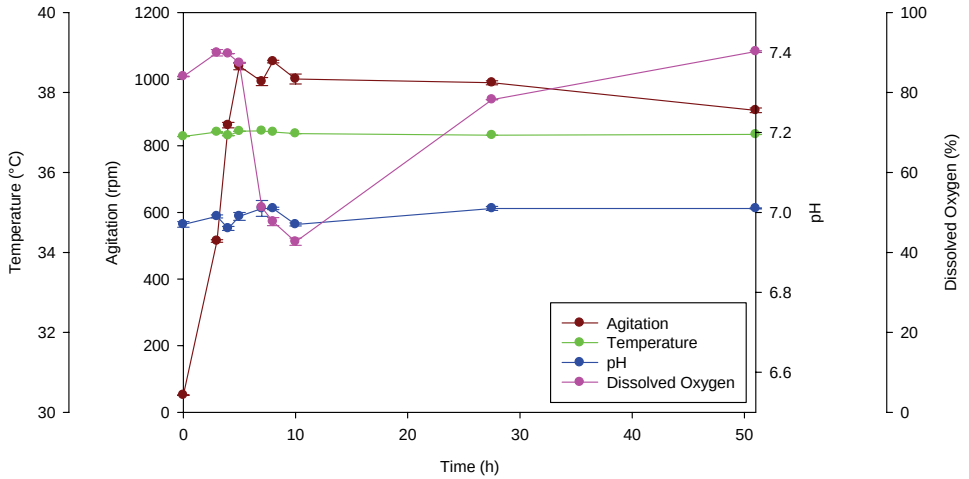

Figure 6.12 Environmental parameters measured during 5 L fed batch fermentation of *Bacillus licheniformis* SJ4628 in yeast malt broth with a glucose feed source, following cryopreservation with 15% v/v DMSO. Profiles of agitation speed (rpm), temperature (°C), pH and dissolved oxygen (%) are shown and error bars represent the range of data collected from two replicate experiments.

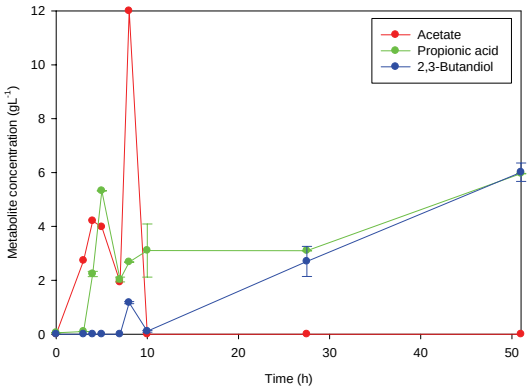

Figure 6.13 Metabolite concentration measured during 5 L fed batch fermentation of *Bacillus licheniformis* SJ4628 in yeast malt broth with a glucose feed source, following cryopreservation with 15% v/v DMSO. Profiles of concentration (gL^{-1}) of acetate, propionic acid and 2,3-butandiol are shown and error bars represent the range of data collected from two replicate experiments.

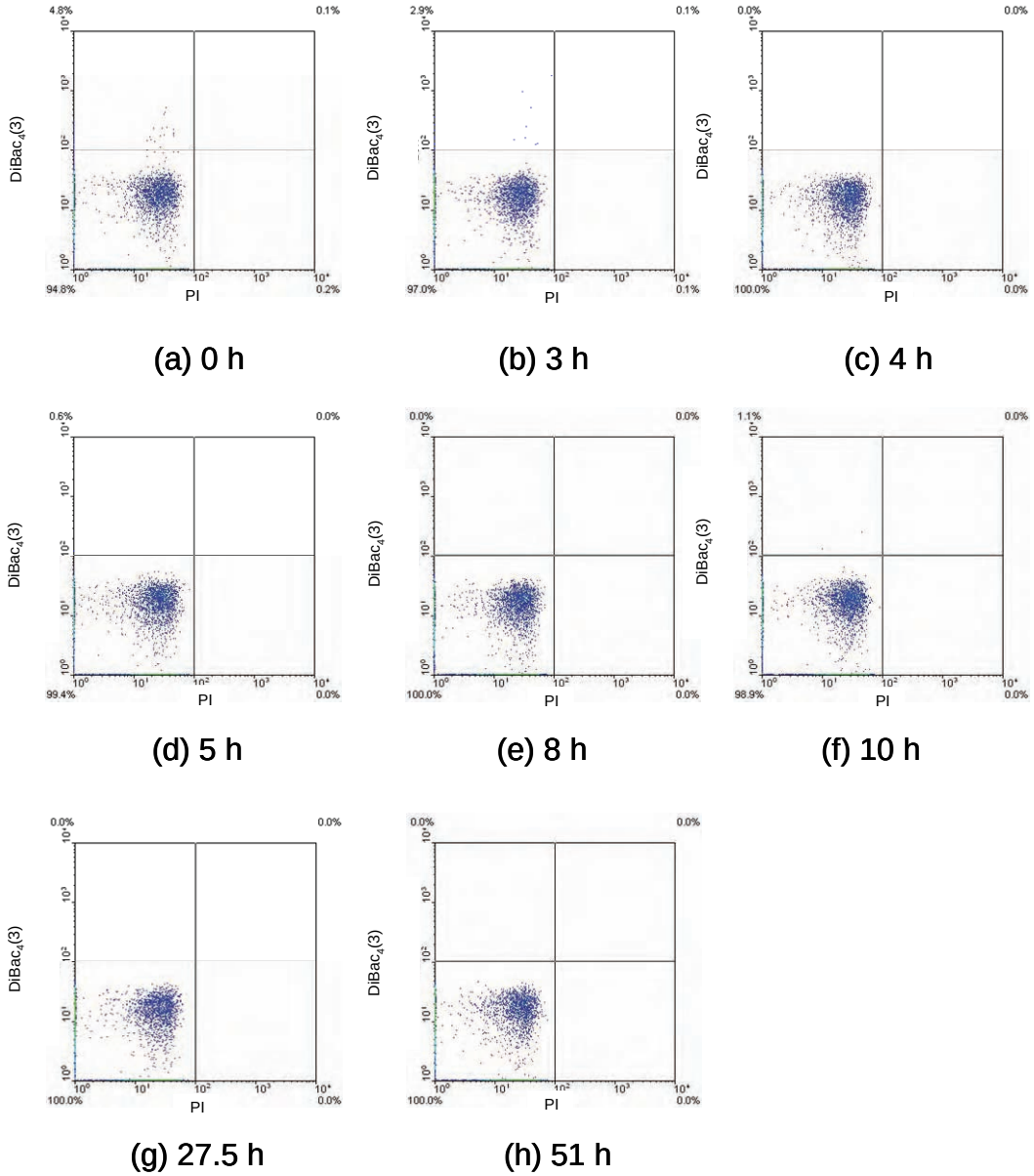

Figure 6.14 Flow cytometry of *Bacillus licheniformis* SJ4628 during 5 L fed batch fermentation in yeast malt broth with a glucose feed source, following cryopreservation with 15% v/v DMSO: (a) 0 h, (b) 3 h, (c) 4 h, (d) 5 h, (e) 8 h, (f) 10 h, (g) 27.5 h and (h) 51 h. Results are shown for the fluorophore combination; $DiBac_4(3)$/PI.

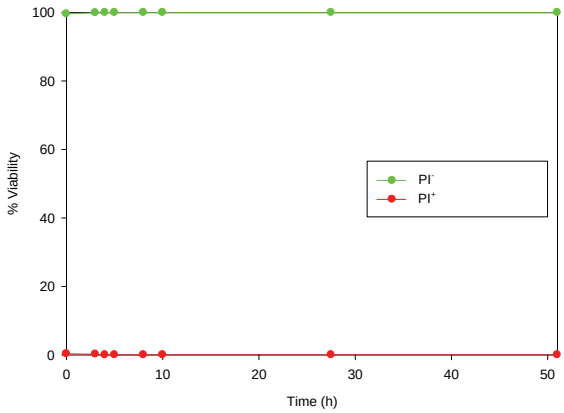

Figure 6.15 Flow cytometry of *Bacillus licheniformis* SJ4628 during 5 L fed batch fermentation in yeast malt broth with a glucose feed source, following cryopreservation with 15% v/v DMSO. Profiles of PI^- (green) and PI^+ (red) are shown for the fluorophore combination; $DiBac_4(3)$/PI.

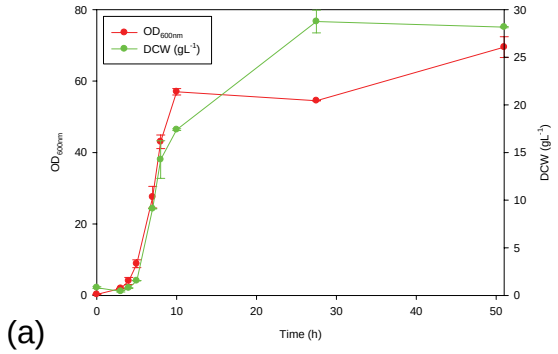

(a)

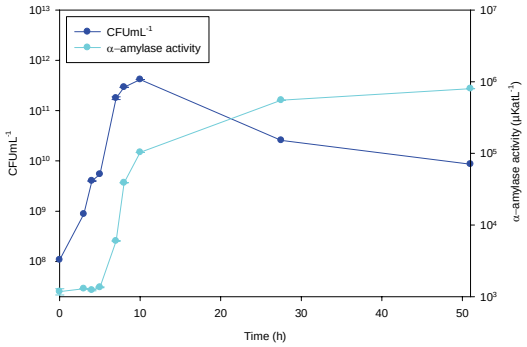

(b)

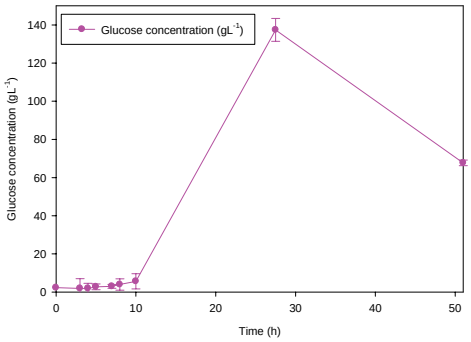

(c)

Figure 6.16 Time course of *Bacillus licheniformis* SJ4628 during 5 L fed batch fermentation in yeast malt broth with a glucose feed source, following cryopreservation with 20% v/v Tween 80. Profiles of (a) OD_{600nm} and DCW (gL^{-1}), (b) $CFUmL^{-1}$ and α-amylase activity and (c) glucose concentration are shown and error bars represent the range of data collected from two replicate experiments.

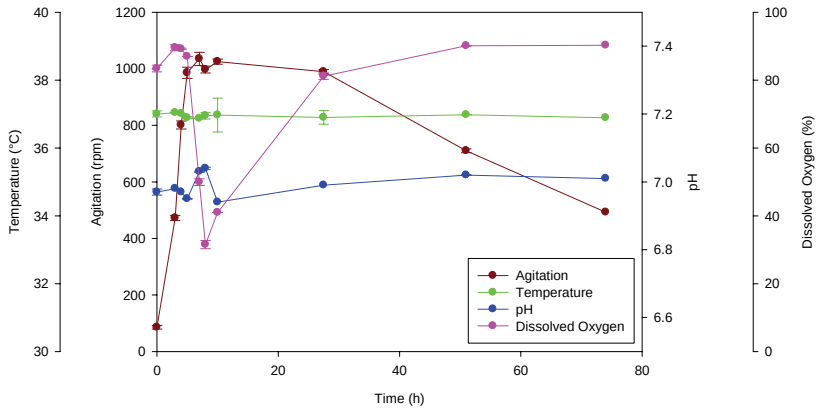

Figure 6.17 Environmental parameters measured during 5 L fed batch fermentation of *Bacillus licheniformis* SJ4628 in yeast malt broth with a glucose feed source, following cryopreservation with 20% v/v Tween 80. Profiles of agitation speed (rpm), temperature (°C), pH and dissolved oxygen (%) are shown and error bars represent the range of data collected from two replicate experiments.

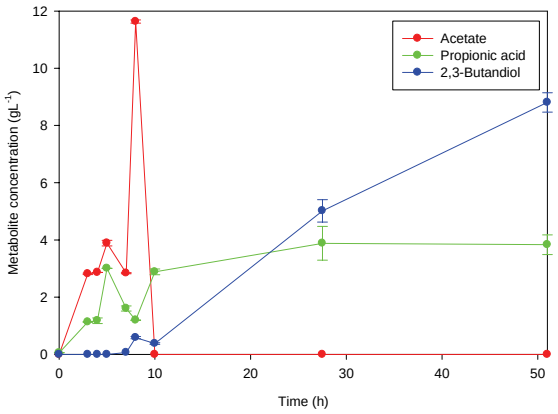

Figure 6.18 Metabolite concentration measured during 5 L fed batch fermentation of *Bacillus licheniformis* SJ4628 in yeast malt broth with a glucose feed source, following cryopreservation with 20% v/v Tween 80. Profiles of concentration (gL^{-1}) of acetate, propionic acid and 2,3-butandiol are shown and error bars represent the range of data collected from two replicate experiments.

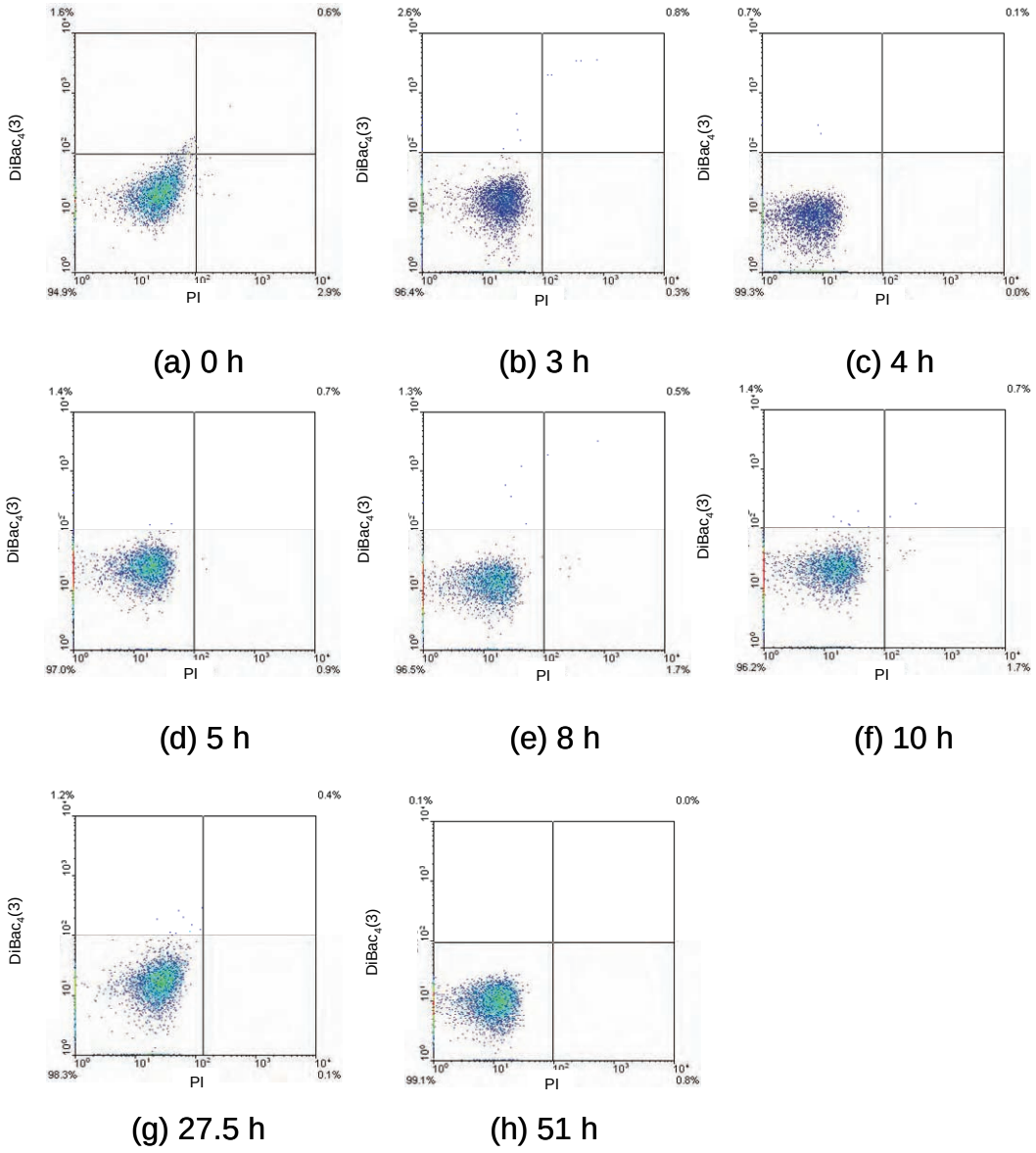

Figure 6.19 Flow cytometry of *Bacillus licheniformis* SJ4628 during 5 L fed batch fermentation in yeast malt broth with a glucose feed source, following cryopreservation with 20% v/v Tween 80: (a) 0 h, (b) 3 h, (c) 4 h, (d) 5 h, (e) 8 h, (f) 10 h, (g) 27.5 h and (h) 51 h. Results are shown for the fluorophore combination; $DiBac_4(3)$/PI.

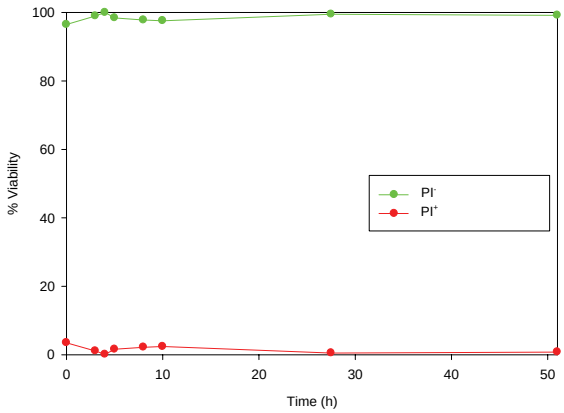

Figure 6.20 Flow cytometry of *Bacillus licheniformis* SJ4628 during 5 L fed batch fermentation in yeast malt broth with a glucose feed source, following cryopreservation with 20% v/v Tween 80. Profiles of PI^- (green) and PI^+ (red) are shown for the fluorophore combination; $DiBac_4(3)$/PI.

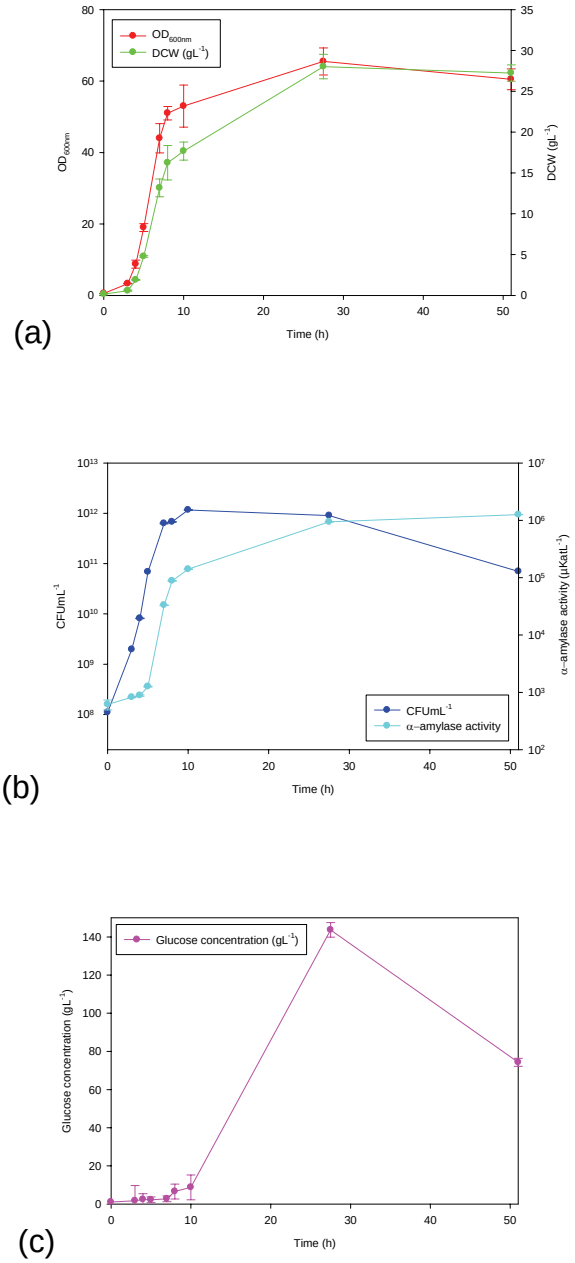

Figure 6.21 Time course of *Bacillus licheniformis* SJ4628 during 5 L fed batch fermentation in yeast malt broth with a glucose feed source, following cryopreservation with no cryopreservant. Profiles of (a) OD_{600nm} and DCW (gL^{-1}), (b) $CFUmL^{-1}$ and α-amylase activity and (c) glucose concentration are shown and error bars represent the range of data collected from two replicate experiments.

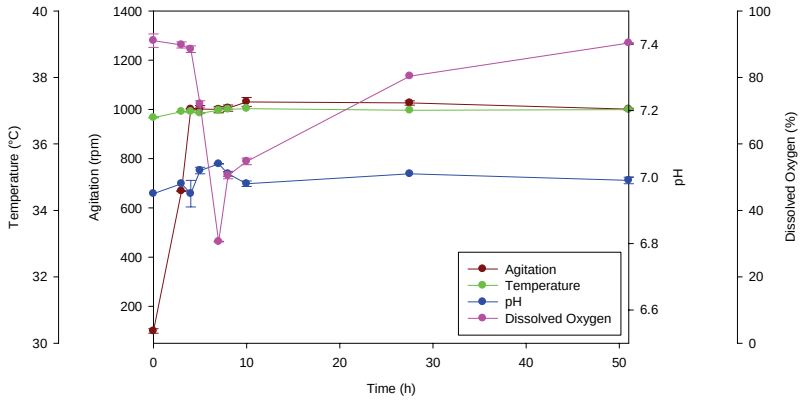

Figure 6.22 Environmental parameters measured during 5 L fed batch fermentation of *Bacillus licheniformis* SJ4628 in yeast malt broth with a glucose feed source, following cryopreservation with no cryopreservant. Profiles of agitation speed (rpm), temperature (°C), pH and dissolved oxygen (%) are shown and error bars represent the range of data collected from two replicate experiments.

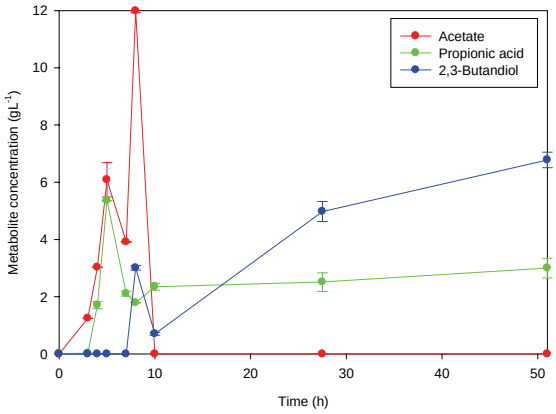

Figure 6.23 Metabolite concentration measured during 5 L fed batch fermentation of *Bacillus licheniformis* SJ4628 in yeast malt broth with a glucose feed source, following cryopreservation with no cryopreservant. Profiles of concentration (gL^{-1}) of acetate, propionic acid and 2,3-butandiol are shown and error bars represent the range of data collected from two replicate experiments.

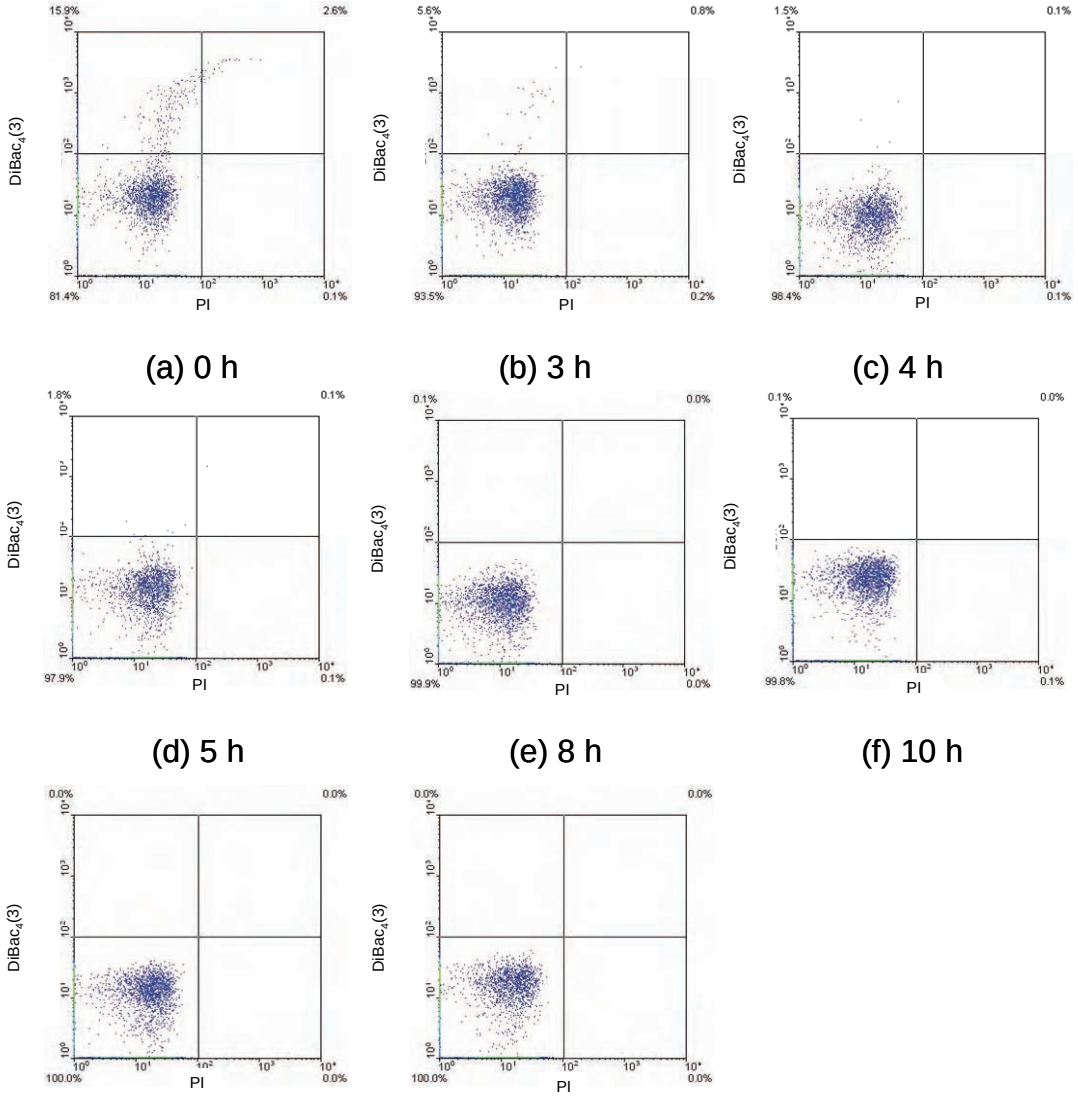

Figure 6.24 Flow cytometry of *Bacillus licheniformis* SJ4628 during 5 L fed batch fermentation in yeast malt broth with a glucose feed source, following cryopreservation with no cryopreservant: (a) 0 h, (b) 3 h, (c) 4 h, (d) 5 h, (e) 8 h, (f) 10 h, (g) 27.5 h and (h) 51 h. Results are shown for the fluorophore combination; $DiBac_4(3)$/PI.

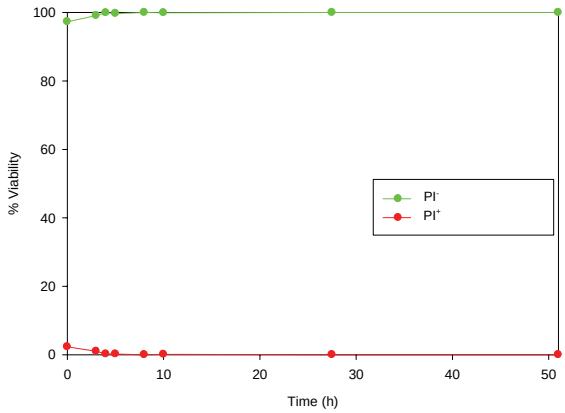

Figure 6.25 Flow cytometry of *Bacillus licheniformis* SJ4628 during 5 L fed batch fermentation in yeast malt broth with a glucose feed source, following cryopreservation with no cryopreservant. Profiles of PI^- (green) and PI^+ (red) are shown for the fluorophore combination; $DiBac_4(3)$/PI.

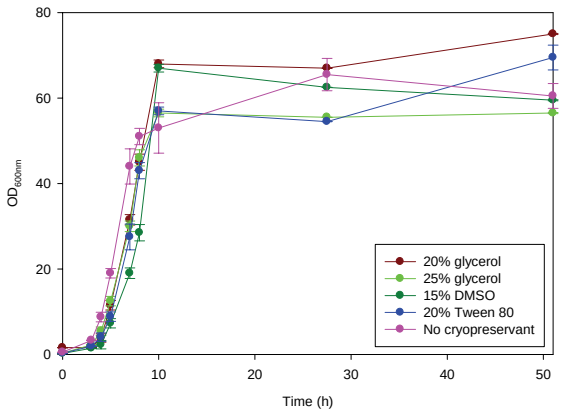

Figure 6.26 Comparison of growth characteristics (OD_{600nm}) of *Bacillus licheniformis* SJ4628 during 5 L fed batch fermentation in yeast malt broth with a glucose feed source, following cryopreservation with each different cryopreservant and no cryopreservant. Each profile is representative of two replicate experiments.

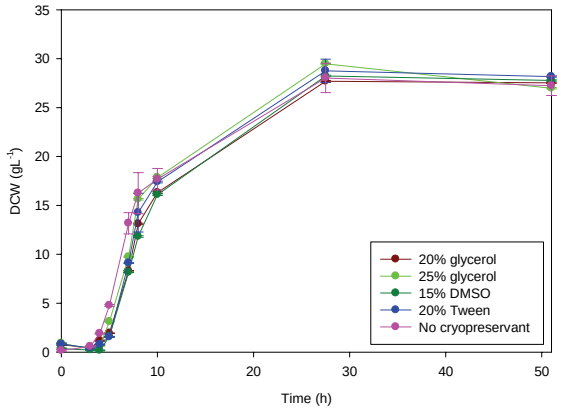

Figure 6.27 Comparison of growth characteristics (DCW (gL^{-1})) of *Bacillus licheniformis* SJ4628 during 5 L fed batch fermentation in yeast malt broth with a glucose feed source, following cryopreservation with each different cryopreservant and no cryopreservant. Each profile is representative of two replicate experiments.

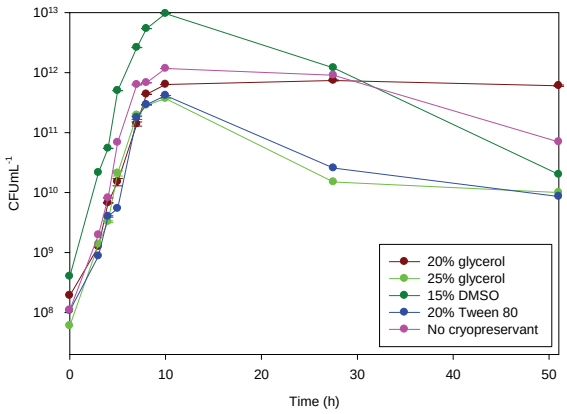

Figure 6.28 Comparison of growth characteristics ($CFUmL^{-1}$) of *Bacillus licheniformis* SJ4628 during 5 L fed batch fermentation in yeast malt broth with a glucose feed source, following cryopreservation with each different cryopreservant and no cryopreservant. Each profile is representative of two replicate experiments.

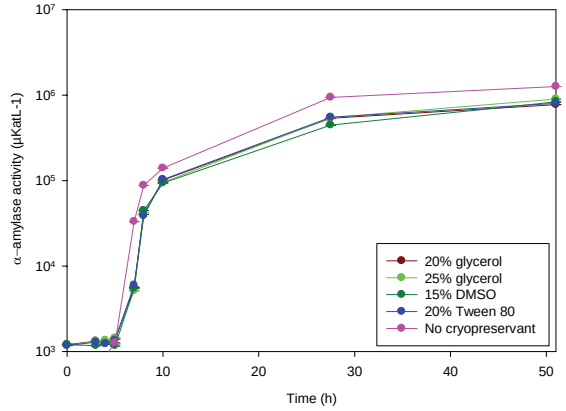

Figure 6.29 Comparison of the α-amylase production ($\mu KatL^{-1}$) of *Bacillus licheniformis* SJ4628 during 5 L fed batch fermentation in yeast malt broth with a glucose feed source, following cryopreservation with each different cryopreservant and no cryopreservant. Each profile is representative of two replicate experiments.

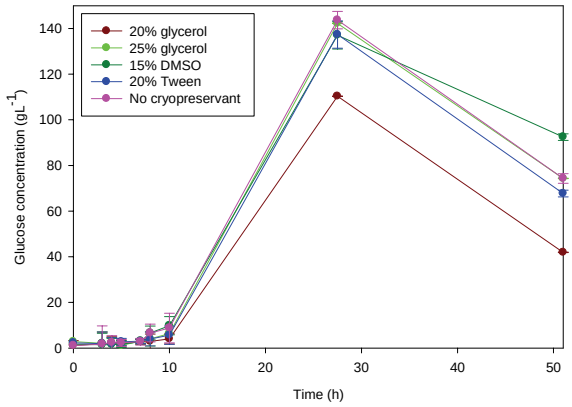

Figure 6.30 Comparison of the glucose concentration (gL^{-1}) during 5 L fed batch fermentation of *Bacillus licheniformis* SJ4628 in yeast malt broth with a glucose feed source, following cryopreservation with each different cryopreservant and no cryopreservant. Each profile is representative of two replicate experiments.

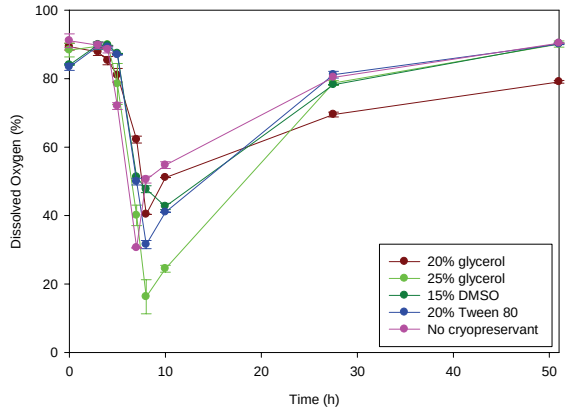

Figure 6.31 Comparison of the dissolved oxygen concentration (%) during 5 L fed batch fermentation of *Bacillus licheniformis* SJ4628 in yeast malt broth with a glucose feed source, following cryopreservation with each different cryopreservant and no cryopreservant. Each profile is representative of two replicate experiments.

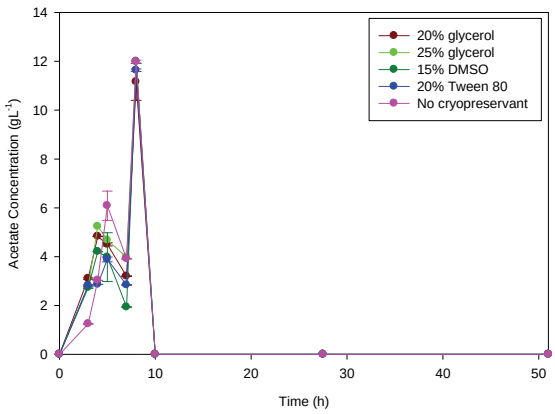

Figure 6.32 Comparison of the metabolite concentration of acetate (gL^{-1}) during 5 L fed batch fermentation of *Bacillus licheniformis* SJ4628 in yeast malt broth with a glucose feed source, following cryopreservation with each different cryopreservant and no cryopreservant. Each profile is representative of two replicate experiments.

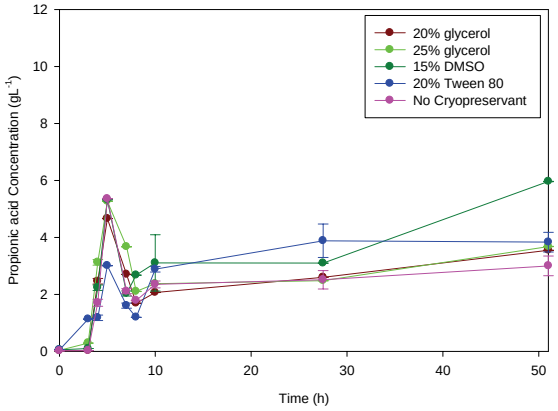

Figure 6.33 Comparison of the metabolite concentration of propionic acid (gL^{-1}) during 5 L fed batch fermentation of *Bacillus licheniformis* SJ4628 in yeast malt broth with a glucose feed source, following cryopreservation with each different cryopreservant and no cryopreservant. Each profile is representative of two replicate experiments.

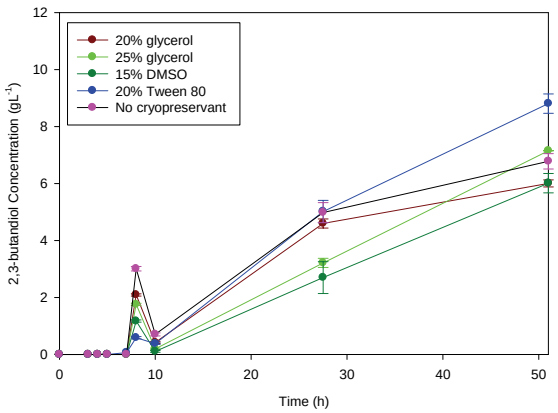

Figure 6.34 Comparison of the metabolite concentration of 2,3-butandiol (gL^{-1}) during 5 L fed batch fermentation of *Bacillus licheniformis* SJ4628 in yeast malt broth with a glucose feed source, following cryopreservation with each different cryopreservant and no cryopreservant. Each profile is representative of two replicate experiments.

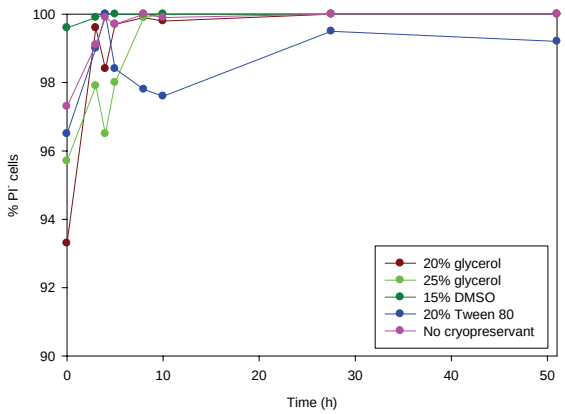

Figure 6.35 Comparison of the total PI^- cells (%) during 5 L fed batch fermentation of *Bacillus licheniformis* SJ4628 in yeast malt broth with a glucose feed source, following cryopreservation with each different cryopreservant and no cryopreservant. Each profile is representative of two replicate experiments.

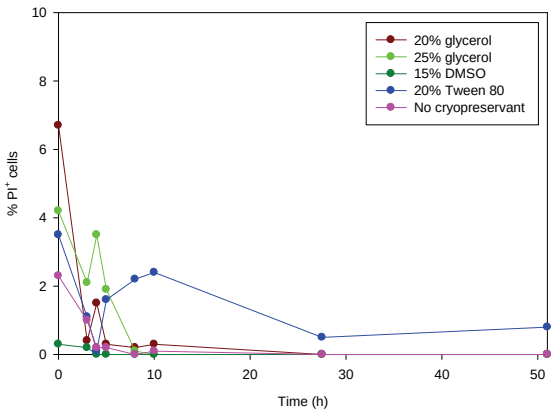

Figure 6.36 Comparison of the total PI^+ cells (%) during 5 L fed batch fermentation of *Bacillus licheniformis* SJ4628 in yeast malt broth with a glucose feed source, following cryopreservation with each different cryopreservant and no cryopreservant. Each profile is representative of two replicate experiments.

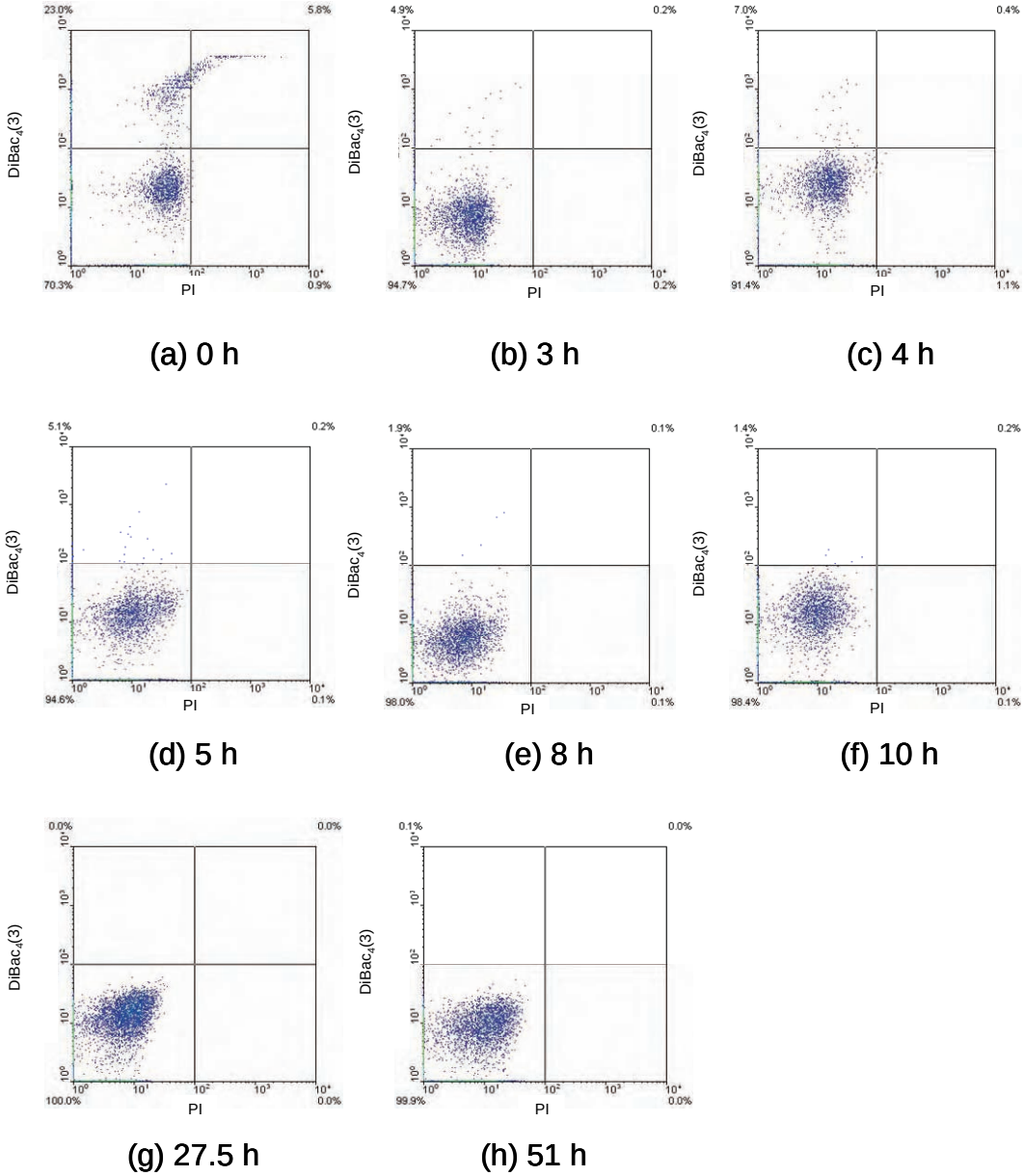

(a) 0 h (b) 3 h (c) 4 h

(d) 5 h (e) 8 h (f) 10 h

(g) 27.5 h (h) 51 h

Figure 6.37 Flow cytometry of *Bacillus licheniformis* SJ4628 during 5 L fed batch fermentation in yeast malt broth with a glucose feed source, following cryopreservation with each different cryopreservant and no cryopreservant: (a) 0 h, (b) 3 h, (c) 4 h, (d) 5 h, (e) 8 h, (f) 10 h, (g) 27.5 h and (h) 51 h. Results are shown for the fluorophore combination; $DiBac_4(3)$/PI and are representative of each of the fermentations.

	20% Glycerol	25% Glycerol	15% DMSO	20% Tween 80	No Cryopreservant
Specific growth rate, μ (h^{-1})	0.13	0.09	0.18	0.11	0.14

Table 6.1 Comparison of the mean specific growth rate during 5 L fed batch fermentation of *Bacillus licheniformis* SJ4628 in yeast malt broth with a glucose feed source, following cryopreservation with each different cryopreservant and no cryopreservant. Each value is representative of two replicate experiments.

Figure 6.26 to 6.30 and Table 6.1 show a summary of the OD_{600nm}, DCW (gL^{-1}) ,$CFUml^{-1}$, α-amylase activity and glucose concentration results for each of the 5 L fed batch fermentations for *B. licheniformis* SJ4628 following cryopreservation with each of the following cell banks: 20% glycerol, 25% glycerol, 15% DMSO, 20% Tween 80 and with no cryopreservant.

Following a short lag phase of 3 h, the mean specific growth rate (μ) was calculated as 0.13 h^{-1} using optical density data from the 7 to 10 h time points for each experiment except the no cryopreserved experiment which used the 5 to 8 h time points. This was lower than found for the shake flask fermentation which was 0.37 h^{-1} (Section 4.1.2.1) and for the batch process which was 0.25 h^{-1} (Section 5.1.1). From 3 to 10 h there was a steep increase in mean optical density, DCW (gL^{-1}), $CFUml^{-1}$ and α-amylase activity which was expected during a fed batch process. The maximum mean optical density was 67 and was calculated using the maximum optical density measurements from each fermentation, and was nearly double that of the batch process; the maximum mean DCW (gL^{-1}) was 28.43 gL^{-1} calculated using the 27.5 h timepoint for each fermentation, and was double that of the batch process. The maximum mean $CFUml^{-1}$ reached 2.46 x 10^{12} and was calculated using the 10 h timepoint for each fermentation. Mean glucose concentration remained consistently low for the first 10 h of each fermentation, from 1.82 gL^{-1} at 0 h to 6.90 gL^{-1} at 10 h, and then increased dramatically to a maximum of 134.14 gL^{-1} at 24 h, before declining to 70.13 gL^{-1} at 51 h. Reproducibility of DCW (gL^{-1}), and alpha amylase measurements were

high (Figure 6.27 and 6.29), OD_{600nm} and $CFUml^{-1}$ (Figure 6.26 and 6.28) measurements were slightly less reproducible reflecting the sensitivities of these techniques. The α-amylase activity was still steadily increasing even after the full 74 h fermentation but the maximum recorded value at 74 h is 1.02 $KatL^{-1}$ which was 63 times higher than the batch process and demonstrates the value of the fed batch process for producing α-amylase. As mentioned previously the a*myE* gene is subject to carbon catabolite repression and the high initial glucose concentrations of the batch process presumably hindered production of α-amylase. It is clear that, despite earlier shake flask experiments (Chapter 4) showing that each of these cell banks had different recovery times after freezing (Figure 4.31), that this had no effect on overall fermentation process performance. This implies that the overnight step process of preparing the inoculum cancelled out any effects caused by the freezing process as it gave the cells long enough to recover. Experiments were conducted with the 15% v/v DMSO (Figure 6.38 to 6.42) and 20% v/v Tween 80 (Figure 6.43 to 6.47) cell banks grown to OD_{600nm} 1.0 without the overnight step as in Figure 4.31 and used to inoculate the 5 L fed batch process no difference was seen in α-amylase yield when compared to cell banks grown to an optical density of 1.0 with an overnight step. The 15% DMSO cell bank was used as it was the slowest cell bank to recover i.e the worst case scenario and the 20% Tween 80 cell bank was chosen as is was the fastest to recover and therefore represents the best possible case scenario.

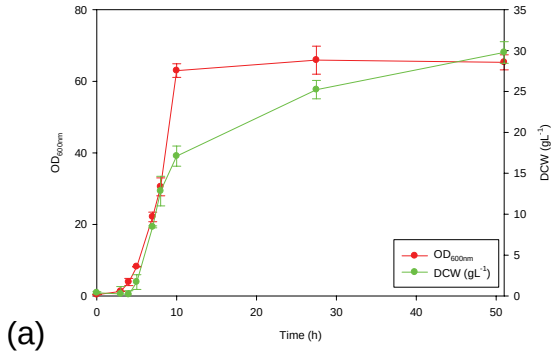

(a)

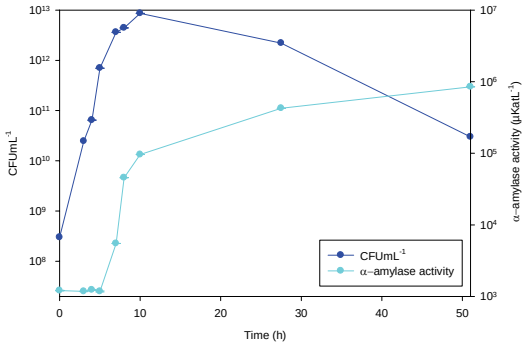

(b)

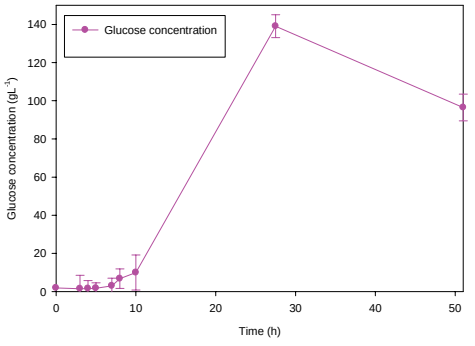

(c)

Figure 6.38 Time course of *Bacillus licheniformis* SJ4628 during 5 L fed batch fermentation in yeast malt broth with a glucose feed source, following cryopreservation with 15% v/v DMSO and with no overnight incubation step on agar. Profiles of (a) OD_{600nm} and DCW (gL^{-1}), (b) $CFUmL^{-1}$ and α-amylase activity and (c) glucose concentration are shown and error bars represent the range of data collected from two replicate experiments.

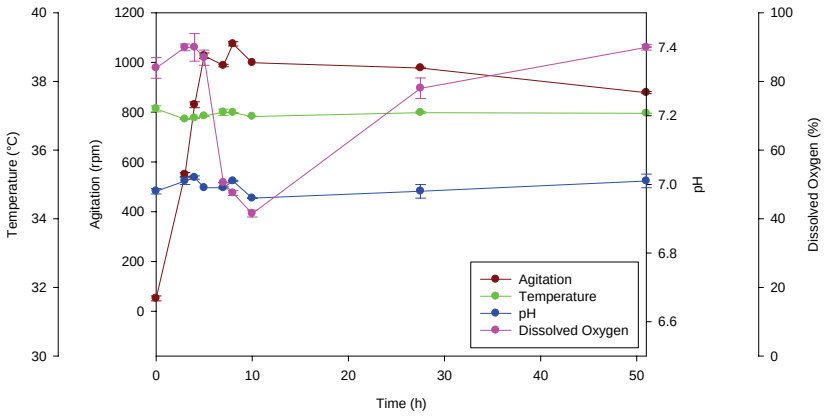

Figure 6.39 Environmental parameters measured during 5 L fed batch fermentation of *Bacillus licheniformis* SJ4628 in yeast malt broth with a glucose feed source, following cryopreservation with 15% v/v DMSO and with no overnight incubation step on agar. Profiles of agitation speed (rpm), temperature (°C), pH and dissolved oxygen (%) are shown and error bars represent the range of data collected from two replicate experiments.

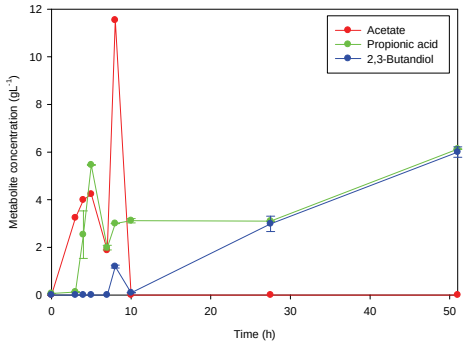

Figure 6.40 Metabolite concentration measured during 5 L fed batch fermentation of *Bacillus licheniformis* SJ4628 in yeast malt broth with a glucose feed source, following cryopreservation with 15% v/v DMSO and with no overnight incubation step on agar. Profiles of concentration (gL^{-1}) of acetate, propionic acid and 2,3-butandiol are shown and error bars represent the range of data collected from two replicate experiments.

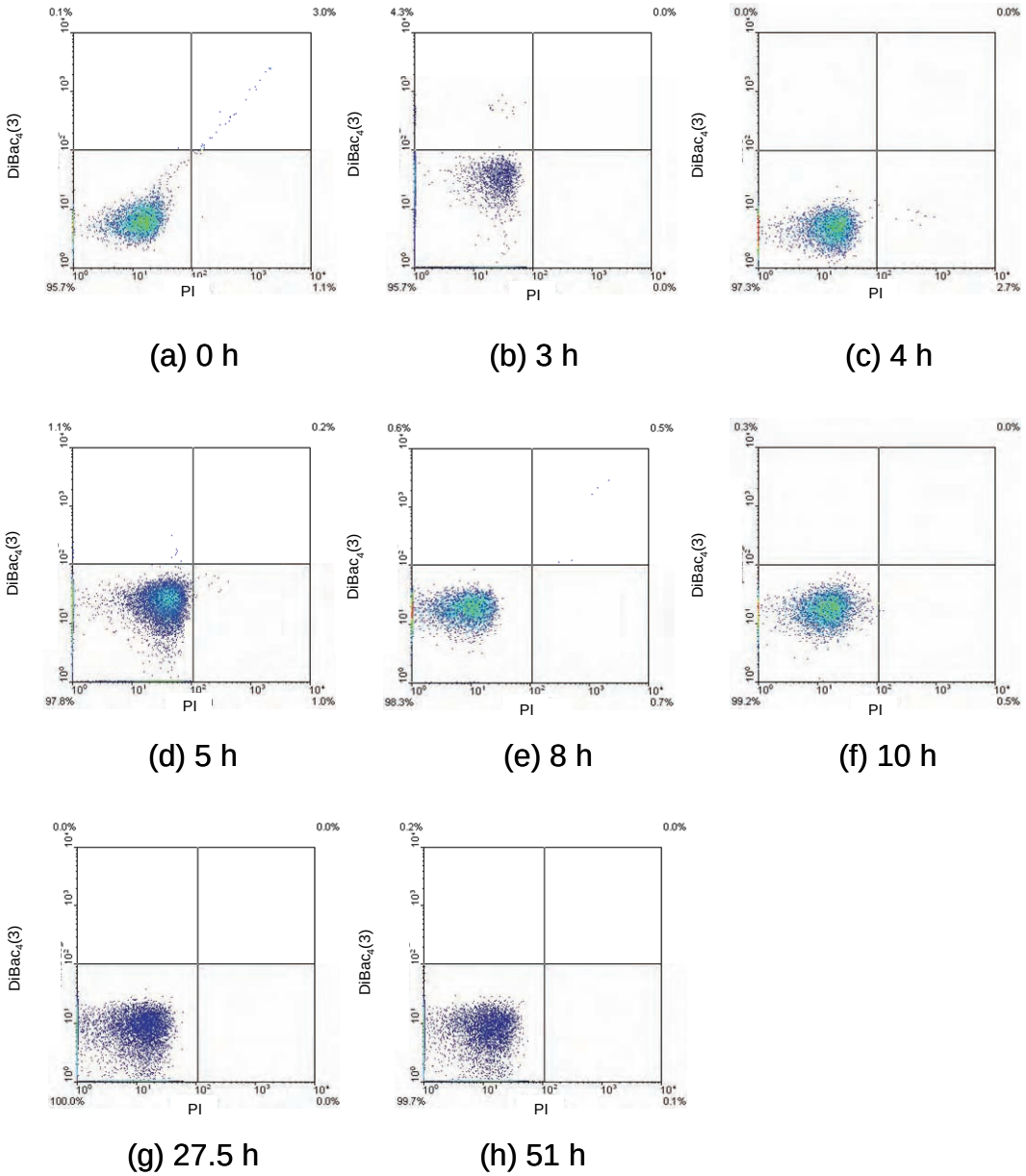

(a) 0 h (b) 3 h (c) 4 h

(d) 5 h (e) 8 h (f) 10 h

(g) 27.5 h (h) 51 h

Figure 6.41 Flow cytometry of *Bacillus licheniformis* SJ4628 during 5 L fed batch fermentation in yeast malt broth with a glucose feed source, following cryopreservation with 15% v/v DMSO and with no overnight incubation step on agar: (a) 0 h, (b) 3 h, (c) 4 h, (d) 5 h, (e) 8 h, (f) 10 h, (g) 27.5 h and (h) 51 h. Results are shown for the fluorophore combination $DiBac_4(3)$/PI.

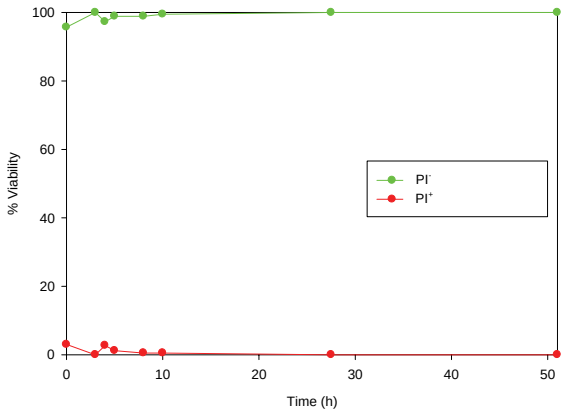

Figure 6.42 Flow cytometry of *Bacillus licheniformis* SJ4628 during 5 L fed batch fermentation in yeast malt broth with a glucose feed source, following cryopreservation with 15% v/v DMSO and with no overnight incubation step on agar. Profiles of PI^- (green) and PI^+ (red) are shown for the fluorophore combination; $DiBac_4(3)$/PI.

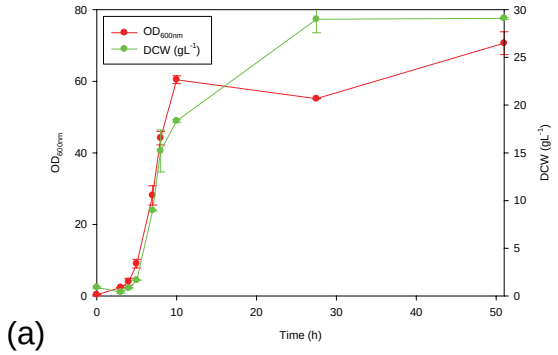

(a)

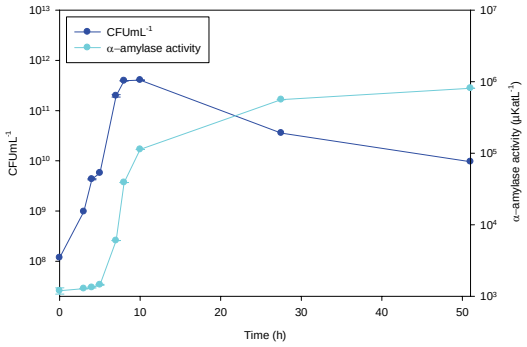

(b)

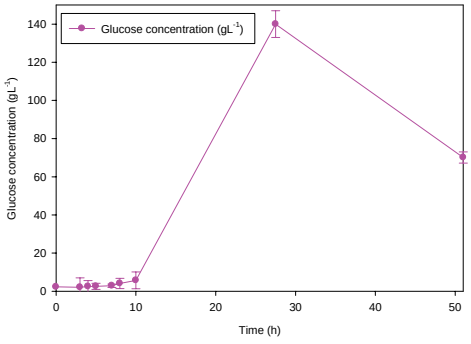

(c)

Figure 6.43 Time course of *Bacillus licheniformis* SJ4628 during 5 L fed batch fermentation in yeast malt broth with a glucose feed source, following cryopreservation with 20% v/v Tween 80 and with no overnight incubation step on agar. Profiles of (a) OD_{600nm} and DCW (gL^{-1}), (b) $CFUmL^{-1}$ and α-amylase activity and (c) glucose concentration are shown and error bars represent the range of data collected from two replicate experiments.

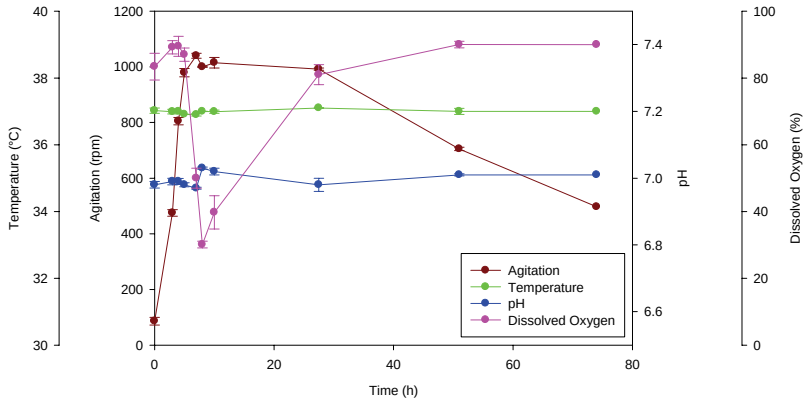

Figure 6.44 Environmental parameters measured during 5 L fed batch fermentation of *Bacillus licheniformis* SJ4628 in yeast malt broth with a glucose feed source, following cryopreservation with 20% v/v Tween 80 and with no overnight incubation step on agar. Profiles of agitation speed (rpm), temperature (°C), pH and dissolved oxygen (%) are shown and error bars represent the range of data collected from two replicate experiments.

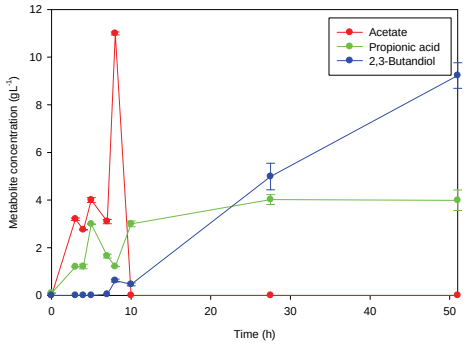

Figure 6.45 Metabolite concentration measured during 5 L fed batch fermentation of *Bacillus licheniformis* SJ4628 in yeast malt broth with a glucose feed source, following cryopreservation with 20% v/v Tween 80 and with no overnight incubation step on agar. Profiles of concentration (gL^{-1}) of acetate, propionic acid and 2,3-butandiol are shown and error bars represent the range of data collected from two replicate experiments.

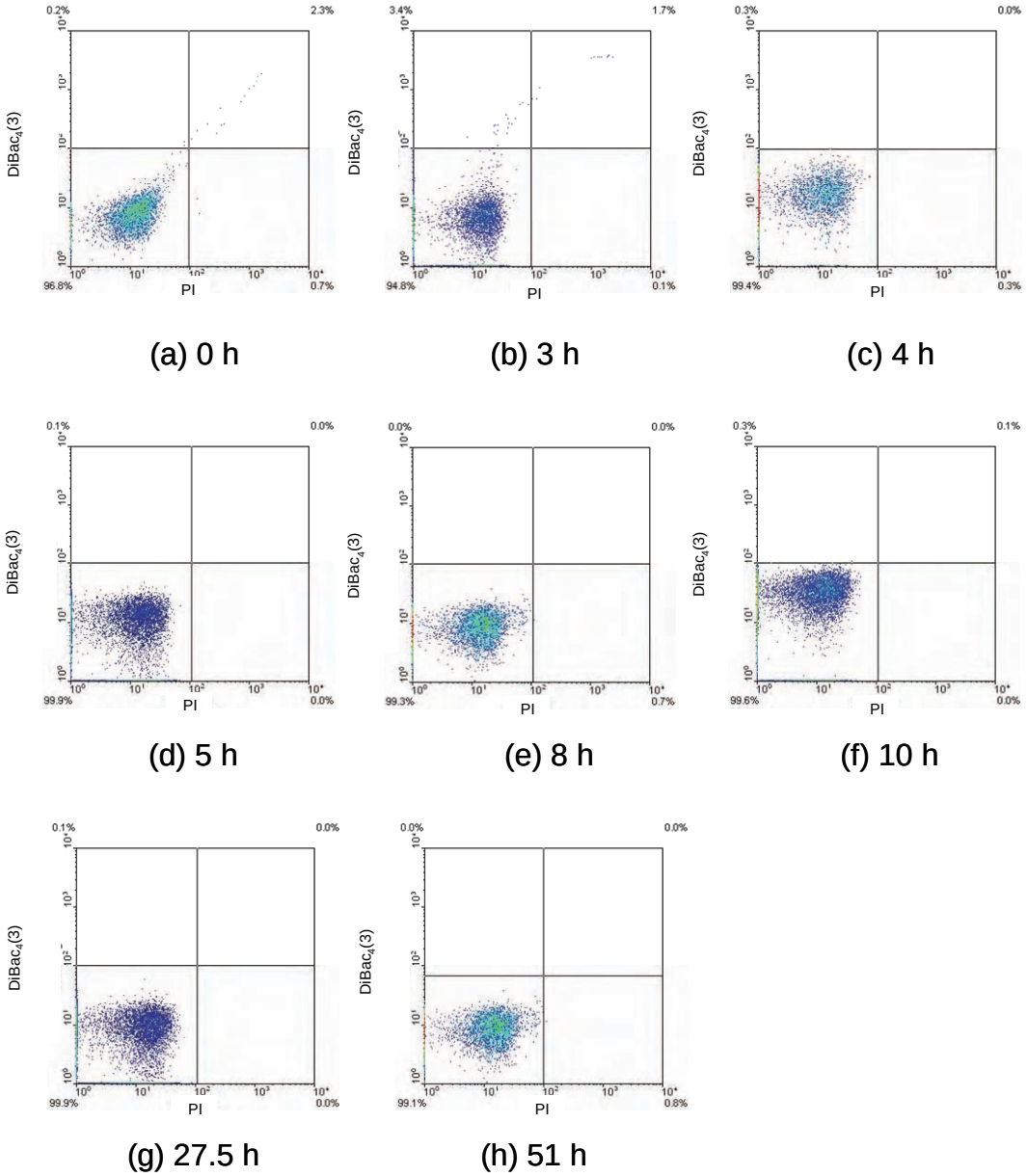

(a) 0 h (b) 3 h (c) 4 h

(d) 5 h (e) 8 h (f) 10 h

(g) 27.5 h (h) 51 h

Figure 6.46 Flow cytometry of *Bacillus licheniformis* SJ4628 during 5 L fed batch fermentation in yeast malt broth with a glucose feed source, following cryopreservation with 20% v/v Tween 80 and with no overnight incubation step on agar: (a) 0 h, (b) 3 h, (c) 4 h, (d) 5 h, (e) 8 h, (f) 10 h, (g) 27.5 h and (h) 51 h. Results are shown for the fluorophore combination $DiBac_4(3)$/PI.

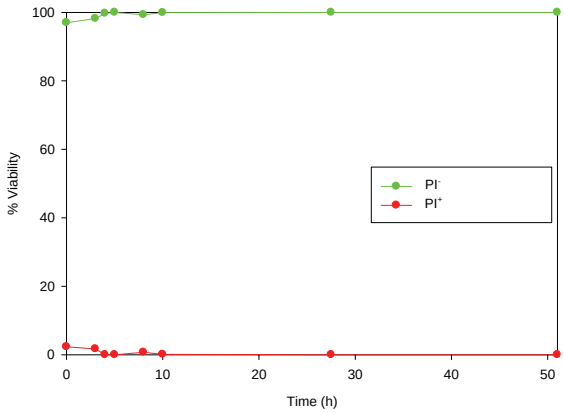

Figure 6.47 Flow cytometry of *Bacillus licheniformis* SJ4628 during 5 L fed batch fermentation in yeast malt broth with a glucose feed source, following cryopreservation with 20% v/v Tween 80 and with no overnight incubation step on agar. Profiles of PI^- (green) and PI^+ (red) are shown for the fluorophore combination; $DiBac_4(3)$/PI.

This indicates that as long as the culture grows to an OD_{600nm} of 1.0 regardless of the time taken then fermentation process performance will be unaffected. This does assume that at OD_{600nm} of 1.0 the cells are fully polarised which has been observed for all of the experiments carried out during this work. This supports the work of Hornbæk and colleagues who noticed that cellular heterogeneity increases the lag phase but not the subsequent growth or final biomass of cultures of *B. licheniformis* SJ4628 (Hornbæk *et al*., 2002) (Chapter 2). This is beneficial to the industrial production process as it means that if an error occurs during the preparation of the cell banks which goes un-noticed, this may not affect the final product yield. The results for *B. licheniformis* SJ4628 5 L fed batch fermentations were very reproducible and reflect the industrial heritage of this organism. Work by Kocharunchitt agrees with this as it shows that production of α-amylase by *B. licheniformis* SJ4628 was largely unaffected by changes in glucose concentration and dissolved oxygen concentration although pH fluctuations were shown to reduce α-amylase yield by 10% (Kochurunchitt, 2007). The robust nature of *B. licheniformis* SJ4628 can in part be attributed to the chromosomal position of the α-amylase gene which overcomes the sometimes temperamental characteristics of plasmid based systems (Summers *et al*., 2005).

Figure 6.31 shows the status of the dissolved oxygen (%) throughout the fermentation process. There was a decline to an average of 32% before a slow increase a trend which closely followed the increase and decrease in cellular

growth.

Figure 6.32 to 6.34 shows the HPLC results for metabolite concentration during the fermentation.

B. licheniformis SJ4628 produced three different metabolites: acetate (Figure 6.32), propionic acid (Figure 6.33) and 2,3-butandiol (Figure 6.34). The concentration of acetate was undetectable at 0 h, then rose to a peak of 4.85 gL^{-1} between 4 and 5 h, and then fell to 3.11 gL^{-1} at 7 h. The mean concentration of acetate then reached a maximum value of 11.75 gL^{-1} at 8 h, finally declining until the end of the fermentation when the concentration of acetate was undetectable. Mean propionic acid concentration was low at the start of the fermentation with a value of 0.04 gL^{-1} at 0 h which rose to a maximum of 4.72 gL^{-1} at 5 h: a steady decline then followed to a value of 1.76 gL^{-1} at 8 h followed by a gradual increase to a final value of 4.0 gL^{-1} at 51 h. The mean concentration of 2,3-butandiol was undetectable until the 8 h time point where it measured 1.72 gL^{-1} and then showed a decline to 0.36 gL^{-1} at 10 h before finally increasing to 6.95 gL^{-1} at 51 h. Figures 6.35, 6.36 and 6.37a to h show the physiological status of the cells throughout the fermentation process.

Cells at the 0 h time point were predominantly polarised with a small de-polarised and permeablised population which quickly recovered and remained polarised throughout the fermentation.

As with the batch process (Chapter 5, Figure 5.3), production of acetate, propionic acid and 2,3-butandiol occurred during the fed batch process. The

concentration of acetate increased up to a maximum at 8 h before falling to a negligible amount from 10 h onwards (Figure 6.32). This corresponded to low glucose levels and falling dissolved oxygen concentrations, which was in contrast to its production in the batch process, indicating that glucose and dissolved oxygen concentration were not the only factors affecting acetate production in this organism. One possibility for this is presence of nitrate in the medium which has been shown to enhance acetate production in *B. licheniformis* NCIB 6346 (Shariati *et al*., 1995). Shariati and colleagues also report that no formate was detected during fermentations of *B. licheniformis* NCIB 6346 where glucose and nitrate were present (Shariati *et al*., 1995). Hornbæk and colleagues have shown that acetate was produced by *B. licheniformis* SJ4628 as a mechanism to correct pH fluctuations, but this is unlikely to be the case here as the pH was maintained at 7.0 throughout the fermentation process (Hornbæk *et al*., 2004). No formate was detected in the present study. The concentration of propionic acid reached a maximum at 5 h during which glucose levels were low and dissolved oxygen levels were high. It showed a decline during the period of declining dissolved oxygen and then an increase when the dissolved oxygen and glucose concentrations started to increase. This again disagrees with the results for the batch process which showed that propionic acid concentration declined with falling dissolved oxygen concentration. The 2,3-butandiol concentration showed a peak at 8 h corresponding with low dissolved oxygen concentrations but then began to increase after 10 h before increasing again as the dissolved

oxygen and glucose levels started to increase. This result may indicate that the high levels of glucose caused 2,3-butandiol production. The production of the same metabolites occured during the batch and fed batch processes. However, the factors affecting their production appear to be different and this may reflect the differences in the fermentation process such as higher glucose concentrations, higher cell biomass, higher α-amylase production and a longer length of fermentation during the fed batch process. The production of these metabolites was, however, in low concentrations (less than 12 gL^{-1}) which was negligible indicating that this organism has been highly selected as an industrial organism to reduce production of these undesirable metabolic products. It also means that the choice of medium used was good as it minimised the production of these products. The viability of *B. licheniformis* SJ4628 during the fed batch process remains high as the number of PI^- cells was above 90% during the 51 h process again highlighting the resilience of this organism.

From these results it can be concluded that despite the different rates of recovery following freezing each of the cell banks showed similar behaviour during the fed batch process and produced similar final biomass and α-amylase concentration. *B. licheniformis* SJ4628 is clearly a very robust and well suited as an industrial production strain.

Chapter 7

Conclusions

1. *B. cereus* NCTC11143 displays a large amount of population heterogeneity when cultured in nutrient broth during shake flask fermentation. This is probably due to its nature as a non-industrial organism.
2. *B. cereus* NCTC11143 is an excellent candidate with which to study the ability of $DiBac_4(3)$, $DiOC_6(3)$ and REDOX sensor green reagent, and PI, to measure microbial viability using multi-parameter flow cytometry.
3. $DiBac_4(3)$, $DiOC_6(3)$ and REDOX sensor green reagent can provide concurrent data about the cellular viability of *B. cereus* NCTC11143.
4. The multi-parameter flow cytometry sorting of *B. cereus* NCTC11143 reveals the presence of “doublets” of live and dead cells joined together.
5. The multi-parameter flow cytometry sorting of *B. cereus* NCTC11143 reveals that cells exposed to the carbocyanine dye $DiOC_6(3)$ can remain viable.
6. *B. licheniformis* SJ4628 displays very little population heterogeneity during shake flask fermentation in yeast malt broth. This is probably due to its nature as an industrial production strain.

7. *B. licheniformis* SJ4628 grows well in concentrations of glycerol not exceeding 25% v/v.
8. Glycerol affects the action of $DiBac_4(3)$ on a flow cytometry plot making the dead cell population appear in a different position than expected.
9. *B. licheniformis* SJ4628 grows well in concentrations of DMSO not exceeding 15% v/v.
10. *B. licheniformis* SJ4628 grows well in concentrations of Tween 80 up to 20% v/v. Higher concentrations may also be non-toxic but, viscosity and foaming problems become problematic.
11. The following concentrations of cryopreservant (v/v) are non-toxic to *B. licheniformis* SJ4628: 20% glycerol, 25% glycerol, 15% DMSO and 20% Tween 80.
12. Cells cryopreserved with 20% v/v Tween 80 showed the fastest recovery rates during shake flask fermentation directly after freezing. Cells cryopreserved with 15% v/v DMSO had the slowest recovery rates. Cells cryopreserved with 20% v/v glycerol, 25% v/v glycerol and no cryopreservant recovered faster than cells cryopreserved with 15% v/v DMSO but not as fast as cells cryopreserved with 20% v/v Tween 80.
13. An increase of 5% v/v glycerol concentration from 20% to 25% v/v displays no advantage during cryopreservation.
14. Yeast malt broth containing 2% v/v polypropylene glycol 2025 is a good cryopreservant by itself.

15. During 5 L batch fermentation in yeast malt broth *B. licheniformis* SJ4628 demonstrates a typical microbial growth profile, with production of α-amylase and produced concentrations of the metabolites acetate, propionic acid and 2,3-butandiol below 10 gL^{-1}.

16. During 5 L fed batch fermentation with each cell bank: 20% v/v glycerol, 25% v/v glycerol, 15% v/v DMSO, 20% v/v Tween 80 and no cryopreservant *B. licheniformis* SJ4628 showed no difference in the production of α-amylase or total final biomass, even though there were differences in the recovery rates of each cell bank directly after freezing. This indicates that the production of the inoculum cancels out the deleterious effects of the freezing process provided that the same optical density is used at inoculation.

17. *B. licheniformis* SJ4628 has grown well and produced reproducible data which is probably attributable to the industrial heritage of the organism and the chromosomal nature of the α-amylase gene.

18. During 5 L fed batch fermentation of *B. licheniformis* SJ4628 in yeast malt broth low concentrations of the metabolites acetate, propionic acid and 2,3-butandiol were measured. This indicates that *B. licheniformis* SJ4628 has been well selected as an industrial organism not to produce large quantities of undesirable metabolites and also that the yeast malt broth is a good choice for growing this organism.

Chapter 8

Further Studies

1. The experiments done during this study show that different cryopreservants have no effect on total biomass or final α-amylase yields during 5 L fed batch fermentations of *B. licheniformis* SJ4628. To further investigate the process, it would be interesting to repeat the procedures with a more recent production strain to see if any differences arose. An organism containing a plasmid based version of the α-amylase gene would be an excellent candidate as it may be a less robust model. The α-amylase gene in *B. licheniformis* SJ4628 is located on the chromosome and is therefore very stable. *B. licheniformis* SJ4628 has been strain selected to over produce α-amylase but is not a recombinant organism. However, many industrial production strains are constructed to over produce products by using recombinant gene technology which involves the use of plasmid DNA. Such organisms can suffer from plasmid instability and it would be interesting to investigate if cryopreservation has an effect on plasmid stability and production of α-amylase.
2. It would be interesting to repeat the experiments done during this study with other micro-organisms that have biotechnological importance such as

the Gram negative organism *E. coli*, the yeast *Saccharomyces* and the fungus *Aspergillus* to find out if fermentation batch to batch reproducibility is affected. The physiological differences of such organisms may play an important role in the way that they respond to cryopreservation.

3. Experiments to scale up the process to something more representative of an industrial scale system would allow further understanding of the process used by Novozymes A/S. Differences exist at the commercial scale compared with the laboratory scale because of the complexity of reactions and interactions that occur in a bioreactor. Larger scale systems have different heat and mass transfer abilities, differences in mixing times mean that pockets of sub-optimal conditions occur for periods of time. There may be differences in the properties of the fermentation broth (viscosity, osmotic pressure, substrate and waste product concentration) and gas and liquid interactions may be different. All of which can affect microbial growth and physiology. At the commercial scale non-producing variant populations can arise from the parent population during the fermentation process. It would be interesting to discover if this occurs with *B. licheniformis* SJ4628 as it could explain differences in batch to batch reproducibility.

References

Amanullah, A., McFarlane, C.M., Emery, A.N., Nienow, A.W. (2001b). Experimental simulations of pH gradients in large scale bioreactors using scale down models. *Biotechnology and Bioengineering*, 73, 390-399.

Arnesen, S., Eriksen, S.H., Olsen, J., Jensen, B. (1998). Increased production of α-amylase from *Thermomyces lanuginosus* by the addition of Tween 80. *Enzyme and Microbial Technology*, 23, 249-252.

Beal, C., Fonseca, F., Corrieu, G. (2001). Resistance to freezing and frozen storage of *Streptococcus thermophilus* is related to membrane fatty acid composition. *Journal of Dairy Science*, 84, 2347-2356.

Bud, R. (1994). The uses of life: A history of biotechnology. *Cambridge University Press*, 1-319.

Chattopadhyay, M.K. (2006). Mechanism of bacterial adaptation to low temperature. *Journal of Biosciences*, 31, 157-165.

Coleman. G. (1970). Distribution of α-amylase forming ability between the membrane and soluble fractions of a cell-free preparation of *Bacillus amyloliquefaciens*. *Biochemical Journal*, 116, 763-765.

Davey, H.M., Kell, D.B. (1996). Flow cytometry and cell sorting of heterogeneous microbial populations; the importance of single cell analyses. *Microbiological Reviews*, 60, 641-651.

Deere, D., Porter, J., Edwards, C., Pickup, R. (1995). Eavaluation of the suitability of *bis*-(1,3-dibutylbarbituric acid) trimethine oxonol, (diBA-C_4(3)$^-$), for the flow cytometric assessment of bacterial viability. *FEMS Microbiology Letters*, 130, 165-170.

Dworkin, M., Falkow, S., Rosenberg, E., Schleifer, K.H., Stackebrandt E. (2006). The prokaryotes: Ecophysiology and biochemistry 3rd edition. *Springer Science*, 124.

Endo, Y., Kamisada, S., Fujimoto, K., Saito, T. (2006). *Trans* fatty acids promote the growth of some *Lactobacillus* strains. *Journal of General and Applied Microbiology*, 52, 29-35.

Fuhrer, T., Fischer, E., Sauer, U. (2005). Experimental identification and quantification of glucose metabolism in seven bacterial species. *Journal of Bacteriology*, 187, 1581-1590.

Fuller, B.J. (2004). Cryoprotectants: The essential antifreezes to protect life in the frozen state. *Cryoletters*, 25, 375-388.

Gil, M.J., Callejo, M.J., Rodríguez, G., Ruiz, M.V. (1999) Keeping qualities of white pan bread upon storage: effect of selected enzymes on bread firmness and elasticity. *European Food Research and Technology*, 208, 394-399.

Gnoth, S., Jenzsch, M., Simitis, R., Lübbert, A. (2007). Process Analytical Technology (PAT): Batch-to-batch reproducibility of fermentation process by robust process operational design and control. *Journal of Biotechnology*, 132, 180-186.

Görke, B., Slülke, J. (2008). Carbon catabolite repression in bacteria: many ways to make the most out of nutrients. *Nature Reviews Microbiology*, 6, 613-624.

Gray, R.D., Yue, S., Chueng, C.Y., Godfrey, W. (2005). Bacterial vitality detected by a novel fluorogenic redox dye using flow cytometry. *www.probes.invitrogen.com*

Gupta, R., Beg, Q.K., Lorenz, P. (2002). Bacterial alkaline proteases: molecular approaches and industrial applications. *Applied Microbial Biotechnology*, 59, 15-32.

Gupta, R., Gigras, P., Mohapatra, H., Goswami, V.K., Chauhan, B. (2003). Microbial α-amylases: a biotechnological perspective. *Process Biochemistry*, 38, 1599-1616.

Gurtovenko, A.A., Anwar, J. (2007). Modulating the structure and properties of cell membranes: The molecular mechanism of action of dimethyl sulphoxide. *The Journal of Physical Chemistry B*, 111, 10453-10460.

Hanai, T. (1999). HPLC: A practical guide. Royal Society of Chemistry, 1-134.

Henrissat, B. (1991). A classification of glycosyl hydrolases based on amino acid sequence similarities. *Biochemical Journal*, 280, 309-316.

Hewitt, C.J., Boon, L.A., McFarlane, C.M., Nienow, A.W. (1998). The use of flow cytometry to study the impact of fluid mechanical stress on *Escherichia coli* W3110 during continuous culture in an aerated bioreactor. *Biotechnology and Bioengineering*, 59, 612-620.

Hewitt, C.J., Nebe-Von-Caron, G. (2001). An Industrial application of multiparameter flow cytometry: Assessment of cell physiological state and its application to the study of microbial fermentations. *Cytometry*, 44, 179-187.

Hewitt, C.J., Nebe-Von-Caron, G. (2004). The application of multi-parameter flow cytometry to monitor individual microbial cell physiological state. *Advances in Biochemical Engineering/Biotechnology*, 89, 197-223.

Hornbæk, T., Nielsen, A.K., Dynesen, J., Jakobsen, M. (2002). Use of fluorescence ratio imaging microscopy and flow cytometry for estimation of cell vitality for *Bacillus licheniformis*. *FEMS Microbiology Letters*, 215, 261-265.

Hornbæk, T., Nielsen, A.K., Dynesen, J., Jakobsen, M. (2004). The effect of inoculum age and solid versus liquid propagation on inoculum quality of an industrial *Bacillus licheniformis* strain. *FEMS Microbiology Letters*, 236, 145-151.

Hornbæk, T., Jakobsen, M., Dynesen, J., Jakobsen, M., Nielsen, A.K. (2004). Global transcription profiles and intracellular pH regulation measured in *Bacillus licheniformis* upon external pH upshifts. *Archives of Microbiology*, 182, 467-474.

Hubálek, Z. (2003). Protectants used in the cryopreservation of microorganisms. *Cryobiology*, 46, 205-229.

Johannsen. E., (1972). Malt extract as protective medium for lactic acid bacteria in cryopreservation. *Journal of Applied Biology*, 35, 423-429.

Kirsop B.E and Snell J.J.S. (1984) Maintenance of microorganisms: A manual of laboratory methods. *Academic Press*. London.

Kocharunchitt, S. (2007). Studies related to the scale up of high cell density *Bacillus licheniformis* fed-batch fermentations: Effect of a changing micro-

environment with respect to pH, glucose and oxygen concentration. PhD *thesis*, University of Birmingham, Birmingham.

Koshland, D.E. (1953) Stereochemistry and the mechanism of enzymatic reactions. *Biological Reviews*, 28, 416-436.

Lee, Y.K. (2006). *Microbial Biotechnology: principles and applications 2nd Edition*. World Scientific, 31.

Lorentz, K. (1998). Approved recommendation on IFCC methods for the measurement of catalytic concentration of enzymes part 9. IFCC method for α-amylase (1,4-α-*D*-glucan4-glucanohydrolase, EC 3.2.1.1). *Clinical Chemistry and Laboratory Medicine*, 36, 185-203.

Lovelock, E.J., Bishop, M.W.H. (1959). Prevention of freezing damage to living cells by dimethyl sulphoxide. *Nature*, 183, 1394-1395.

Martin, C., Smith, A. (1995). Starch biosynthesis. *The Plant Cell*, 7, 971-985.

Meroueh, S.O., Bencze, K.Z., Hesek, D., Lee, M., Fisher, J.F., Stemmler, T.L., Mobashery, S. (2006). Three-dimensional structure of the bacterial cell wall peptidoglycan. *PNAS*, 103, 4404-4409.

Miller, J.B., Koshland, D.E., Jr. (1978). Effects of cyanine dye membrane probes on cellular properties. *Nature*, 272, 83-84.

Moes, J., Griot, M., Keller, J., Heinzle, E., Dunn, I.J., Bourne, J.R. (1984). A microbial culture with oxygen sensitive product distribution as a potential tool for characterizing bioreactor oxygen transport. *Biotechnology and Bioengineering*, 27, 482-489.

Nakano, M.M., Hulett, F.M. (1997). Adaptation of *Bacillus subtilis* to oxygen limitation. *FEMS Microbiology Letters*, 157, 1-7.

Nebe-von-Caron, G., Stephens, P.J., Hewitt, C.J., Powell, J.R., Badley, R.A. (2000). Analysis of bacterial function by multi-colour fluorescence flow Cytometry and single cell sorting. *Journal of Microbiological Methods*, 42, 97-114.

Onyeaka, H., Nienow, A.W., Hewitt, C.J. (2003). Further studies related to the scale-up of high density Escherichia coli fed-batch fermentations: The additional effct of a changing microenvironment when using aqueous ammonia to control pH. *Biotechnology and Bioengineering*, 84, 474-484.

Pagliaro, M., Rossi, M. (2008). The future of glycerol: New uses of a versatile material. Royal Society of Chemistry, 1-10.

Paulo da Silva, G., Mack, M., Contiero, J. (2008). Glycerol: A promising and abundant carbon source for industrial microbiology. *Biotechnology advances*, 27, 0-39.

Polge, C., Smith, A.U., Parkes, A.S. (1949). Revival of spermatozoa after vitrification and dehydration at low temperatures. *Nature*, 164, 666.

Preist, F.G. (1977). Extracellular enzyme synthesis in the genus *Bacillus*. *Bacteriological Reviews*, 41, 711-753.

Presecan-Siedel, E., Galinier, A., Longin, R., Deutscher, J., Danchin, A., Glaser, P., Martin-Verstraete. (1999). Catabolite regulation of the *pta* gene as part of carbon flow pathways in *Bacillus subtilis*. *Journal of Bacteriology*, 181, 6889-6897.

Pum, D., Neubauer, A., Györvary, E., Sára, M., Sleytr, U.B. (2000). S-layer proteins as basic building blocks in a biomolecular construction kit. *Nanotechnology*, 11, 100-1007.

Ragunathan, R., Swaminathan, K. (2005). Growth and amylase production by *Aspergillus oryzae* during solid state fermentation using banana waste as substrate. *Journal of Environmental Biology*, 26, 653-656.

Ratledge, C., Kristiansen, B. (2001). Basic Biotechnology 2nd Edition. *Cambridge University Press*, 43.

Rey, M.W., Ramaiya .P., Nelson, B.A., Brody-Karpin, S.D., Zaretsky, E.J., Tang, M., Lopez de Leon, A., Xiang, H., Gusti, V., Clausen, I.G., Olsen, P.B., Rasmussen, M.D., Andersen, J.T., Jørgensen, P.L., Larsen, T.S., Sorokin, A., Bolotin, A., Lapidus, A., Galleron, N., Ehrlich, S.D., Berka, R.M. (2004). Complete genome sequenceof the industrial bacterium *Bacillus licheniformis* and comparisons with closely related *Bacillus* species. *Genome Biology*, 5, R77.

Robinson, T.P., Wimpenny, J.W.T., Earnshaw, R.G. (1991). pH gradients through colonies of *Bacillus cereus* and the surrounding agar. *Journal of General Microbiology*, 137, 2886-2889.

Russell, J.B., Cook, G.M. (1995). Energetics of bacterial growth: balance of anabolic and catabolic reactions. *Microbiological Reviews*, 59, 48-62.

Shapiro, H.M. (2000). Membrane potential estimation by flow cytometry. *Methods*, 21, 271-279.

Shapiro, H.M. (2003). Practical flow cytometry 4th edition. *Wiley-Liss*, New York.

Shariati. P., Mitchell, W.J., Boyd, A., Priest, F.G. (1995). Anaerobic metabolism in *Bacillus licheniformis* NCIB 6346. *Microbiology*, 141, 1117-1124.

Schallmey, M., Singh, A., Ward, O.P. (2004). Developments in the use of *Bacillus* species for industrial production. *Canadian Journal of Microbiology*, 50, 1-17.

Sikkema, J., DeBont, J.A.M., Poolman, B. (1995). Mechanisms of membrane toxicity of hydrocarbons. *Microbiological Reviews*, 59, 201-222.

Simione, F.P. (1998). Cryopreservation manual. Nalge Nunc International Corp, 1-8.

Sleytr, U.B., Huber, C., Ilk, N., Pum, D., Schuster, B., Egelseer, E.M. (2006). S-layers as a tool kit for nanobiotechnological applications. *FEMS Microbiology Letters*, 267, 131-144.

Smith, A.U. (1950) Prevention of haemolysis during freezing and thawing of red blood cells. *Lancet*, 2, 910-911.

Smittle, R.B., Gilliland, S.E., Speck, M.L. (1972). Death of *Lactobacillus bulgaricus* resulting from liquid nitrogen freezing. *Applied Microbiology*, 24, 551-554.

Smittle, R.B., Gilliland, S.E., Speck, M.L., Walter, W.M. (1974). Relationship of cellular fatty acid composition to survival of *Lactobacillus bulgaricus* in liquid nitrogen. *Applied Microbiology*, 27, 738-743.

Sneath, P.H.A., Mair, N.S., Sharpe, M.E., Holt, J.G. (1986). Bergey's manual of systematic bacteriology, Volume 2. Baltimore, Williams and Wilkins.

Sonenshein, A.L. (2007). Control of key metabolic intersections in *Bacillus subtilis*. *Nature Reviews Microbiology*, 5, 917-927.

Strandberg, L., Andersson, L., Enfors, S. (1994). The use of fed-batch cultivation for achieving high cell densities in the production of recombinant protein in *Escherichia coli*. *FEMS Microbiological Review*, 14, 53-56.

Sum, A.K., de Pablo, J.J. (2003). Molecular simulation study of the influence of dimethylsulfoxide on the structure of phospholipid bilayers. *Biophysical Journal*, 85, 3636-3645.

Summers, D.K., Sherratt, D.J. (2005). Bacterial plasmid stability. *BioEssays*, 2, 209-211.

Suutari, M., Laakso, S. (1994). Microbial fatty acids and thermal adaptation. *Critical Reviews in Microbiology*, 20, 285-328.

Swain, M.R., Ray, R.C. (2007). Alpha-amylase production by *Bacillus subtilis* CM3 in solid state fermentation using cassava fibrous residue. *Journal of Basic Microbiology*, 47, 417-425.

Talsania, M. (2007). The application of multi-parameter flow cytometry to study the effects of different preservation techniques on the cell physiology of *E.coli* W3110 and *B.cereus* NCTC 11143. PhD *thesis*, University of Birmingham, Birmingham.

Uitdehaag, J.C.M., Mosi, R., Kalk, K.H., Van der Veen, B.A., Dijkhuizen, L., Withers, S.G., Dijkstra, B.W. (1999). X-ray structures along the reaction pathway of cyclodextrin glycosyltransferase elucidate catalysis in the α-amylase family. *Nature Structural Biology*, 6, 432-436.

Van der Maarel M.J.E.C., Van der Veen., B., Uitderhaag, J.C.M., Leemhuis, H., Diijkhuizen, L. (2002). Properties and applications of the starch- converting enzymes of the α-amylase family. *Journal of Biotechnology*, 94, 137-155.

Veith, B., Herzberg, C., Steckel, S., Feesche, J., Maurer, K.H., Ehrenreich, P., Bäumer, S., Henne, A., Liesegang, H., Merkl, R., Ehrenreich, A., Gottschalk, G. (2004). The complete genome sequence of Bacillus licheniformis DSM, an organism with great industrial potential. *Journal of Molecular Microbiology and Biotechnology*, 7, 204-211.

Vértesy, L. (1972). Proticin, a new phosphorus-containing antibiotic. Characterisation and chemical studies. *Journal of Antibiotics*, 25, 4-10.

Voigt, B., Antelmann, H., Albrect, D., Ehrenreich, E., Maurer, K.H., Evers, S., Gottschalk, G., van Dijl, J.M., Schweder, T., Hecker, M. (2009). Cell physiology and protein secretion of *Bacillus licheniformis* compared to *Bacillus Subtilis*. *Journal of Molecular Microbiology and Biotechnology*, 16, 53-68.

Webb. C., Kamat, S.P. (1993). Improving fermentation consistency through better inoculum preparation. *World Journal Of Microbiology and Biotechnology*, 9, 308-312.

Weidenmaier, C., Peschel, A. (2008). Teichoic acids and related cell-wall glycopolymers in Gram-positive physiology and host interactions. *Nature*, 6, 276-287.

Williams, C.M., Richter, C.S., M$_{AC}$Kenkie JR, J.M., Shih, J.C.H. (1990). Iasolation, identification, and characterization of a feather-degrading bacterium. *Applied and Environmental Microbiology*, 56, 1509-1515.

Wittman, V., Lin, H.C., Wong, H.C. (1993) Functional domains of the penicillinase repressor of *Bacillus licheniformis*. *Journal of Bacteriology*, 175, 7383-7390.

Zhang, Y.M., Rock, C.O. (2008). Membrane lipid homeostasis in bacteria. *Nature Reviews Microbiology*, 6, 222-233.

http://www.novozymes.com

http://www.lsbu.ac.uk/biology/enztech/starch.html

http://textbookofbacteriology.net/index.html

http://home.cc.umanitoba.ca/~oresniki/210/LEC31-01r.pdf

http://www.fda.gov/cder/OPS/PAT.htm